APPLICATIONS OF SCINTILLATION COUNTERS TO THE STUDY OF γ-RAY EMISSION PROCESSES

by

G.M.LEWIS

Thesis submitted for the Ph.D. degree of the University of Glasgow.

ProQuest LLC.
789 East Eisenhower Parkway
P.O. Box 1346
Ann Arbor, MI 48106 – 1346

PREFACE

The work described here was carried out in the department of Natural Philosophy of Glasgow University, over a period of approximately five years, ending in February 1954. The investigations are described in chapters 1, 2, and 3 of the text, and three interlocking aspects of the γ-ray process are essentially considered, viz. spectroscopy, lifetime, and spatial distribution. The introduction first indicates the background of the scintillation method, and then deals with the underlying theory and basic work associated with the three γ-ray aspects in turn.

The author acknowledges suggestions from Dr. S. C. Curran concerning the two crystal method (Ch. 1, §2), and the La^{140} decay scheme (Ch. 1, §3); also measurement work on La^{140} by Dr. R. C. Bannerman who determined figs. 6 and 9.

Sm^{151} and Eu^{155} (cf. Ch. 1, §4) were being studied in the laboratory by Dr. H. W. Wilson using proportional counter methods; the author was approached to investigate aspects requiring scintillation counters.

Concerning Ch. 2, §3, (i-vi), Mr. A. T. G. Ferguson assisted by preparing some of the ancillaries and by suggestions.

The author collaborated with Mr. A. T. G. Ferguson in the work referred to in Ch. 2, §4, by suggestions, by providing auxiliary equipment, and by carrying out the measurement work of figs. 36 and 37.

In conclusion, the author wishes to thank Prof. P. I. Dee for his interest in the work, Dr. S. C. Curran for discussions on radioactive decay, and Drs. J. G. Rutherglen and R. D. Smith for access to the high tension set at one stage of this work.

July 1954.

INDEX

§3/

§4/

INTRODUCTION

INTRODUCTION.

GENERAL SURVEY.

On the classical theory, the incidence of the smallest amount of γ-radiation in matter was expected to be followed by scattering. It is now known, however, that a group of several quanta can pass through relatively large bulks of material without effect. The impact of a γ-ray in matter is in general attended by the energising of one or more particles, usually electrons, which in turn can produce excitation and ionisation. Observation of the latter effects leads to information on the liberated particles and thence to a specification of the γ-ray concerned.

The often inefficient, and inherently indirect form of detection and measurement has made γ-ray work difficult. Whilst individual events could be studied by cloud chamber methods, and more recently by photographic techniques, larger surveys have been undertaken by spectrometers and various forms of gas counter, the γ efficiencies of which are in general low. The requirement for a counter permitting efficient detection and measurement of γ-ray energy has been a very real one, particularly for coincidence studies.

The introduction and development of the scintillation counter, activated by the fluorescent light from excited atoms and molecules usually in condensed materials, has satisfied this need over large γ-ray energy regions.

Though the scintillation counter has found most immediate usage/

usage in the field of γ-ray work, attributes and developments, such as those associated with fast response, have given it considerable value in other fields of investigation.

With the availability of a method for examining individual γ-ray events quantatively and effectively, detailed studies can be made of the processes associated with these events. Three types of information, generally interlinked, on γ-rays and the γ-ray processes are required, and will be considered. They can be listed as follows:-

1. Spectroscopic data, concerning the γ-ray energy and intensity.
2. Lifetime figures, referring to the ordering and timing of events.
3. Spatial specifications of the γ-rays, intrinsically related to spin.

In the text it will be found convenient to associate with the term spectroscopy, also prompt coincidence spectroscopy, involving a knowledge of those events which are, broadly speaking, time coincident with one another, i.e., which belong to the one parent disintegration. As for lifetime work, since the scintillation counter plays a dominant role in the short lifetime region, emphasis will be placed on this. The spatial relationships can concern γ-ray angular distribution and correlation investigations. These three aspects can be linked with the three characteristic properties of the scintillation counter, viz., uniformity, speed, and efficiency of the response, respectively. In the following pages/

pages of the Introduction, the essential properties of the scintillation counter are first discussed, with special reference to γ-ray absorption and technique; the three aspects of a γ-ray process are then considered in more detail.

§ 1. THE DEVELOPMENT OF THE SCINTILLATION COUNTER FOR γ-RAY WORK.

(1) The Scintillation Counter.

Fluorescence has played an important role in the bulk detection of radiations. Ultra violet light produced direct optical excitation; cathode rays, X rays, and the early radioactive radiations produced particle excitation of the appropriate optical levels. In view of these applications, many parts of the subject have been closely studied in the past, particularly those relating to cathodoluminescence (cf. e.g., Stokes (1852), Röntgen (1895), Becquerel (1896), Lenard (1903)). The scintillation detection of single heavy particles was of much importance in early radioactive work (cf. e.g., Crookes (1903)), but the visual method of detection gave way to various forms of electrical counter.

The Photoelectric effect (cf. e.g., Hallwachs (1888)), and the discovery of secondary emission (Austin and Starke (1902)) permitted the ultimate development of the photomultiplier (cf. for instance Zworykin, Morton and Malter (1936)). The detection of α-particle scintillations using a photomultiplier was effected by Curran/

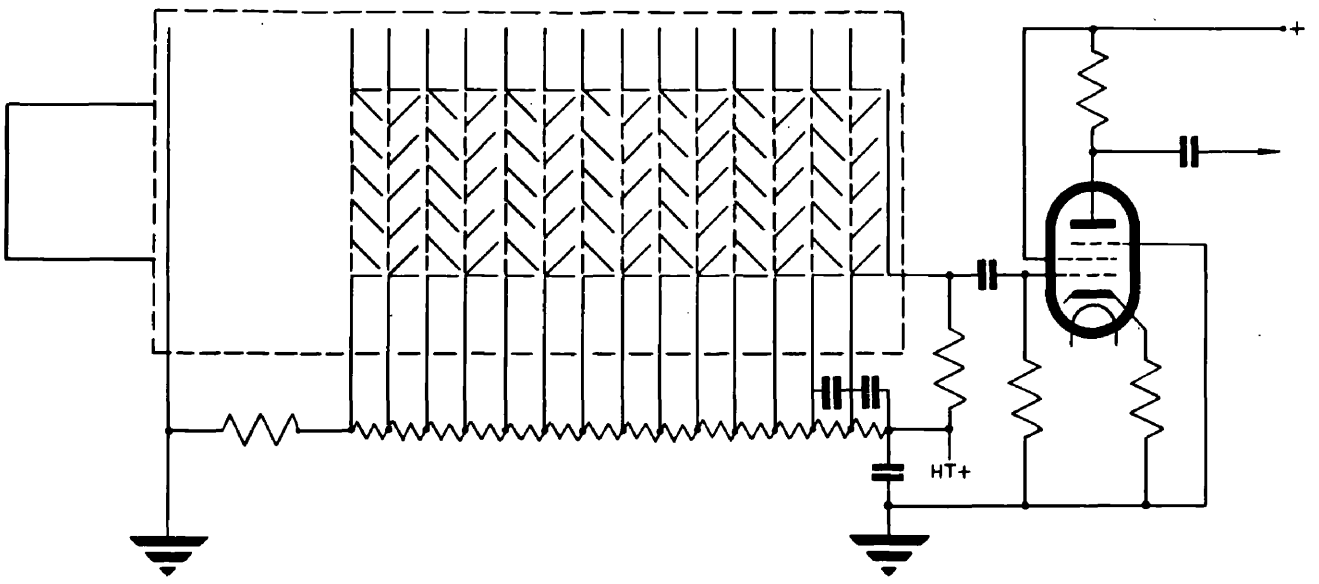

Fig. 1. Schematic diagram of photomultiplier showing scintillator in place, and preamplifier connections.

Curran and Baker (1944). Independently Broser and Kallman (1947)ab detected particles and γ-quanta, reporting uniformity of response for α-particles. A new return to older methods followed.

A schematic diagram is shown in fig. 1 of a scintillation counter. Connections with a preamplifier are shown for completeness though other attachments are equally appropriate. As a result of irradiation that part of the emitted light which is not absorbed by the mass of scintillater passes out as fluorescence and ejects photoelectrons at the cathode. Successive multiplication occurs and finally electrons charge up the effective collector capacity, the charge received being subsequently allowed to leak away.

Tubes having tungsten sensitivities around 30μa/lumen were realizable. Making some allowance for the wider response band of the photomultiplier relative to the eye this corresponds roughly to about 1 photoelectron per 20 quanta of 3 e.v. . For a very efficient phosphor like zinc sulphide, which under α bombardment required at best only 9 e.v. per quantum (Chariton and Lea (1929)) it could be anticipated that 1Me.v. of α energy might liberate about a thousand photoelectrons allowing for some loss through geometry (cf. 1P21, R.C.A. tubes). With a gain of 10^6, and a collector system capacity of 20 pf. an output of several volts could then be expected. Both thermal and shot electrical noise in the following preamplifier and circuity would therefore be of no consequence, being restricted to the microvolt region with proper design, even for bandwidths of several megacycles. (cf. Nyquist (1928) and Williams (1936)). This indicates, together with the wide band character of the amplification/

amplification, the particular merits of the multiplier action. The phototube has however a dark current of its own. This is to some extent temperature dependent, as it is partly due to thermal electron emission, but at high interstage voltages the noise increases. This tube noise limits the performance of the counter at energies liberating only a few electrons from the cathode.

Following on the introduction of the counter and the use by Broser and Kallman (1947)b of naphthalene for detection of γ-rays, other γ-ray scintillators were proposed, amongst them anthracene (Bell (1948)) and thallium activated sodium iodide (Hofstadter (1948) Whilst the response of the organic materials was not as good as that of the impurity activated inorganic materials the rise time was shorter.

On the multiplier side the production of tubes with side and small end window cathodes by E.M.I (types 4140 & 5060) improved the geometrical efficiency of commercial multipliers (cf. Sommer and Turk (1950)).

This was approximately the position when the work described in this thesis began. Because of the exploratory character of much of the early work referred to above, preliminary measurements were made on the method. The scintillation responses of some materials were examined including those of some liquids and solutions, particularly with a view to possible γ-ray use. A rough assessemnt of the absolute response of anthracene was also made.

The/

The initial aim was to determine how the scintillation counter could be best set up for measuring γ-ray energy, since this type of measurement had not been made, and consideration had to be given to the preparation of blocks of material of adequate size. Before introducing more specifically the γ-ray side of the technique reference should be made to some later developments of the counter itself which have helped in this connection. On the scintillator side reference should be made to the use of terphenyl in solutions (Reynolds, Harrison, and Salvini (1950)), which have an efficiency ~I/3 that of anthracene, and a fast rise time; (e.g., for terphenyl in toluene a rise time of 2×10^{-9} sec. has been measured (Post R.F. 1950)). Mention should be made too of the commercial availability of certain crystals in bulk by Harshaw, and Hilger, for instance. On the photomultiplier side, the development of the 1" & 2" cathode E.M.I 11 & 14 stage tubes the R.C.A. tube 58I9, and the more recent high sensitivity Du Mond tubes should be referred to.

(ii) γ - ray absorption.

γ -ray absorption is essentially determined over large energy ranges by the three processes; photoelectric effect, Compton process, and pair production. The first of these is accompanied by the emission of an X-ray, in general, which can induce subsequent photoeffects. The second involves production of a scattered γ-ray of lower energy. The third involves provision of 1.02 Mev for pair creation/

creation, which reappears subsequently when annihilation occurs.

The photoelectric effect implies electron ejection from one of the various K, L, M ---- shells of the atom. The electron is emitted preferentially along the electric vector, i.e., at right angles to the momentum of the γ-ray. The nucleus has therefore to provide a momentum increasing with γ-ray energy (K_0). In consequence of this the photoeffect is not of importance at higher energies especially for materials of low atomic number z; furthermore that from the K-shell is dominant. At lower energies the K-shell photoeffect cross section φ_K is, per atom:

$$\varphi_K = \varphi_0 \frac{Z^5}{137^4} 4\sqrt{2}\left(\frac{\mu}{K_0}\right)^{7/2} \qquad (1)$$

where $\varphi_0 = 8\pi r_0^2/3 = 6.57\times10^{-25}$ cm^2 and μ is the electron mass. (cf. e.g. Heitler (1947), Stobbe (1930)).

In the Compton process, Compton (1923), involving free electrons a large portion of the incident γ-energy is in general reradiated, partly to accord with momentum considerations. At the lower energies the electron cross section $\bar{\varphi}_0$, corresponding to an atomic cross section $Z\varphi_0$, is given by the Thomson scattering formula, the scattering intensity being symmetric about the electric vector. The theoretical formula has been deduced by Klein and Nishina (1929). At higher energies radiation in the backward direction falls off rapidly, and with it the total absorption cross section. The atomic cross section φ_c for the Compton process is given at high energies by the asymptotic relations.

$$\varphi_c = Z\,\varphi_0 \frac{3}{8} \frac{\mu}{K_0}\left(\frac{1}{2} + \log\frac{2K_0}{\mu}\right) \qquad (2).$$

In/

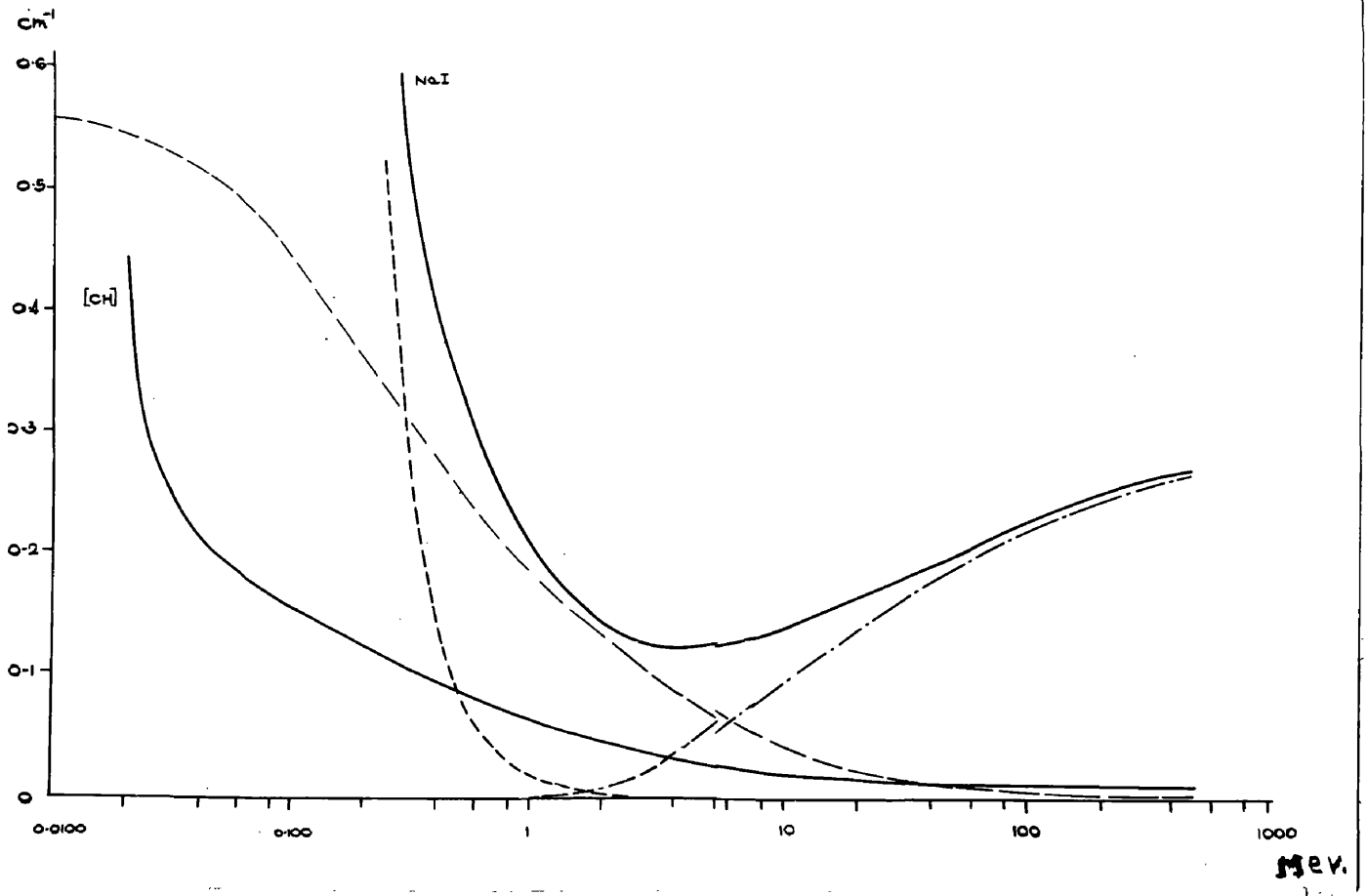

Fig. 2. γ-ray absorption coefficients for NaI crystal and for a hypothetical organic crystal of density 1 containing equal numbers of C and H atoms.

In the pair production process, electrons are ejected from negative energy states Dirac (1928) Blackettand Occhialini(1933). Momentum is provided by the nucleus, and the absorption increases with coulomb attraction of the nucleus, being proportional to Z^2. Beyond the threshold of 1.02 MeV the absorption slowly increases with frequency, the increasing amount of phase space available to two particles at the higher energies offsetting restrictions in providing the momentum for balance. At high energies, the cross section φ_p is given by: $\varphi_p = \frac{Z^2}{137}\varphi_0\left(\frac{1}{6\pi}\right)\left(7\log\frac{2k_0}{\mu} - \frac{109}{6}\right)$ (3)

(cf. Heitler and Sauter (1933))

A screening correction for the coulomb attraction due to the electrons in the atom has generally to be included.
Much further experimental work in connection with these γ -ray absorption processes has been carried out; detailed comparisons with theory are given by Heitler (1947) and by Spring (1950). Results will be referred to in the text of energy and related measurements with scintillation counters on the photoelectric and Compton process here which accord with the theory.

On the basis of the above and data given by Heitler (1949) the variation of γ-ray absorption coefficient with energy in any material may be obtained. Fig. 2 shown the variation in absorption coefficient τ per cm. for scintillators of activated sodium iodide; and also for a hypothetical organic material having equal numbers of carbon/

carbon and hydrogen atoms and density unity. It further shows the contribution to absorption in the case of the sodium iodide crystal, of the three processes dealt with above. The allowance for screening in the pair effect at the highest energies shown is only approximate.

(iii) γ-ray energy measurement with scintillation counters.

It is necessary to consider, in energy measurements, the range of the electrons produced. At low energies this is roughly proportional to density being $\sim$ 1 mm. for an electron of $\frac{1}{4}$ MeV energy in a material of density 1. At higher energies the range may be large and may be a more important factor than the γ-ray absorption; further the energy loss by Bremsstrahlung may become important.

If the photoelectric cross-section is high in a block of scintillating material, there is a high probability that the characteristic X-rays liberated during the γ -ray photoelectric absorption are themselves absorbed in the material together with the subsequent characteristic X-radiations involved. A single peak should then occur. This effect in sodium iodide was demonstrated by West, Meyerhof, Hofstadter (1951). It is particularly important for energies below $\sim \frac{1}{4}$ MeV (cf. fig. 2). Effects in other materials are referred to in Ch.1.

For capturing the considerable amounts of radiation from Compton scattering relatively large amounts of material are in general required, adequate width as well as length having to be provided./

provided. In the initial stages of development searches were being made for such γ-ray peaks using single crystals. Some work of this kind is mentioned in Ch. 1. With smaller amounts of material a method using two crystals in coincidence could be employed, one activated by back scattered Compton γ-rays, the other selecting the corresponding electrons of maximum energy. Results by this method were published by Hofstadter and McIntyre (1950)a. Preliminary measurements had been carried out by the writer, and these and later measurements are described.

The pair effect is important for the detection of high energy radiation, the particles produced being initially directed forwards. Breadth as well as length has to be provided in the scintillator to allow for scattering and Bremsstrahlung. Mention should be made of the experiment by Johannson (1950) who selected pulses in a central crystal giving annihilation quanta in two subsidiary crystals in coincidence.

In using single crystals for energy measurements, care has to be taken to sort out the photoelectric and pair peaks and the Compton edge. This could be avoided in the region $\sim$ 100 KeV to $\sim$2 MeV by using an organic phosphor where only the Compton edge occurs. Use is made of this property in the work referred to in Ch. 1 on La^{140} (cf. Bannerman, Lewis and Curran (1951). At the present time with the larger crystals of sodium iodide now available, it is possible to produce a single peak, over large energy ranges, by capture of secondary quanta.

§2 THE γ-RAY EMISSION PROCESS AND NUCLEAR SPECTROSCOPY.

An examination of the γ-ray energies associated with nuclear transitions gives the level differences of the nuclear states, and coincidence studies involving the various emitted radiations lead to mass difference assignments. Conversely the available energy in a radioactive transition limits the number of excited states accessible to investigation by decay methods. In isobaric transitions to a stable state, this energy roughly falls with atomic number, being generally greater for unstable odd odd, than for odd A, nuclei; a trend in line with the semi empirical Weizsäcker predictions (cf. too Bitter 1950, p 123).

In considering γ-ray emission the nature of the states involved is of prime importance, particularly the charge distribution and energy; fundamentally these must depend on the nuclear forces. As exact information on the states is not available, interpretations of them are of great value. Some reference will be made in this work to one such interpretation, viz., the shell model (cf. e.g., Meyer 1949). On this model spin and parity assignments can be postulated for both ground and low lying excited states Moreover qualitative estimates can be hazarded about the energy changes involved, Thus odd A nuclei can be expected to have lower first levels than even even nuclei, and the shift of a particle within a shell can be expected to involve only a small energy. The power of the method is best gauged by specific instances (cf. e.g., Goldhaber and Sunyar 1951). Other models are useful in other cases/

cases (cf. e.g., Guggenheimer (1943), Hafstad (1938)).

The nature of the single γ-emission process is considered in (ii) below. It is desirable first to consider in (i) the characteristics of a multipole order radiation field, since much emphasis will be placed on this in some of the work that follows (cf. §4 and ch. 3).

The case of two and three γ-rays being emitted simultaneously from an electron positron system will be raised along with other matter in §3 .

(i) Multipole order radiations.

The emission of a photon by an orbital charged particle has long been associated with changes in angular momenta (cf. Abraham (1914)). The quantisation of the angular momentum of an atomic or nuclear system could therefore be expected to have an important bearing on the type of radiation fields produced.

In quantum physics for spherically symmetric Hamiltonians, the rotational operators $\frac{\partial}{\partial \varphi}$ (where φ is the azimuthal angle), etc., are associated with constants of the motion (cf. Dirac (1935), p.121). For the rotationally invariant electromagnetic field equations therefore those solutions, which are eigenstates of the rotational operators, will possess important constants of the motion. These can be shown to be angular momentum constants.

Solutions of the electromagnetic equation in vector form can be obtained, viz:

$$\vec{E} = \text{curl } (\vec{r}\psi); \quad \text{or again } \vec{H} = \text{curl } (\vec{r}\psi) \qquad -(4)$$

where ψ is a solution of the equation $\nabla^2\psi + K^2\psi = 0$.

and/

and $\vec{r}$ is the radius vector. In spherical polar co-ordinates (r,θ,φ), ψ can be given by $\psi = Y_{\ell m}(\theta,\varphi).\ f(r)$ (5). where f(r) is an appropriate function of r, and φ enters $Y_{\ell m}$ (the spherical harmonic) as $e^{im\varphi}$ here, {cf., for instance, Heitler (1936), Stratton (1941) p.415}.

These forms (4) are associated with magnetic, and electric, multipole radiation respectively of order ℓ, the radial components of $\vec{E}$ and $\vec{H}$ vanishing, respectively.

These fields are eigenstates of the vector rotation operator $\frac{\partial}{\partial\varphi}$; thus under a rotation of co-ordinate axes;

$$\frac{\partial}{\partial\varphi}(\text{curl}\ \vec{r}\psi) = m\ (\text{curl}\ \vec{r}\psi) \qquad (6)$$

in a manner analogous to the equation:

$$\frac{\partial}{\partial\varphi}\ Y_{\ell m} = m.Y_{\ell m}.$$

for scalar wave functions (cf. Franz (1950)..

By expressing the angular momentum in terms of Poynting's vector Franz has shown the quantum characters ℓ and m are associated with the total angular momentum and axial resolute of angular momentum respectively of the multipole radiation. Moreover the solutions form a complete set of solutions of the equations.

The emission probability of a quantum in a small solid angle about the direction (θ, φ) is a function of θ only for the above (ℓm) multipole radiation and can be designated $F\ell^m(\theta)$. (cf. e.g., Falkoff and Uhlenbeck (1950)).

(ii) <u>The emission probability</u>.

It is necessary to mention γ-ray intensity considerations, which will be needed in ch. 1; (and the closely linked lifetime matters/

matters which will be referred to further in §3 and Ch. 2).

On the classical theory the emission probability of long wave length multipole radiation (ℓm), due to an oscillatory charge density ρ, distributed through a volume V is proportional to the (moment integral)^2: $\left| \int r^{\ell} . Y_{\ell m}^{+}(\theta,\varphi) . \rho(r) . dV \right|^2$

{cf. Blatt and Weisskopf (1952), p.590, who deduce the transition probabilities (7), (8), (9) below}.

The emission probability $q_{\ell m}$ of a quantum of electric multipole radiation (ℓm) from a single nucleon of charge e in a transition from state ϕ_a to φ_b may be written in quantum theory, as

$$q_{\ell m} = \frac{4\pi\gamma e^2}{\hbar} . k^{2\ell+1} . \left| \int r^{\ell} . Y_{\ell m}^{+}(\theta,\varphi) . \varphi_b^{*}(\tau) . \varphi_a(\tau) . d\tau \right|^2 . \qquad (7)$$

where $$\gamma = \frac{2(\ell+1)}{\{1.3.5.....(2\ell+1)\}^2}$$

The integration over τ including the spin variables and the volume; where the wavelength $2\pi/k$ is long compared with the linear dimensions of the nucleus. If the nucleon possess a magnetic moment an additional term, generally small, should be included within the modulus. Using the independent particle model of the nucleus of radius R, the transition probability $q_{\ell m}$ has been shown to be

$$q_{\ell m} = \frac{\gamma e^2}{\hbar} . k^{2\ell+1} . R^{2\ell} . S. \qquad (8)$$

where S is a factor of order unity for a favoured transition, depending on the angular momentum of the nucleon involved before and after. For a nucleus of $A \sim 50$, emitting a γ-ray of energy $\sim$ 1 MeV, lifetimes of $\sim 10^{-16}$ and $\sim 10^{-11}$ secs can be predicted against electric dipole and quadrupole transitions respectively.

The expected magnetic multipole radiation (ℓm) probability, has/

has been shown to be less by the approximate ratio

$$\left\{\frac{MCR}{\hbar}\right\}^2 \cdot \frac{1}{10} \sim 100 \qquad (9)$$

where M is the mass of the nucleon.

Whilst these formulae of Blatt and Weisskopf serve to predict γ-intensities in general, consideration has to be given to the internal conversion coefficients before assessing the lifetime of states, of high atomic number Z, emitting lower energy radiations. Moreover the experimental determination of these coefficients can serve as an independent check on the multipole order and type of radiation. They can be assessed theoretically without knowledge of nuclear structure; (cf. e.g., Dancoff and Morrison (1939)). { Passing reference should be made to multipolarity determinations in the higher energy region using internal pair effects (cf. e.g., Jaeger and Hulme (1935), Latyshev (1947)}.

Experimental verifications of the above intensity and related theory exist. One of many instances involves the 411 Kev. state of H_g^{198}, examined by short lifetime methods referred to in §3 below, by Graham and Bell (1951); also by Davey and Moon (1953) and Malmfors (1952). The lifetime is of order 10^{-11} sec. implying an E.2 transition. This assignment is confirmed by the internal conversion results (cf. Elliott and Wolfson (1951)).

(iii) Experimental work here involving γ-ray spectroscopy.

Some of the γ-ray work on radioactive sources was initiated as indicated in §I to investigate certain aspects of scintillation counter work, then in an early state these involved γ-ray energy and intensity measurements, and subsequently the development and use/

use of certain coincidence methods which would correlate the γ-ray energies involved. An investigation of the γ-rays of La^{140} is described from this viewpoint, which led to information concerning the decay of this element.

Some early work on the radioactive elements Sm^{151}_{62} and Eu^{155}_{63} is also described which suggested possible decay schemes for these nuclei(cf. too Wilson and Lewis (1952)). These nuclei occur in a region of Z and A where much data is required.

An investigation was carried out too on naturally radioactive Rb^{87}, which has, on occasions been supposed other than a pure β-emitter. The mode of decay, lifetime and β - ray characteristics were of much interest. This source seemed particularly suitable for study by the scintillation method, and crystals of RbI (Tl I) were made and examined in connection with the work. Purely β-ray aspects of the study are referred to briefly in the Appendix (cf. too Lewis (1952)b).

With the development of the scintillation technique spectroscopic studies requiring more involved procedure became possible. The study and some applications of delayed coincidence spectroscopy are referred to in <u>§ 3</u> below.

§3 DETERMINATION OF SHORT LIFETIMES, POSITRON AND POSITRONIUM LIFETIMES AND ASSOCIATED SPECTRA.

The lifetime of an excited state against single quantum emission has been referred to in principle. The work in the text (ch.2) will also relate to the spectra and lifetimes associated with the annihilation of a positron electron system, where two or/

or three quanta are emitted simultaneously, a matter introduced below in (iii). A fast coincidence unit using scintillation counters served as a basis of measurement and the development of this is referred to briefly in (i), and its application is indicated in (ii).

(i) Fast coincidence units.

The pulses from a scintillation counter could be expected to rise quickly (cf. S1) and a coincidence unit with resolving time at least in the 10^{-8} sec. region seemed realisable. In 1949 Bell and Petch referred to the construction of a fast unit using 1P21 multipliers, discriminating after mixing. A requirement concerning work in ch. 3 had led the author to investigate units of these resolving times to cut down random counts. The use of fast discriminators and the like did not take adequate advantage of the fast multiplier pulses, and it was decided to incorporate the suggestion of discriminating after mixing. Appropriate line and other circuitry was designed and made. Development work and operational methods for high speed γ -ray work are referred to mostly in the text. Reference too should be made to the work of de Benedetti using a different input system.

(ii) Short lifetime determinations involving γ -rays and associated spectroscopy.

The main method of short lifetime determination at the present time employs delayed coincidence technique, utilising scintillation counters. In this if the formation of an excited state be announced by the emission of radiation this can be allowed to trigger one channel/

channel of a high resolution coincidence device, allowing the subsequent decay of the nucleus to be followed by the other channel. By this means Graham and Bell (1951) showed the lifetime of Hg^{198} to be less than 3×10^{-11} sec. (cf. §2 ii). This method will be used in the text; its application to the determination of fast periods, and more than one period, will be considered in detail. This method has the further merit of permitting delayed coincidence spectroscopy to be carried out, an aspect required in the text. Developments of this technique are detailed there, together with applications.

[In passing, mention should be made of the complementary γ-line width (Γ_γ) method of measuring very short lifetimes. Resonance scattering has been observed for Hg^{198} by Davey and Moon (1953), Malmfors (1952) (cf. §2 ii); Γ_γ has been found for proton capture when the total width is large (cf. Fowler and Lauritsen (1949)). Other special methods exist (cf. Thirion and Telegedi (1953)), Elliott and Bell (1949), Delbrück and Gamow (1931)].

(iii) Positron and positronium lifetimes and associated spectra (including work relating to Na^{22} and Co^{60} lifetimes).

The field of study of positron electron systems was one with many subjects requiring investigation, both two and three quantum-wise. These investigations were all fundamentally suited to the scintillation method with its high γ-ray efficiency, its ability to distinguish energies, and its very fast response time.

Annihilation/

Annihilation of positrons can occur by one, two or three quanta. One quantum emission implies a momentum contribution from another particle. The predicted effect was small (cf. Jaeger and Hulme (1936)); cf. too Meric (1949).

The two quantum process of annihilation was formulated by Dirac (1930) before the discovery of the positron by Anderson (1932), and Blackett and Ochialini (1933). It has been estimated to occur partly in flight and mostly at rest. With positrons of Kinetic energy $\frac{1}{2}$mev. less than 3% of the annihilations should occur in flight. The expectations for annihilation in flight have been confirmed recently by Colgate and Gilbert (1953) and by Kendall and Deutsch (1953); this process will, essentially, not be discussed in ch. 2.

The two quantum process at rest has been confirmed in several ways (cf. the γ-ray measurements of Du Mond, Lind, and Watson (1949), and the angular correlation experiments of Beringer and Montgomery (1942). If N denote the number of atoms per unit volume, $r_0 = e^2/mc^2$, the lifetime against annihilation has been assessed on the above theoretical formulation at τ where

$$\tau = \frac{1}{NZ\pi r_0^2 c} \qquad (10)$$

if all the electrons be assumed available, e.g., for lead τ would be $\sim 6 \times 10^{-11}$sec. The work of Deutsch (1951) had shown that the annihilation time in gases was not always inversely proportional to pressure. The proportionality existed for oxygen, but not for freon, in the latter the annihilation time had been shown to be approximately 1.4×10^{-7}sec. at various lower pressures. The two quantum/

quantum process of annihilation of slowly moving positrons and electrons requires the system to be in a singlet state, spin 0, (cf. Wheeler 1946, cf. also Ch. 2 where a deduction is given on the basis of the Dirac equation).

Ore and Powell (1949) showed theoretically that three quantum annihilation can occur from the triplet state of spin 1, and they showed that the process was 1110 times less likely than annihilation from a singlet state. If therefore annihilation occurred by collision between free positrons and electrons the two quantum process would occur 370 times as often as the three quantum process. The factor of 3 entered because of the higher statistical probability of forming a triplet state. The lifetime of the bound singlet state had been given by Wheeler as 1.25×10^{-10} sec. The lifetime of a bound triplet state would be 1.4×10^{-7} sec. when once formed. It seemed therefore that the freon lifetime coincided with that of triplet postronium. Deutsch and Dulit (1951) showed the presence of annihilation radiation below 510 KeV using freon, and de Benedetti and Siegel (1952) had obtained three quantum coincidences from positrons decaying in freon. It seemed desirable to select out the delayed radiation associated with the long period (1.4×10^{-7} secs.) using delayed coincidence scintillation technique and to compare the spectrum with that theoretically predicted by Ore and Powell. It seemed of value to determine that in oxygen also, in view of its different pressure behaviour, for comparison. These experiments are described in Ch. 2 (cf. too Lewis and Ferguson (1953)).

The/

The lifetime at higher pressure in freon was of interest, together with a comparison of the decay time in oxygen with the theory of free collision annihilation. A search was also made for the fast decay in freon at a later date with the same unit. The search for a fast decay in gases could have important bearings on the annihilation process. The fraction of triplet state was also determined directly by this method (Ch.2, § 3, (vi)).

Work of an analogous nature, and on an extended scale needed to be carried out for condensed materials, liquids and solids. In an abstract De Benedetti and Richings (1951) indicated that the lifetime difference between metallic potassium and lead was less than 10^{-9} sec. In Ch. 2, § 4 (cf. Ferguson and Lewis (1953)) various relative measurements of lifetime are referred to, and an account is given of absolute annihilation time measurements of positrons in aluminium and involving work on Na^{22} and Co^{60}. A discussion is given of a second period in solids. Suggestions for operating high speed coincidence units with any type of radiations, particularly γ-radiations, materialised. In the meanwhile, further publications have appeared relating to condensed materials by De Benedetti and Richings (1952), also by Bell and Graham (1952), (1953).

§4 NUCLEAR SPINS AND THE ANGULAR CORRELATION OF SUCCESSIVE γ-RAYS

(1) The nature of the relationship.

Strong angular correlations have been referred to in §3 concerning the simultaneous quanta produced in annihilation processes. The suggestion that angular correlations can occur between/

between successive γ-rays in nuclear emission was made by Dunworth (1940). Calculations were made by Hamilton (1940). The high efficiency of scintillators is of great value in this application, and the method was successfully demonstrated by Brady and Deutsch (1947, 1948)a,b) for Co^{60}.

The spatial distribution of a single γ-emission of given multipole order (cf. §2 ii) is related to the angular momentum of the wave and so to the spin change of the nucleus concerned. If a nucleus be initially orientated at random, and a γ-ray be detected in a certain direction the spin of the nucleus is related, in a sense aligned, to this direction, and a subsequent γ-ray emitted of given multipole order will have its spatial characteristics, to some extent, predetermined. Conversely the angular correlation leads to spin assignments for the nuclei. The work can be generalised to include the case of cascade γ-emission following particle capture.

The method is of particular value for determining the spins of short lived states, which cannot be determined spectroscopically. Corroborative evidence may sometimes be obtained by the methods indicated in §2. The use of polarisers enables a distinction to be made between magnetic and electric transitions. Moreover if mixed transitions be suspected the angular correlation method can be a sensitive method of assessing the components.

The nature of the correlation relationships will be referred to in some detail below and in the main text; particularly the case/

case of γ -γ intensity correlations from a radioactive nucleus (double γ cascade); and the case of γ -γ intensity correlations from a nucleus formed by particle capture (triple cascades).

A single instance of angular relationships can first be given to exemplify the method which will be followed, involving a nucleus of initial spin $j_o = o$. If a spinless particle travelling along the z direction, with orbital momentum l_o be captured by the nucleus only states having z resolutes of momentum defined by $m_1 = o$ would be formed. If instead a γ quantum (of intrinsic spin 1) of multipole order l_o had been emitted along the z direction, only states $m_1 = 1$ would have occurred. Taking $l_o = 1$, so that the spin produced either way is $j_1 = 1$, one may suppose subsequent γ-emission in both cases to a state $j_2 = o$. The emission probability at angle θ to the z-axis would then be $\sin^2\theta$ (classical dipole along $\vec{z}$), for the spinless particle case; and $(1 + \cos^2\theta)$, (classical dipoles along $\vec{x}$ & $\vec{y}$), for the γ quantum case. (The particle case is generally referred to as an angular distribution process).

The explicit value of the population density of the first intermediate state (cf. $j_1 m_1$, above) will be shown of importance in all cascades. For triple cascade processes the determination of the generally unequal population densities is a first stage only, attention having to be paid subsequently to coherency factors. Detailed consideration of triple cascade processes is left to ch. 3. For double γ-cascades the formation and emptying of the intermediate states are reciprocal processes and this aspect will/

will be stressed in the treatment given below (cf.eqn.(12c))

Consider the population density of the first intermediate state reached, either by photon emission or by particle capture, from an unorientated nucleus (jomo) with mo randomly distributed.

For photon emission, of multipole order l_o, along the axis of quantisation, the relative population of the first intermediate state $(j_1 m_1)$ is given immediately by χ'_{m_1} where

$$\chi'_{m_1} = (j_o\, l_o\, m_1 - 1,\ 1 \,|\, j_1 m_1)^2 + (j_o\, l_o\, m_1 + 1,\ -1 \,|\, j_1 m_1)^2 \qquad \text{(11a)}$$

where m_1 has been determined at mo +1, and mo - 1, in the two Clebsch Gordon coefficients (cf., too, Condon and Shortley (1951) p.73).

For the capture of a particle, of any intrinsic spin s, incident along the axis z of quantisation, upon the unorientated nucleus (jomo) the channel spin S is defined as the vector sum of jo and s. The quantum numbers $sjoSS_z$ represent effectively the intrinsic spin properties of the particles, and the substates (S, S_z) are randomly distributed. (S_z is the z-resolute of the channel spin S.) If all the channel spins S were equally available the population density of the first intermediate states $(j_1 m_1)$, allowing for the additional orbital momentum of the particle (l_o), would be therefore,

$$\Sigma_S (S\, l_o\, S_z\, 0 / j_1 m_1)^2 \quad \text{where } S_z = m_1.$$

If $\alpha(S)$ however denote the relative probability of the spin S in the reaction process, the population density of $(j_1 m_1)$ will be χ''_{m_1}, where

$$\chi''_{m_1} = \Sigma_S\ \alpha(S).\ (S\, l_o\, m_1\, 0 / j_1 m_1)^2 \qquad \text{(11b)}$$

(cf. too Devons and Hine (1949)

Double cascade processes involving at least one γ -ray are now considered./

considered. Reference may be made in this connection, too, to Biedenharn, Arfken and Rose (1951), also Falkoff and Uhlenbeck (1950); Hamilton (1940) derived the formula of type (12b) for γ - γ cascades utilising theorems of random phase. Suppose γ -emission along the z direction (or capture of a particle travelling in the z direction), to occur, followed by photon emission of multipole order l_1. The probability of appearance of this second emission in a given solid angle at (θ, φ) can be written P, where

$$P = \sum_{m m_2 p} \left| \sum_{m_1} (j_0 m | H_0 | j_1 m_1)(j_1 m_1 | H(\vec{A}) | j_2 m_2) \right|^2 \quad (12a)$$

Here m stands for mo in the photon case, (or m stands for S_z, S in the particle case, cf. 11b), Ho and $H(\vec{A})$ specify the appropriate interaction operators in the two successive processes. $\sum$ refers to summation over the initial and final magnetic quantum numbers (m and m_2) and over the polarisations p of the γ-rays involved (one or two as the case may be), e.g. circular polarisations.

It might appear from inspection of (12a) that the summation over m_1 involves cross terms (coherency). However, by the special choice of the axis of quantisation above, m_1 is uniquely specified by m (or conversely m is specified by m_1) (cf. derivation of (11a) and (11b) above), and (12a) becomes immediately:

$$P = \sum_{m_1, m_2, p, (\text{and } S \text{ for particle case})} |(j_0 m | H_0 | j_1 m_1)|^2 \cdot |(j_1 m_1 | H(\vec{A}) | j_2 m_2)|^2 \quad (12b)$$

Here m_1 has replaced m under the symbol $\sum$ in the photon case; (or similarly m_1 and S have replaced m under the symbol $\sum$ in the particle case).

The first term yields the population density χ_{m_1} (i.e. either

m_1/

$\chi_{m_1'}$ or $\chi_{m_1''}$). The second term on summing over the relevant polarisation variables involves the probability of multipole order radiation intensity $F\ell_1^{m_1-m_2}(\theta)$ (cf. §2 (ii)). Consequently (12b) can be written immediately as:

$$P = \sum_{m_1 m_2} \left[\chi_{m_1} \cdot (j_1 m_1 \ell_1 m_2 - m_1 \mid j_2 m_2)^2 \cdot F_{\ell_1}^{m_1-m_2}(\theta) \right] \quad (12c)$$

and P is a function of θ only.

The use of multipole order radiation theory here makes clear the fundamental basis of the correlation method.

Considering only γ - γ cascades (cf. e.g., Biedenharn and Rose, (1953)) $P(\theta)$ has been shown a polynominal in $\cos^2\theta$. The highest power of $(\cos^2\theta)$ does not exceed either of the two multipole orders (ℓ_0, ℓ_1) nor does it exceed the angular momentum number j_1 of the intermediate state.

The expression for triple cascade processes will imply a generalisation of (12a) and will involve cross terms (coherency) usually. This will be referred to again in ch.3.

(ii) Experimental Work.

The first experiments carried out on angular correlations utilised Geiger counters (Kikuchi, Watase, and Itoh (1942), Beringer (1943), and Good (1948). For Na^{24}, Br^{82}, Y^{88} and Co^{60} little evidence of anisotropy was found. Assuming the lifetime to be sufficiently short to avoid reorientation between successive emissions some anisotropy would have been expected for these even even nuclei. For these and other reasons Brady and Deutsch (1947, 1948) investigated several sources including Na^{24}, Co^{60} and Y^{88} using/

using scintillation counters. For Co^{60} and Na^{24} an anisotropy $f(\theta)$ consistent with:-

$$f(\theta) = \frac{1}{8}\cos^2\theta + \frac{1}{24}\cos^4\theta$$

was found, suggesting a 0 - Q- 2 - Q - 4 transition. The anisotropy for Yb^{88} was less. The increased efficiency and shorter resolving time of these experiments using naphthalene as scintillator permitted a counting rate roughly 100 times greater than that of the gas counter experiments which they superseded. The experiments were extended by Metzger and Deutsch (1950) so that the polarisation was also examined and the parity changes determined.

γ -ray angular distribution experiments were carried out by Devons and Hine (1949) and by Jacobs, Malmberg and Wahl (1948) using gas counters. Initial γ-ray angular distribution studies of preliminary type using a scintillation counter were reported on by Kern, Moak, Good and Robinson (1951) for the case of proton capture by B^{11}.

The work described in Ch. 3 started with a check experiment on the angular correlation of Co^{60} γ-rays. As no work at all had been done on γ-γ -ray angular correlation involving particle reactions, and as this work was complementary to angular distribution measurements, it was decided to investigate the angular correlation between the two cascading γ-rays emitted by the proton capture process of B^{11}, leading to the even even nucleus C_{12}, and this work is described, in ch.3 (cf. too, Lewis (1952)a). Work involving/

involving $\gamma - \gamma$ ray angular correlation in a different plane was published independently by Hubbard, Nelson, and Jacobs (1952).

It should be mentioned that while it has been found convenient to refer this work done here on angular correlations to Chapter 3, it was actually carried out before the main work of Chapter 2; it in fact preceded the study of Rb^{87}.

In conclusion mention should be made of the effects of environment in correlation work. The environment can under certain circumstances affect the initial orientation as well as the reorientation. Moreover if the initial orientation is sufficiently pronounced an angular relation should be obtained for only one γ -ray relative to some determining axis. The effect of environment in $\gamma - \gamma$ angular correlations was demonstrated by Aeppli, Bishop, Frauenfelder, Walter and Zuntli (1951) for Cd^{111} produced from In^{111}, where the lifetime of the intermediate state was long, about 10^{-7}sec. The anisotropy varied between 0 and 16% for various source environments., Orientation of the initial state has been observed by Daniels, Grace and Robinson (1951), (cf. too Bleaney (1951)); other methods of orientation have been proposed.

CHAPTER 1

γ-RAY MEASUREMENT AND SPECTROSCOPY

CHAPTER I.

GAMMA RAY MEASUREMENT AND SPECTROSCOPY.

§ 1 EARLY PRELIMINARY WORK.

(i) Phosphor Comparison Tests.

The first experiments carried out were intended to examine the general characteristics of the scintillation method, within the limits imposed at that time. Zinc sulphide, anthracene, naphthalene and activated sodium iodide had been reported on in the literature (cf. introduction). Rough tests were therefore carried out on some common fluorescent and transparent materials to determine their response to radiations, in particular to the α-rays of polonium, the β-(and γ) rays of a radon seed (effectively the radiations of RaD and RaE), and γ radiations, including those of Co^{60}. An E.M.I. side window multiplier type 4140 was primarily employed.

The advantage of anthracene over naphthalene was first confirmed, and the α response of these seemed to be low compared with the β-response. The superiority of anthracene over naphthalene was shown to continue when a 1 P28 multiplier matching the emission bands of naphthalene was employed, in fact by a factor of about 3. It is interesting to note that the response of anthracene exceeds that of a $\sim 2\frac{1}{2}\%$ mixture of anthracene in naphthalene, also by a factor of 3. Among the substances investigated were fluorspar and solutions of anthracene in benzene. The peak response of fluorspar to β,γ rays was inferior to that of anthracene./

anthracene. Weak scintillations only were obtained from the solutions.

Very weak effects were produced in various glasses and other transparent materials. This latter can arise in several ways; for electrons some of it is due to Cerenkov radiation (Cerenkov 1934).

(ii) Crystallisation.

Following this, methods of purifying and crystallising anthracene were examined by the author and crystals of approximate size 1 cm. diameter x $\frac{1}{2}$ cm. thick were prepared from a small amount of melt. The presence of an inert gas was found necessary. The material was placed in a small tube, suspended in a glass pot containing the inert gas kept at or near atmospheric pressure by means of a reservoir. The pot was immersed in a bowl of liquid paraffin, electrically heated. Slow crystallisation of the melt could be arranged by keeping the bath appropriately heated, in view of the insulating properties of the gas surrounding the melt.

Subsequently, when the need arose, naphthalene crystals were also prepared, and these were relatively easy to make. Blocks $\sim$ 1" cube could be obtained by permitting the melt to cool slowly in a pot immersed in a large bath of water. Later large crystals $\sim$ 2" cube were prepared by very slow surface cooling of the melt, the water bath being kept almost at the melting point.

Crystals of sodium iodide, thallium activated, were prepared by a different method. The materials were placed in a capsule tapered at the one end, (to initiate crystal growth later), and sealed up near the melting point after extracting the air. The capsule/

capsule was then allowed to fall slowly through a vertical temperature gradient, first permitting melting, and subsequently, slow cooling.

(iii) Phosphor Efficiency.

It seemed worth while investigating roughly the absolute efficiency of anthracene, to determine approximately how great the energy wastage was. One of the crystals made above was irradiated by fluorescent X-rays of copper ($\sim$ 8Kev.), obtained from X-ray photoelectric absorption in a copper foil. This fluorescent radiation would yield photoelectrons and Compton electrons in the anthracene. The approximate maximum pulse height obtained was compared with that developed by single photons which were allowed to leak in (which would liberate single electrons from the cathode). Lead glass was used to shield the photocathode from direct X-radiation, since the X-rays otherwise produced an appreciable direct effect on the multiplier. A signal to noise ratio of about 8/1 on the cathode ray tube display was achieved, i.e., about 1 Kev of energy per photoelectron. Adopting the maker's specification for the μa /lumen sensitivity of the E.M.I. multiplier type 5060 used, the observations corresponded to about 60 evof energy/photon and an anthracene efficiency near 5%. Because of the now known non linear response it should be somewhat greater at higher energies (cf. Hopkins 1951). It is of interest to note that recent work by Furst, Kallman and Kramer (1953) using integral methods lead to an efficiency of 10% though peak methods listed there have given results in the region of ($\frac{1}{4}$ - 4)%; reference/

reference too should be made to the results of Birks and Szendrei (1953). Experiments of Jackson and Harrison (1953) indicate there is at least some small loss of energy by long term phosphorescence which would not register in peak methods of measurement.

(iv) Tube Noise.

Early investigations on the response of a crystal to γ-rays showed substantial contributions to the pulse height distributions at lower energies where tube noise effects were present. With the E.M.I. tubes operating at $\sim$ 120 Volt/stage, the noise fell about 5 times for a 40°C. fall in temperature from room temperature (cf. too Engstrom 1952). To reduce regenerative effects at higher voltages the cathode and containing can are run at earth potential. In working near the noise level care has to be taken to avoid satellite pulses from the tube or phosphor (cf. e.g., § 5).

§ 2 γ -RAY ABSORPTION AND MEASUREMENT.

Attention was initially focussed on the Compton energy region for organic scintillators, ($\sim$ 100Kev to $\sim$ 2 Mev), where unambiguous specification of γ -ray energy could be hoped for. The form of the Compton response to be expected is discussed below.

In the Compton process the probability $d\varphi$, of obtaining a quantum of energy K scattered between angles θ and ($\theta + d\theta$) to the direction of incidence of the initial radiation Ko is given by the Klein Nishina formula:-

$$d\varphi = \pi r_0^2 \frac{K^2}{K_0^2} \left(\frac{K_0}{K} + \frac{K}{K_0} - \sin^2\theta \right) \sin\theta \, d\theta \qquad (13a)$$

(cf. Heitler (1947)p(154)eqn.(51))

In/

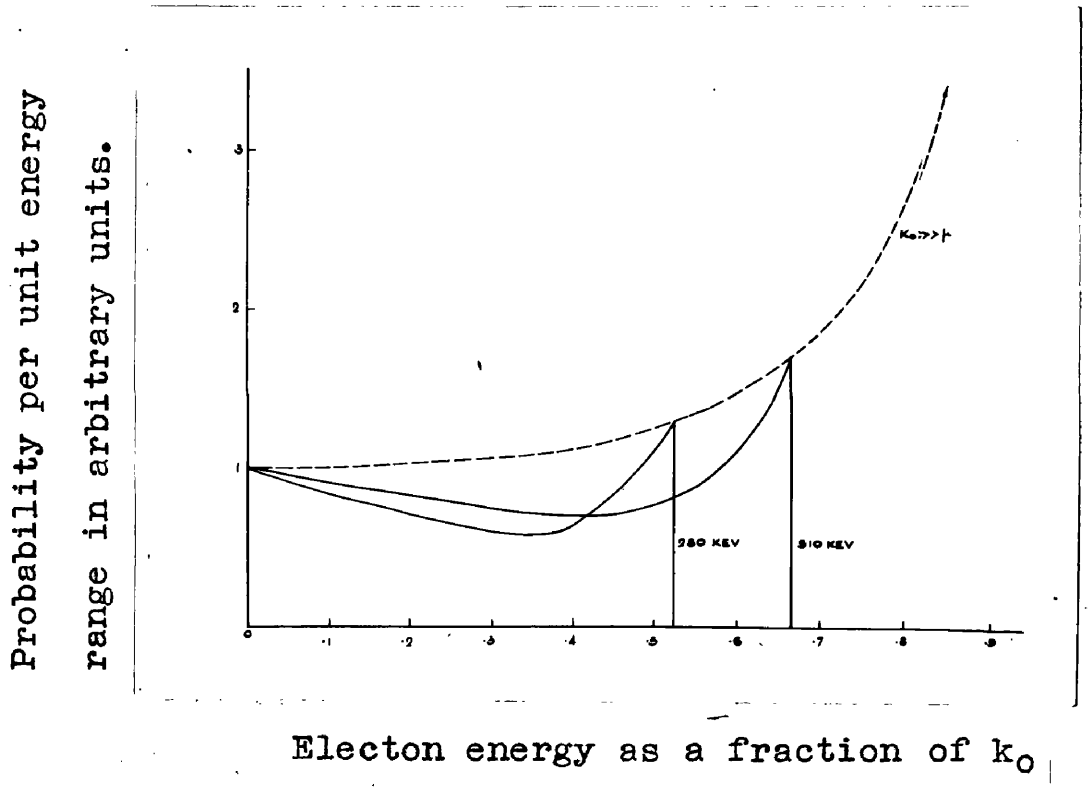

Fig.3. Expected electron energy distribution due to Compton effect, for γ-ray energies k_0 of 280 kev., 510 kev., and for large energies.

In view of the momentum relation;

$$K = \frac{K_0 \mu}{\mu + K_0(1-\cos\theta)} \qquad (13b)$$

where μ is the electron rest mass,

$$\frac{dK}{d\theta} = \frac{-\mu K_0^2 \sin\theta}{[\mu + K_0(1-\cos\theta)]^2} = -\frac{K^2}{\mu}\sin\theta \qquad (13c)$$

The distribution of electron energy $E = (K_0 - K)$, for a fixed Ko will be essentially given them by:-

$$-\frac{d\varphi}{dK} = \frac{\pi r_0^2 \mu}{K_0^2}\left(\frac{K_0}{K} + \frac{K}{K_0} - \sin^2\theta\right) = \pi r_0^2 \frac{\mu}{K_0^2}\left[\frac{K_0}{K} + \frac{K}{K_0} + \left(\frac{\mu}{K_0} - \frac{\mu}{K}\right)^2 + 2\left(\frac{\mu}{K_0} - \frac{\mu}{K}\right)\right] \qquad (13d)$$

For very large Ko ($K_0 \gg \mu$), the ratio Ko/K is large for the back scattered quanta of energy $\sim \mu/2$ and the distribution peaks very sharply for electron energies close to the maximum energy $(K_0 - \mu/2)$.

The distribution for $K_0 \gg \mu$ is illustrated by the dotted curve of fig. 3, as a function of E/Ko, in the energy region below the Compton edge (which is not shown) at E/Ko close to 1. The distributions for γ -ray energies of 510 Kev and 280 Kev are shown for comparison (cf. too Hofstadter and McIntyre (1950)b).

It should be noted in passing, using equation (13c), the scattered quantum energy K is only a slowly varying function of θ, for backward scattered quanta having θ close to 180°. The electron energy liberated in the crystal associated with backward scattered quanta is therefore relatively homogeneous. This is made use of in the two crystal method described below.

Early investigations were often made using discriminator bias curves. With the early tubes and crystals the discriminator curves here and elsewhere continued to rise sharply at the lower energy end. At this stage the two crystal method was tried out. One crystal/

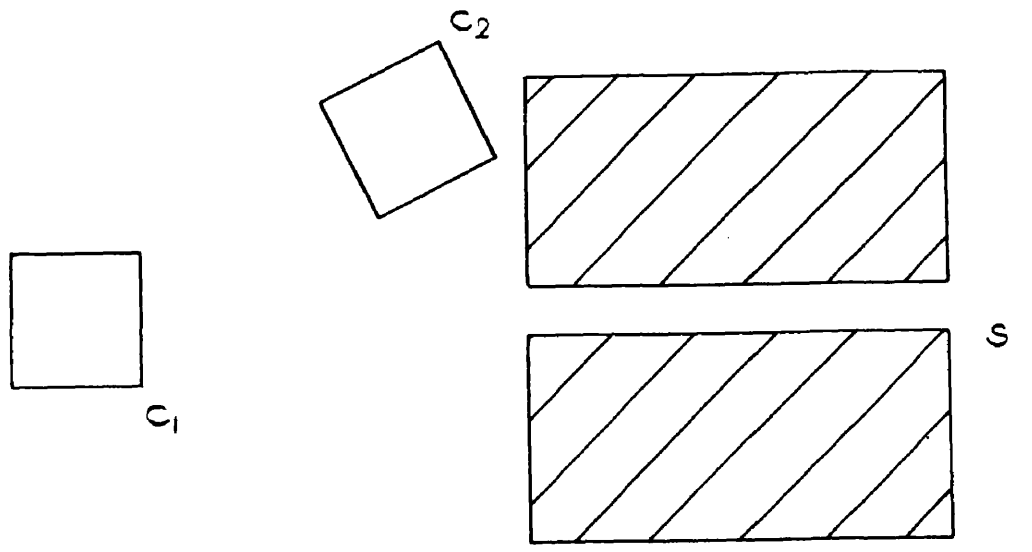

Fig.4.Two crystal method of determining γ-ray energy.

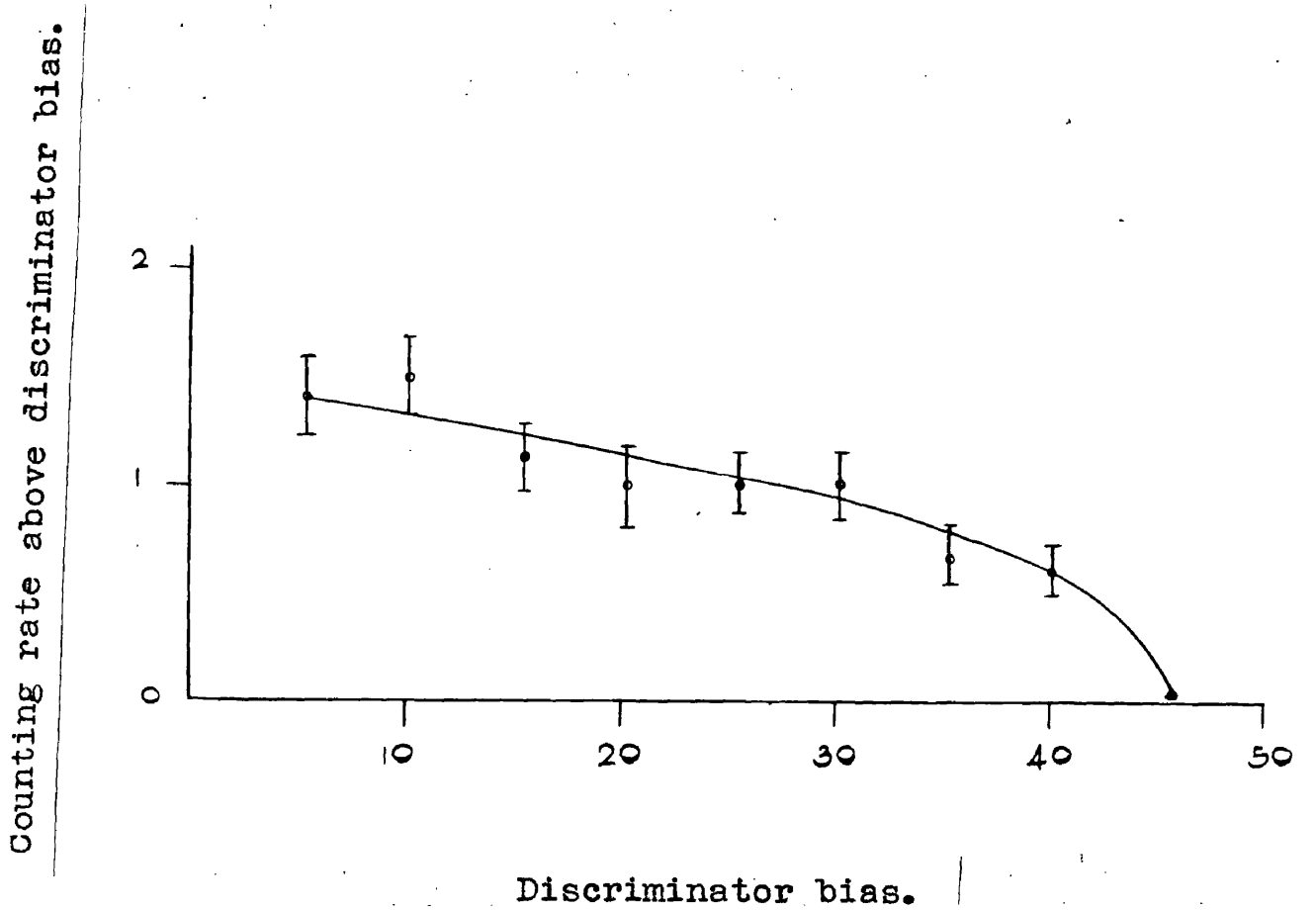

Fig.5. Preliminary discriminator curve for Co^{60} γ-rays using two crystal method.

crystal was irradiated by collimated γ-rays as shown in fig. 4 and was used to determine the electron energy (ko-k). The other crystal, in coincidence with it, was screened from direct radiation and picked up back scattered radiation. Only the electrons of highest energies, in the immediate neighbourhood of the Compton edge in the first crystal could therefore contribute to the firing of the coincidence unit. The first crystal (C_1) was a small cube of naphthalene, and the second (C_2) was a conglomerate of thallium activated sodium iodide crystals. The two multipliers were the side window tube. E.M.I. type 4140, and the 1 cm. cathode E.M.I. tube type 5060 (the only tubes available then). The outputs from the two counters led after amplification to two discriminators, which could activate a coincidence unit. The amplifier systems were designed to maintain a fast response, output leads being kept short, so that the discriminators could fire together. The coincidence unit had a resolving time of $\sim 1\ \mu$sec. The counter C_2 had to be well screened to cut down random counts. The discriminator associated with the crystal C_2 was placed at a fixed setting. The bias on the other discriminator was varied and the coincidence counts were determined as a function of discriminator bias.

A plot of these very preliminary results is shown in fig. 5, when a source of Co^{60} was employed. The discriminator curve shows a partial plateau as expected, but no real sign of two plateaux. It was realised that the use of a variable discriminator was not very satisfactory and that the optical arrangements were not good. Nevertheless/

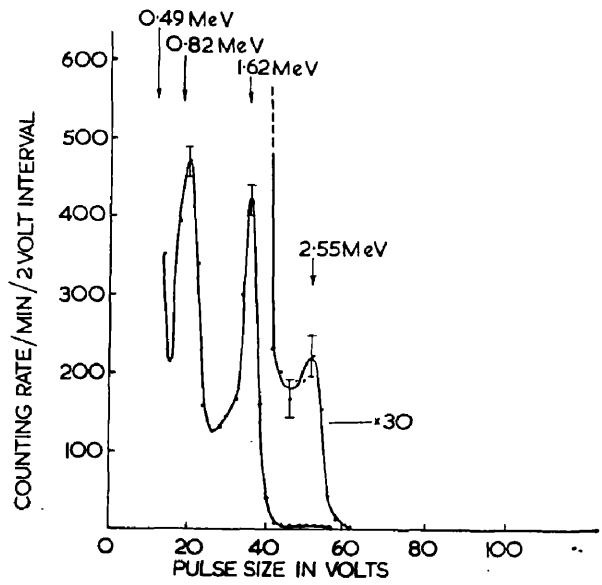

Fig.6 Electron energy distribution in the scatterer ,in the two crystal method,for La^{140}.

Nevertheless the considerably improved response over that obtained using only a single crystal at this time served to emphasize the advantage of the two crystal method from an energy resolution viewpoint. Steps were therefore taken to secure an improved experimental arrangement, incorporating kicksorter technique. Additional tube performance and selection tests, e.g., using line β sources were also probed. Whilst this later work was proceeding, Hofstadter and McIntyre (1950)a established conclusively the two crystal method and its merits. The method was later used here for investigations on the γ-rays of La^{140}, and a curve utilising the method is indicated in fig. 6 (cf. Bannerman, Lewis, and Curran (1951) and preface). It permits intensity assignments to be made of the γ-rays associated with the individual peaks. The direct observation of the weak high energy γ-ray measured to be 2.55 Mev $\pm$ 2% was of particular interest. It had been previously measured by the photodisintegration of deuterium (Wattenberg (1947), Hanson (1949). Bishop, Wilson and Halban (1950)). Further reference to the γ-ray spectrum of La^{140} and its decay scheme is deferred until later.

The two crystal method, whilst allowing an assessment of relative intensity as well as an assignment of energy, suffers from solid angle restrictions. Some improvement can be effected by making the second crystal ring shaped about the incident direction.

For comparison purposes the single crystal Compton effect is demonstrated/

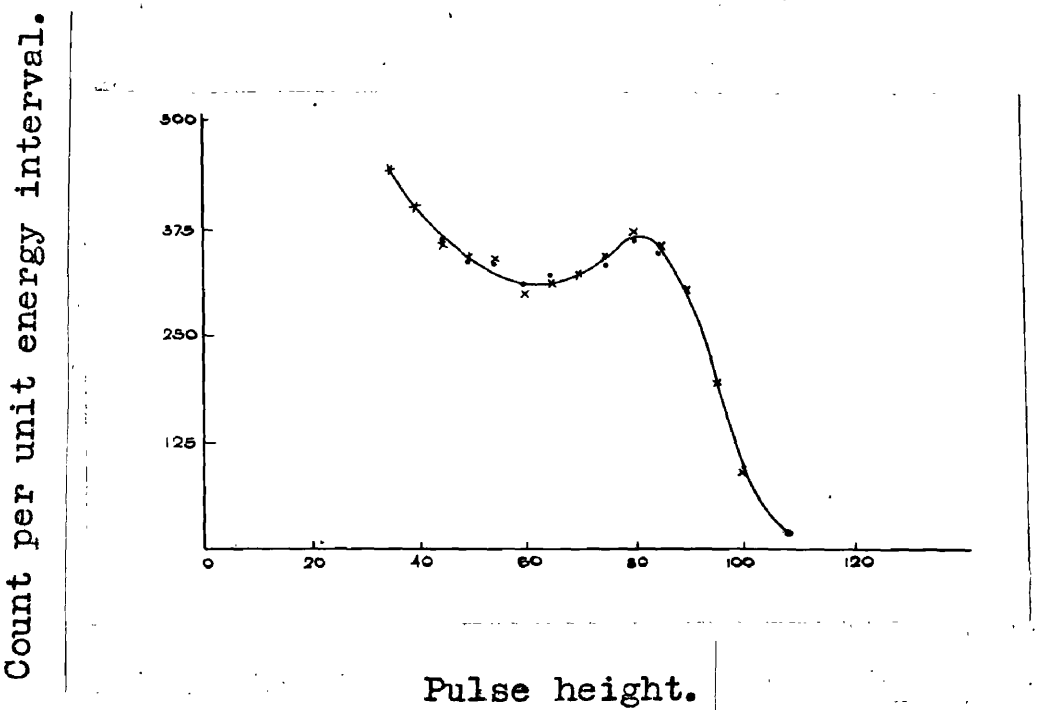

Fig. 7. Response of 1 cm^3 crystal of anthacene to the 280 kev. γ-ray of Hg^{203}.

demonstrated experimentally by the more recent fig. 7, for the 280 Kev γ-rays of H_g^{203} in 1 cm.^{3} anthracene. The Xradiation though not screened off is of little effect in the region shown. The high energy part of the spectrum accords approximately with theory, allowing for the finite resolution. The low energy part rises partly because of back scattering from the multiplier glass work. Fig 36 is another instance of the single crystal Compton effect

The development of single crystal technique has been throughout a dominant problem, as all scintillation work is ultimately dependent upon the response of a single crystal. Items often appearing maybe relatively trivial in retrospect enabled considerable advance to be made. Reference can be made to two aspects. The first refers to discolourations in crystals, actually surface discolourations which hindered progress, the introduction in connection with this work here of the simpler organic solvents, and the development by others of the dry box methods, helped in this direction. The second was the suggestion by others of magnesium oxide as a scintillation reflector as a substitute for aluminium and other metallic reflectors. The commercial production of crystals and improvements in multipliers and the ability to select have played a vital part (cf. introduction).

As an example of the use of these techniques reference may be made to fig. 25 which shows the peak obtained from $\frac{1}{2}$ mev radiation, by the coincidence of the total photopeak and multiple Compton peak, in a composite block of sodium iodide effectively $1\frac{1}{4}$" cube.

Lastly it should be mentioned that in determinations of γ-ray and/

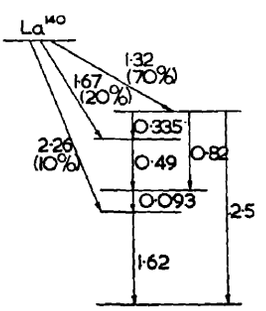

Decay scheme of La^{140}.

Fig. 8.

and related energies the linearity of the measuring apparatus has always been checked, and appropriate calibrations made. The photomultiplier output signal voltage was low. The work of Raffles and Robbins (1952) emphasizes the need for care in this direction with E.M.I. multipliers, especially with the faster organic phosphors.

§ 3 COINCIDENCE METHODS; THE γ-RAYS AND DECAY OF La^{140}

The efficiency and speed of scintillation counters render them of exceptional value in the study of coincidences. With the development of the technique, the γ-rays, as well as the particles, involved in the decay, become accessible to coincidence study from an energy viewpoint. In examining the coincidence methods available the decay of La^{140} was investigated further. The double crystal method (cf. fig. 6) had indicated the lines at 0.49, 0.82, 1.62 Mev to be the intense ones. The 2.55 Mev γ-ray and a 0.335 Mev γ-ray were equally weak. The decay scheme of La^{140}, put forward by Beach, Peacock and Wilkinson (1949) is illustrated in fig. 8, and was based essentially on magnetic spectrometer measurements. Previously β-γ and γ-γ coincidences had been reported without direct evidence of the γ-ray energies involved. (cf. Osborne and Peacock (1946); Mitchell, Langer, and Brown (1947); Mandeville and Scherb (1948)).

The suggestion was therefore made that γ-γ coincidences be observed, using anthracene in one of the two counters. Those of the anthracene pulses which feature in coincidences could be recorded/

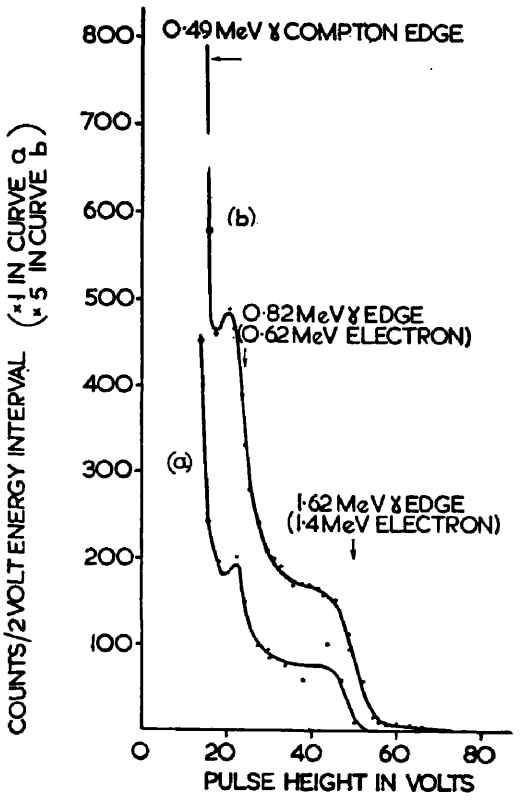

Fig. 9. Pulse height distributions in a small anthracene crystal due to absorption of La^{140} γ-rays; (a) with coincidence control, (b) without control.

recorded by a kicksorter. The use of anthracene would enable each γ-ray to be recognized by its Compton edge effect. Ambiguities which might arise using sodium iodide in this position would be avoided. If two γ-rays would be observed in the kicksorter display then these would be in cascade with one another. If three or more were to appear in the kicksorter display, further tests would have to be applied to determine their relationship. The simplest method then would require the introduction of an appropriate discriminator setting in the other channel.

Care must be taken to keep the random pulses low since the random coincidences will display the full normal pulse distribution of the anthracene crystal without coincidence control. Fig. 9 shows some of the results obtained by this method (with β particles screened off). The full pulse height distribution of the crystal, when all the γ-rays are allowed to record without coincidence control, is shown for comparison. (cf. Bannerman, Lewis and Curran (1951) and preface).

In this determination a pulse arriving at the anthracene counter was capable of being displayed on a cathode ray tube and a brightened spot appeared at a coincidence, the displacement of the spot vertically being a measure of the pulse height. The brightened spots could be photographed. Alternatively, a fixed photomultiplier (linked to a scaler) could be arranged to view (and scan) the brightened spots through a fixed horizontal slit; a variable known bias voltage being applied to the Y plates of the cathode/

cathode ray tube.

The 1.62, 0.82, 0.49 Mev γ-rays appear clearly in the coincidence curve. The relationship of the γ-rays could be made clear by subsequently discriminating in the other counter so that coincidences with the 1.62 Mev γ-ray were recorded.

With the availability of large blocks of sodium iodide at the present time giving single peaks in certain energy regions some of the advantages of anthracene have disappeared. Using two γ -ray counters with such blocks, the respective pulses could be exhibited as X and Y shifts and the display filmed. Furthermore a considerable amount of β-γ coincidence work could be done in similar manner, each γ -ray displaying its own β spectrum. For instance the precise shape of each of the three β rays of La^{140} could be determined individually without having to estimate the form of the components of the composite β curve.

In measuring spectra with very efficient crystals care has to be taken to keep the source sufficiently distant from it, otherwise cascading γ -rays, γ_1 and γ_2, say, will also give an addition peak ($\gamma_1 + \gamma_2$). Alternatively this property can be made use of in establishing the presence of cascade processes (cf. the integrating method Bannerman, Lewis and Curran 1951).

Evidence has been given (Bannerman, Lewis and Curran (1951)) that the .093 γ ray of fig. 8 is weak and therefore not a member of the main cascade (cf. too Pruett and Wilkinson (1953)). This is of interest too in view of the angular correlation experiments a little later by Robinson and Madansky (1951) on the 0.82 and 1.62 Mev/

Mev γ -rays. Assuming the two γ -rays to be directly in cascade they suggested a possible 4 -Q- 2 - Q- 0 sequence. Certain points finally regarding spin may be mentioned. The work of Beach, Peacock and Wilkinson (1949) indicated strong internal conversion of the 0.335 Mev γ-ray. This would suggest an $\ell = 2$, or higher transition; and the comparable intensities of the 0.335 and 0.82 Mev γ -rays, allowing for energy, would suggest similar spin changes for both these emissions. The absence of a ground state β decay and the high ft values for the β decays suggest the spin of La^{140} to be at least 2. The internal pair coefficient of the strong 1.62 Mev γ-ray would appear worth investigating from these viewpoints.

§ 4 THE DECAY OF Sm^{151} and Eu^{155}.

In the investigation of the disintegration processes of Sm^{151} and Eu^{155} (cf. Wilson and Lewis (1952)) a requirement arose for the study of — coincidences. Neutron capture by pure samarium results in the formation of the long lived β-emitters Sm^{151} (Inghram, Hayden, and Hess (1947,1950), Marinsky (1949) and Eu^{155} (produced by the decay of short lived Sm^{155}), (Hayden, Reynolds and Inghram 1949). The pure K-capture source Sm^{145} (Butement 1951) would also be produced, and small traces of β emitting Eu^{154}, (stable Eu^{153} is obtained from the short lived pile product Sm^{153}, and its neutron cross section is high).

The radiations of Sm^{151} and Eu^{155} seemed well suited to proportional/

proportional counter techniques and a study of the pile product from this aspect had been started (cf. preface). It had been hoped that one or other of these radioactive materials would be predominant, in a sample irradiated for 8 weeks at a thermal neutron flux of $3.5 \times 10^{10}/cm^2/sec$, but preliminary measurements had indicated they were present with relative intensities of 1:4. In view of the involved chemistry, a study was made without chemical separation.

(i) The radiations emitted.

The β -spectrum of Sm^{151} was known to have an end point of ~75 Kev (cf. Agnew (1950), Marinsky (1949)). The β spectra of Eu^{155} had end points of ~150 and ~250 Kev (cf. too Marinsky). The proportional counter work on the source (cf. Wilson and Lewis (1951)) confirmed the presence of these end points and the presence of a weak spectrum showing end points at 400 and 700 Kev associated with Eu^{154} (cf. Hayden, Reynolds and Inghram (1949)).

The γ -rays were of particular interest. Proportional counter studies indicated that γ -rays of 19.3 Kev. and 15.2 Kev. were emitted by the source (Wilson and Lewis (1951)). Scharff Goldhaber, der Mateosian, McKeown, and Sunyar (1950) had detected 21 Kev γ radiations from Sm^{151} as a fission product, and the 19.3 Kev γ -ray is presumably to be identified with this. Further Marinsky and others using a magnetic spectrometer found two γ -radiations with Eu^{155} of energies 85 and 99 Kev, and it is reasonable to relate the 15.2 Kev radiation to the difference, i.e., to assume the 85 and/

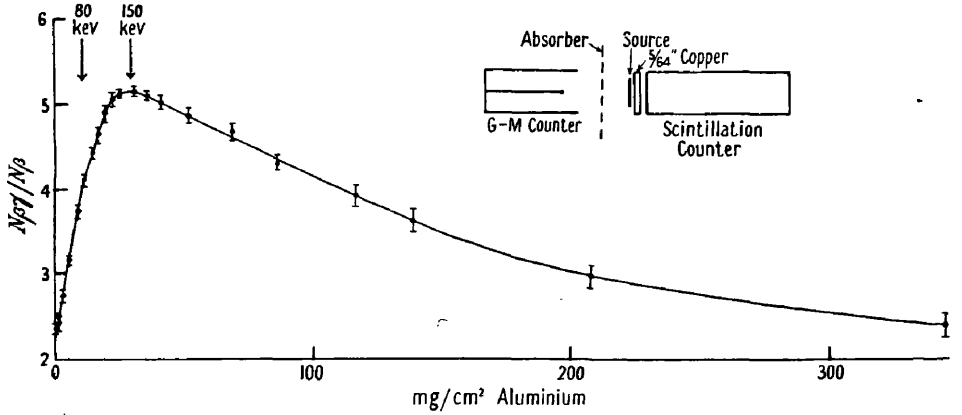

Fig.10. Ratio of number of β–γ coincidences to number of β-counts as a function of aluminium absorber thickness.

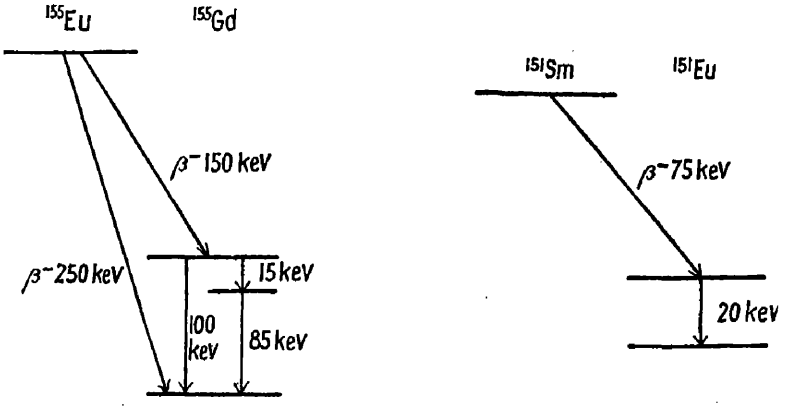

(a) Fig. 11. (b)

Fig.11. Possible decay schemes of Eu^{155} and Sm^{151}

and 15.2 Kev radiations are in cascade.

The presence of L & K X-radiations was also noted. The K-X-rays were associated with K capture in Sm^{145}, and internal conversion of the γrays of Eu^{155} (X-rays of Pm. and Gd. respectively).

(ii) Beta-gamma coincidences; and discussion.

Though nowadays this experiment would be carried out probably using two scintillation counters and Kicksorter techniques (cf. § 3, and Ch.2), for this source it was convenient to record coincidences, using absorption techniques on the β -side. A scintillation detector picking up the γ-radiation was shielded by 5/64" of copper to stop electrons and soft X rays. A thin window (1.7 mgm/cm^2) β -Geiger type counter was employed. The coincidence curve is shown in fig. 10, where β - γ coincidences per β -particle are plotted in terms of the aluminium thickness between the source and the β -counter.

The results of fig. 10 and the findings referred to in (i) above receive an interpretation in terms of the possible decay schemes shown in fig. 11. The initial steep rise can be associated with the elimination of the 75Kev β rays of Sm^{151}, since the 19.3 Kev γ -radiation would not be detected by the γ -counter. The subsequent slow rise to 150 Kev may be associated with the elimination of the β -rays of higher energy (~ 250Kev) which do not give β - γ coincidences. The elimination of coincidences with β -rays of 150 Kev is consistent with the schemes. The remaining part of the curve is associated/

associated with the Eu^{154} contamination referred to above.

Marinsky found no γ - γ coincidences for Eu^{155} and it is probable amongst other reasons that the 15 Kev quanta are highly converted. An attempt to investigate this issue by examining β -soft γ coincidences showed that β rays of energy higher than 75 Kev were in coincidence with K & L X-radiation. By admitting β -rays of all energy the number of β - γ coincidences per β remained almost constant (cf. Wilson and Lewis 1952) suggesting that the Sm^{151} particles are in coincidence with soft γ quanta or with X rays arising from their internal conversion.

Further work, using separated isotopes and or chemical separation was necessary at this stage.

In the meanwhile work on these rare earth isotopes continues to be reported (cf. Hollander, Perlman and Seaborg (1953)). Reference should be made in particular to the investigations involving enriched Sm isotopes by Lee and Katz (1954), also to the work of Rutledge, Cork and Burson (1952), apparently also with enriched isotopes. Additional weak γ -rays have been reported for Eu^{155} near 60 and 130 Kev.

§ 5. THE NATURAL RADIOACTIVITY OF Rb^{87}, AND SOME γ -RAY SCINTILLATION PROPERTIES OF THALLIUM ACTIVATED RUBIDIUM IODIDE

(cf. too Appendix).

Reasons for investigating the Rb^{87} decay by a scintillation method have been briefly referred to in the introduction. The mode/

mode of decay had been investigated in various ways and there has been uncertainty regarding the process of decay. The forbidden nature of the disintegration is of much importance in β decay theory, and the lifetime has geological interest. Lastly rubidium has chemical associations with the most efficient γ -ray phosphor.

In an investigation in 1941, Ollano reported several conversion peaks. Haxel, Houtermans and Kemmerich (1948) reported finding β -e coincidences. Proportional counter work by Curran, Dixon and Wilson (1951) found no evidence of conversion electrons. More recently McGregor and Wiedenbeck (1952) found no electron electron coincidences. In earlier measurements Libby and Lee (1939) found a β -ray end point energy of 130 Kev. More recently Bell, Cassidy and Davis (1950) stated it to be 270 Kev. Curran, Dixon and Wilson (1951) obtained a forbidden plot of end point energy 275 Kev. Many lifetime measurements have been made, recent values being near 6×10^{10} years. Charpak and Suzor (1951) have however alleged that the proportional counter figure obtained by Curran, Dixon and Wilson should be 7.6×10^{10} years and not 6.2×10^{10} years if further back scattering corrections be applied.

It seemed worth while investigating the scintillation properties of thallium activated rubidium iodide, and providing they were suitable, to investigate the mode of decay of Rb^{87} using 4π geometry and the integrating method (cf. § 3). Moreover the method would provide a means of studying the particle emission free from self absorption and back scattering errors at the low energy/

energy end, and could record it at the high energy end. Such a crystal could be adequately screened so that background effects would present no difficulty.

In this section of Ch. 1 an account will be given of the scintillation response of thallium activated rubidium iodide crystal to X, γ , and line electron radiations, and evidence will be presented for the absence of γ and conversion lines in the Rb^{87} decay process.

The properties of the β -spectrum, the lifetime determination and theoretical considerations relating to it are referred to briefly in the appendix (cf. too Lewis (1952)a).

(i) Crystal preparation and response.

The crystals were prepared in a manner similar to that used previously for making activated sodium iodide crystals. A few grams of rubidium iodide, activated with various percentages of thallium iodide, were placed in a quartz container, which was heated. The air was extracted near the melting point, and the container sealed. It was then allowed to drop slowly down the temperature gradient of the furnace mentioned earlier. In this manner several crystals of size approximately 3-4 mms. cube were made. The author acknowledges the help of the chief technician, Mr. J. T. Lloyd with this furnace work.

The crystals obtained were clear, and did not readily absorb moisture. Nevertheless in most of the experiments the crystal under test was coated with a small amount of paraffin. One such crystal was/

was mounted on an E.M.I. tube type VX5032, and a thin aluminium container a little larger than need be, from a containing aspect, enclosed the crystal. Lead blocks surrounded the system to a depth of two inches. The tube was run at moderately low voltages to keep the noise level low, and the amplified pulses observed. The pulses observed under γ-excitation were less than those of thallium activated sodium iodide by a factor of ~6. Whilst the rise time was better than about 1 μ sec., it was noticed at an early stage that a background of very small spurious, spasmodic pulses was also present. Bombarding the crystal directly with α-particles on a triggered cathode ray tube established conclusively the presence of a phosphorescence lasting in all the order of a millisecond. Varying the amount of activator from much below $\frac{1}{2}\%$ to 2% did not get rid of the phosphorescence effect. Crystals of activated rubidium iodide prepared from the carbonate using freshly prepared hydriodic acid did not remove it either. (The response of these latter crystals was somewhat lower, due probably to traces of free iodine in the hydriodic acid).

It was therefore arranged to suppress the spurious pulses by electronic paralysis methods. Normally the amplified pulses from the multiplier were recorded on a single channel cathode ray tube Kicksorter similar to that referred to previously (§ 3)through a gating unit normally triggered by the pulse itself, directly. This gating unit lengthened and brightened the trace so that a bright spot appeared on the cathode ray tube face. To suppress the spurious low/

γ-ray of RaD.

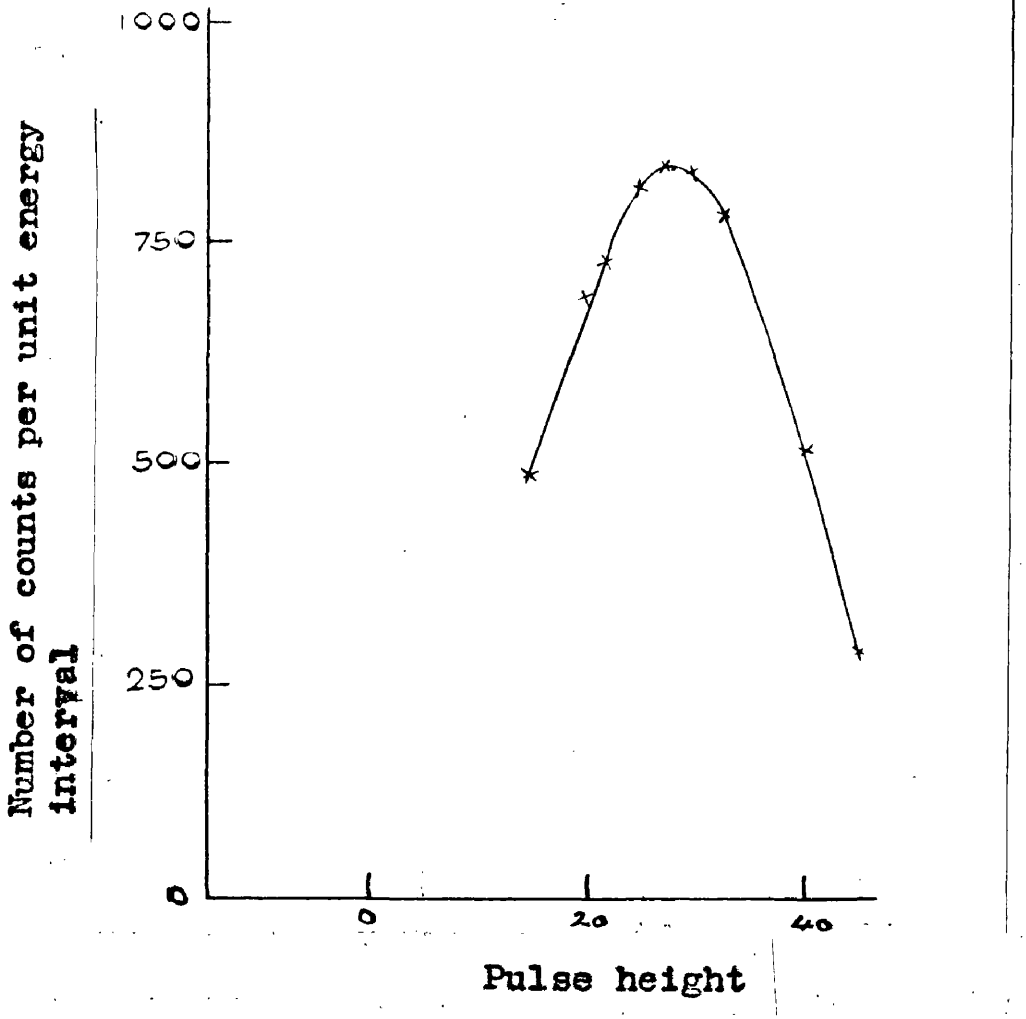

Fig. 13. Response of RbI(Tl) crystal to the 280 kev. γ-ray of Hg^{203}.

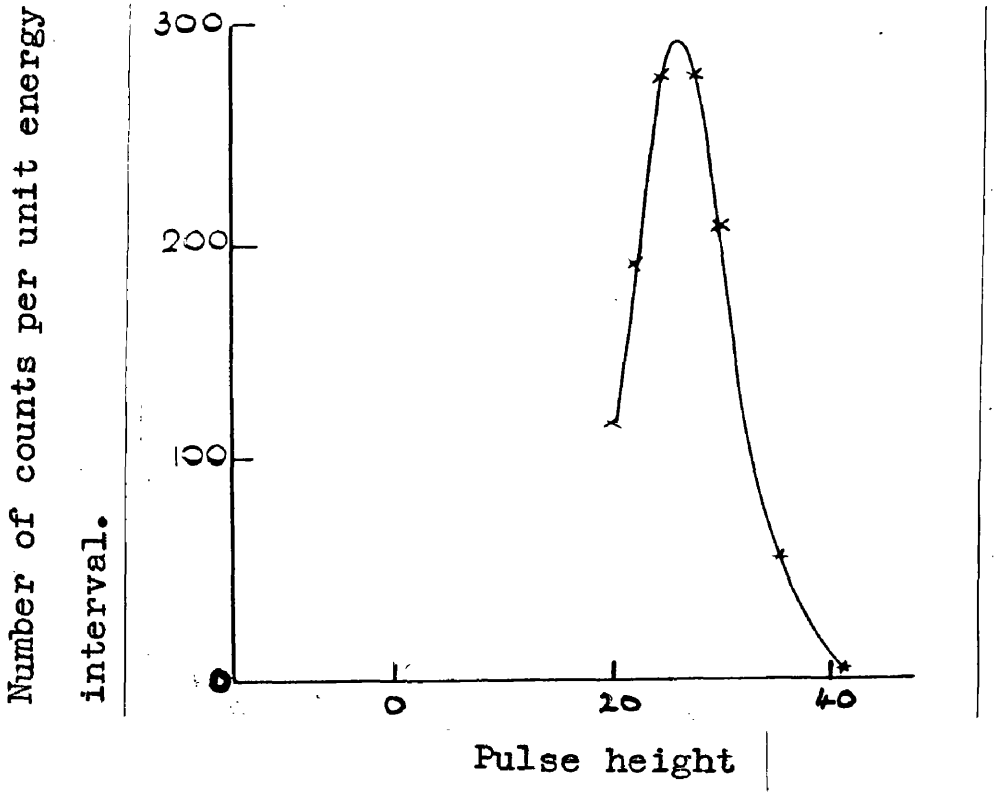

low energy pulses following the main pulse, a paralysis circuit driven by a discriminator was constructed and inserted before the gating unit. An alternative circuit used, incorporated paralysis in the gating unit itself, by altering the length of the pulse it delivered. At the lowest energies paralysis times of 1 - 3 milliseconds were employed. Tube noise became then the ultimate restriction.

Figs. 12 and 13 show two of several photoelectric peaks, obtained in the course of the work and shows the response to RaD (.467Kev) and Hg^{203} (280 Kev) γ-rays, using a crystal approximately 4 mms. x 4 mms. x $2\frac{1}{2}$ mms.

The half width at half height in the 280 Kev γ-ray case is near 15%. This width was roughly consistent with that obtained with activated sodium iodide under similar conditions, allowing for the greater peak response of the latter substance. (The width is essentially determined, within a factor of order unity, by the statistical fluctuations in the number of useful photoelectrons emitted by the photocathode per γ-ray (cf. Garlick and Wright (1952)).

Calibration was carried out on the crystal with various radiations, the Kα x rays of molybdenum filtered by zirconium (17.5 Kev), the fluorescent Kx rays of silver (~22Kev), In^{114} (Kx ~24 Kev, & conversion electrons), RaD (46.7 Kev γ ray), Hg^{203} (Kx 72Kev, γ-ray 280 Kev), Cs^{137} (conversion electrons). In the calibration work on conversion electrons, a 0.0005" aluminium reflector was used, (having somewhat poorer reflecting power), the/

Fig 14a. Response of RbI(Tl) to In^{114} & Cs^{137} conversion electrons, in turn, relative to that of the Hg^{203} γ-ray. (a 0.0005" aluminium reflector was used)

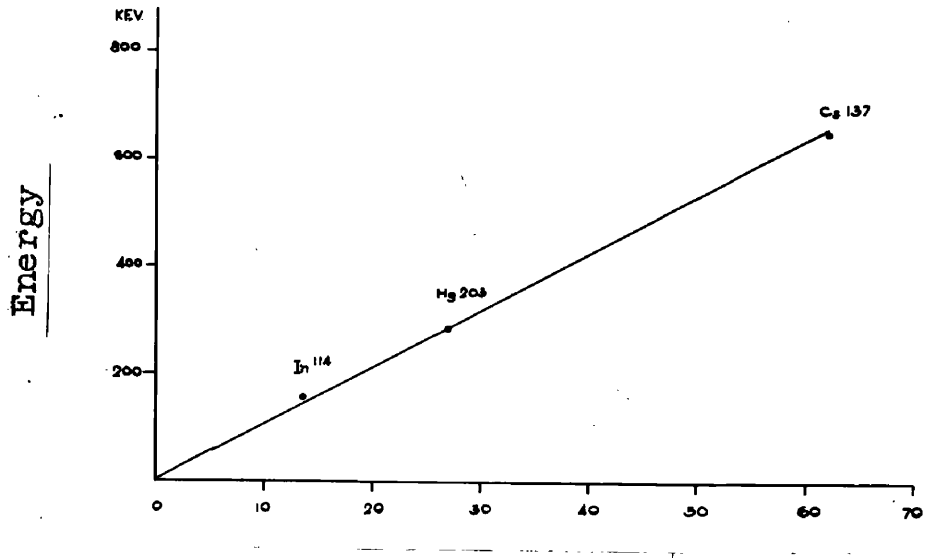

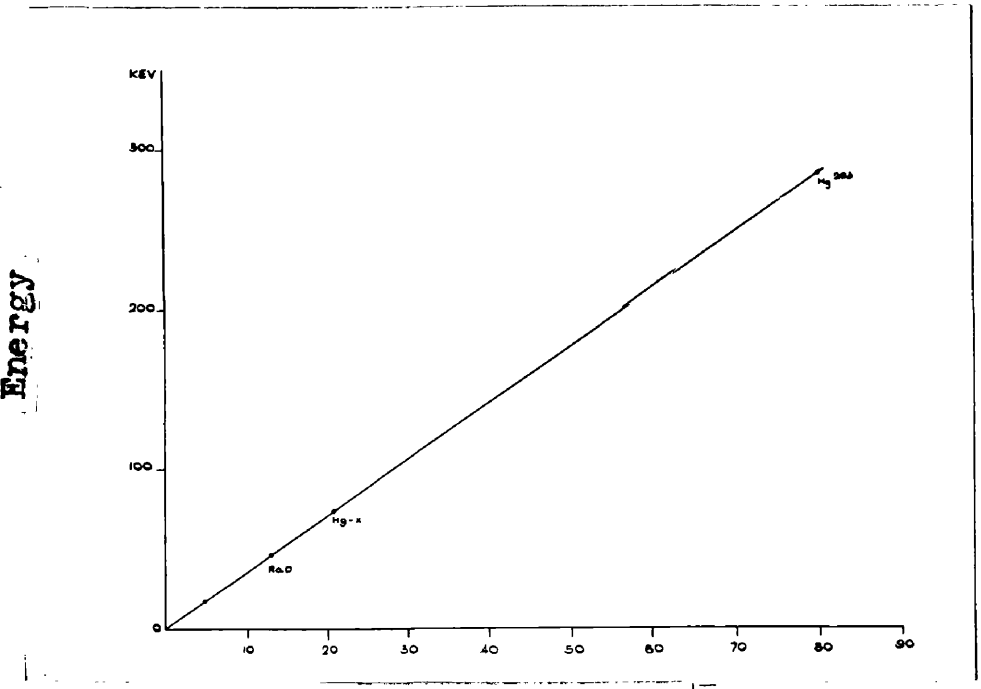

Fig. 14b. RbI(Tl) crystal calibration using γ-ray photopeaks.

Fig. 14c. Low energy calibration of the RbI(Tl) crystal using γ-ray photo-electric effect.

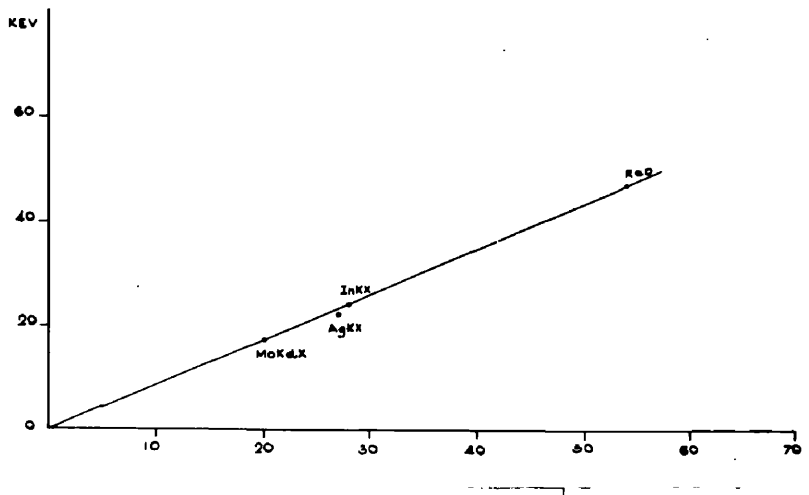

the energy loss being allowed for in the calibration curves.

Figs. 14a, 14b, and 14c show the linear nature of the response. The response of the crystal to γ-rays utilising the photoelectric effect, of course generally implies capture in the crystal of the various K,L.... $\overset{\text{iodine}}{\wedge}$ x-rays emitted in the crystal. It therefore involves the energising of a number of electrons in rapid succession. The fact that the calibration points fall on a straight line through the origin implies a linearity of response below the figure of 17 Kev, the lowest figure at which reliable calibration could be obtained.

(ii) Rb^{87} pulse height distribution.

The spectral pulse height distribution using the above crystal is shown in fig. 15a. The background counts were checked using a small crystal of sodium iodide (thallium activated), and examining it at equivalent working points allowing for the better efficiency of the latter crystal. The background was a negligible factor. Noise counts in the multiplier had to be allowed for only at the lowest energies, and the correction from this cause was small. The curve involved three sets of points, two sets being taken at lower energy with a greater amplifier gain. The points indicated by triangles necessitated paralysis, but points at higher energies using paralysis fell on the curve drawn - these points have been omitted for clarity. The curve is smooth in form and additional intermediate points support this view. One point has been included in the figure (at ~ 13 Kev) assuming the linear response/

Fig. 15a.

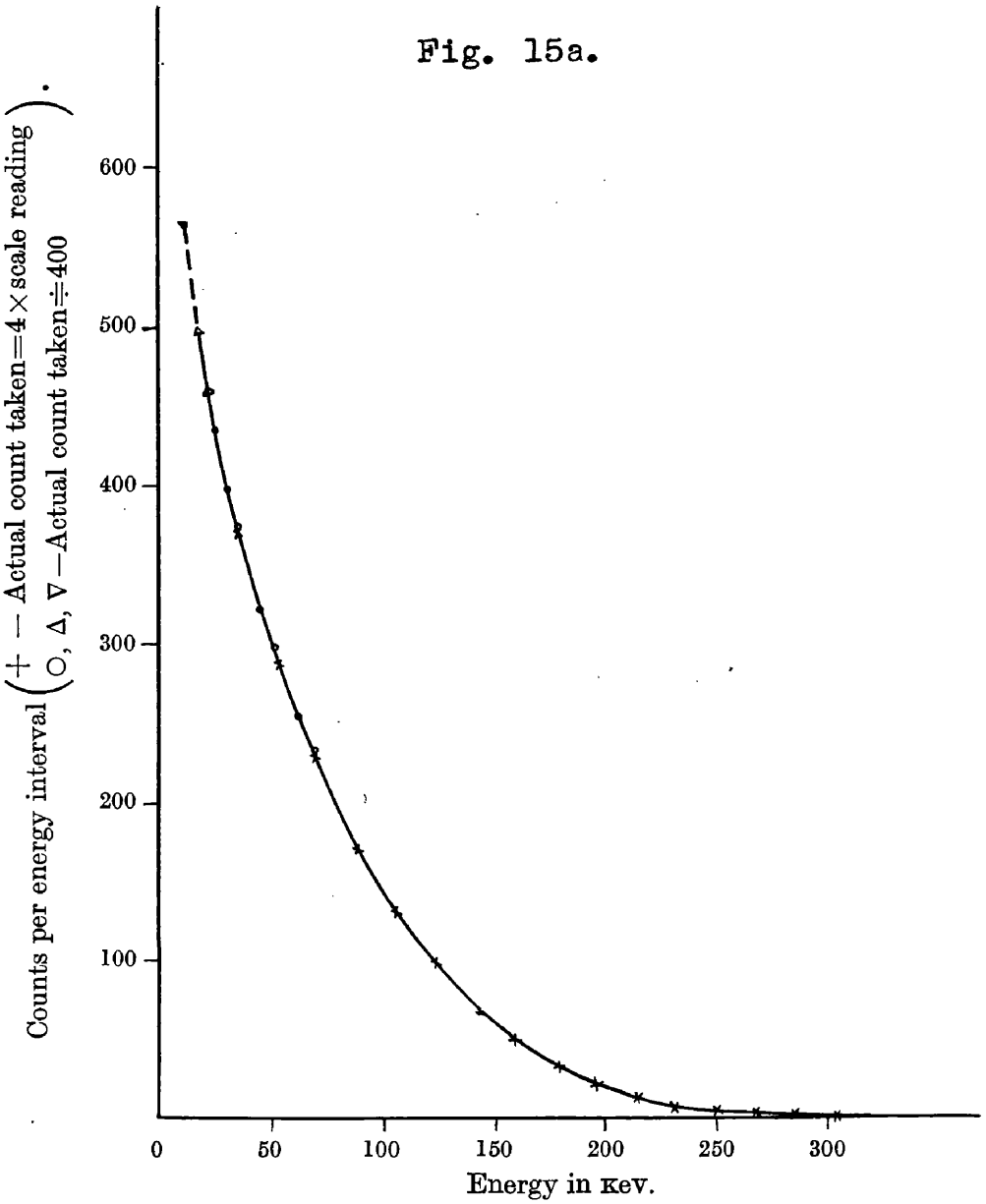

Spectrum of ^{87}Rb obtained using an activated rubidium iodide crystal. × Amplifier at low gain ; ○, Δ, ∇ amplifier at higher gain (points Δ, ∇ were taken in runs with paralysis ; point ∇ involves slight extrapolation of linear calibration).

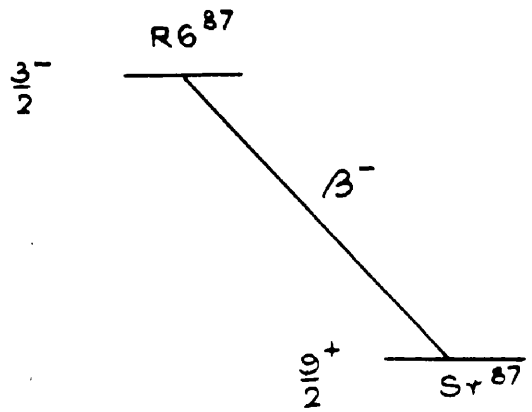

Fig. 15b. Decay scheme of Rb^{87}.

response to be valid below - 17 Kev (cf. (1) above). Similar results to these were obtained using another crystal of activated rubidium iodide.

The smooth form of the curve indicates the absence of conversion peaks and γ-rays in the range investigated. As has been mentioned, the integrating method (§ 3) using 4π geometry would displace the complete β-curve if simultaneous conversion peaks and associated K, L, ... radiation were present, or simultaneous low energy γ-rays existed. Higher energy γ-rays would have appeared in the main structure of the curve, due to the imperfect absorption. Delayed radiation would do likewise. It should be stated that Curran, Dixon and Wilson (1951) could find no evidence of K & L X rays in their investigation. The results indicate Rb^{87} is a pure β-emitter.

The shape of the β-spectrum, the similarity with that obtained by the proportional counter method, and the theoretical significance of the results, are referred to in the appendix. (Recent findings by another method (McGregor and Wiedenbeck (1954)) are also quoted). The lifetime is there estimated at $(5.90^{\pm 0.1}) \times 10^{10}$ years. The decay is given by fig. 15b.

The spin of Rb^{87} is $\frac{3}{2}$, that of $^{87}_{38}Sr$ is 9/2. On the independent particle model the first excited state of Sr^{87} might be expected to be given by the shift of the odd neutron, leading to a lower spin state in the same shell, e.g., $p\frac{1}{2}$ or maybe $p3/2$, $f5/2$ (cf. Mayer, Moszkowski and Nordheim 1951) leading then to a faster β transition. The energy change is therefore too great for these states to be formed by the decay of Rb^{87}. The experiments of Mann and/

and Axel (1951) show the existence of $p\frac{1}{2}$ and $p3/2$ excited states of Sr^{87} at 390 Kev. and 875 Kev. above the ground state.

CHAPTER 2

FAST DELAYED COINCIDENCES AND THE ANNIHILATION RADIATION OF POSITRON ELECTRON SYSTEMS

CHAPTER 2. FAST DELAYED COINCIDENCES AND THE ANNIHILATION RADIATION OF POSITRON ELECTRON SYSTEMS.

§ 1 THE DESIGN AND CHARACTERISTICS OF A HIGH SPEED COINCIDENCE UNIT USING SCINTILLATION COUNTERS.

(i) General Arrangement.

As this chapter deals with time and time related measurements, first consideration will be given to the electronic design of the high speed mixing unit.

The multiplier pulses, rising rapidly, are allowed to produce roughly fixed size pulses by the cutting off of a limiter valve. By having a suitably arranged shorted line these main channel pulses can be made of an approximately fixed small duration also. Two such pulses from different multipliers arriving within roughly twice this time duration of one another register in a mixing system, and deliver at least twice the response which each could provide separately. The pulses are lengthened and ultimately sorted out by a discriminator.

The precise shapes of the clipped pulses are dependent on the amplitude of the multiplier pulses. If these latter are not adequately large the limiting valve will be only slowly cut off, and pulses rather wider than desirable will enter the mixing system. These are removed by discriminating after mixing (cf. introduction §3 - Bell and Petch 1949). In this, additional outputs are taken from each multiplier, either from the multiplier collector through an attenuator, or better from a dynode. The amplified response provided/

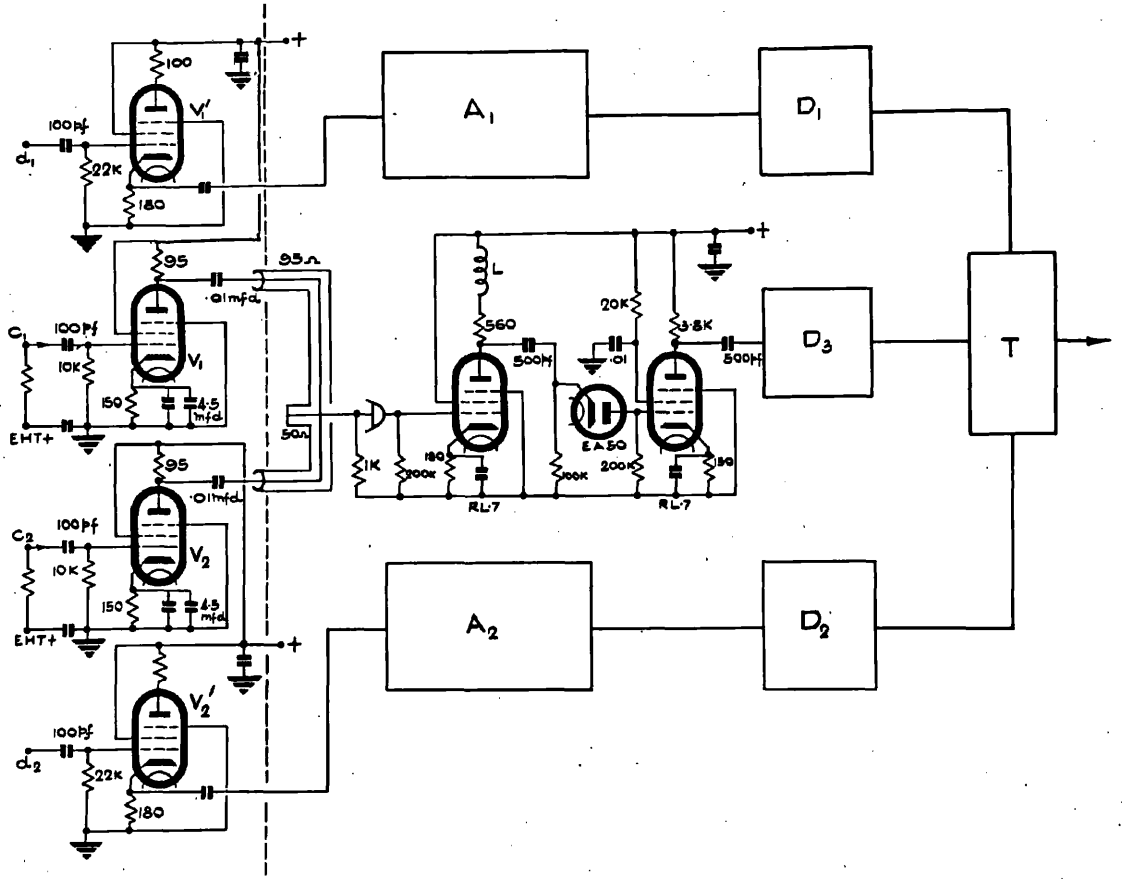

Fig. 16. Fast coincidence unit as used at lower resolving times. C_1 C_2 -photomultiplier collectors, V_1 V_2 -limiters , V_1' V_2' -side channel head valves, d_1 d_2 -photo multiplier dynodes. A_1 A_2- amplifiers T- Triple coincidence unit. For faster resolving times the mid channel amplifier is replaced by a fed back amplifier of higher gain.

provided a signal roughly proportional to the amount of light emitted by the phosphor. Each such side channel signal operated a discriminator. The two side channels and the main channel discriminators together operated a triple low speed coincidence unit. The output pulses of the latter could by appropriate choice of discriminator settings be associated therefore (a) with coincident pulses, (b) with initial pulses of adequate heights in the two multipliers.

The unit detailed below used generally two stages of centre channel amplification. It could operate with a diode as mixer between the two valves, or at higher speeds using a crystal diode as mixer in front. The convenient resolving time range was then about 10^{-7}sec. to 5×10^{-9}sec. This unit was used in the work on gases of § 3 (i - vi). For the high speed work on gases (§ 3 vii) additional centre channel amplification (with feed back) was inserted to obtain the shorter resolving time (3×10^{-9} sec.) necessary there.

Another complete unit employing four stages of centre channel gain complementary in range to the two stage unit above, operating conveniently in the 10^{-8}sec. to 10^{-9}sec. region is referred to in § 4 (cf. preface) (Ferguson and Lewis (1953))

(ii) Main Channel System.

Fig. 16 indicates the circuit arrangements of the complete system. Fig. 17 illustrates the pulses formed at successive points of the main channel system.

The/

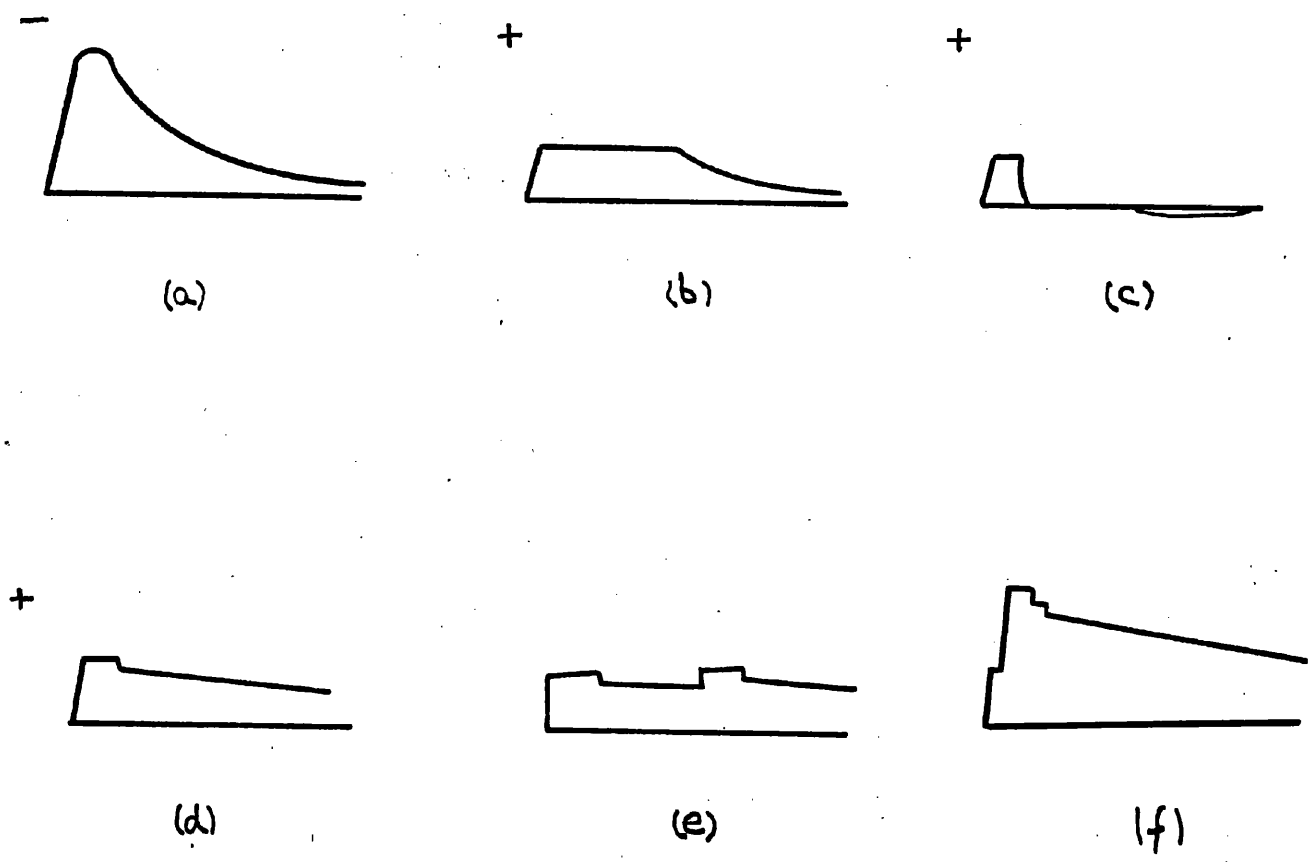

Fig.17. Pulse forms.(a) Multiplier output,(b)Limiter output,(c) Clipped pulse; (d) (e) (f) lengthened outputs due to,a single pulse, two non coincident pulses , two pulses coincident within the resolving time,respectively,illustrating how non coincident pulses can be eliminated in the main channel system.

The main output pulse (fig. 17a) from the multiplier collector cuts off the limiting value (type Cv138, in earlier work an R.L.7), mounted near the multiplier on the same metalwork. The grid leak is suitably low, in the case of organic scintillators decay times of 1/5 μ sec. were used, to prevent overloading at high rates. (The low leak resistance also reduced the possibility of leakage voltage from the collector which would alter the cv138 standing current). To keep the grid base short, cathode decoupling is employed, it has to be well decoupled to prevent any appreciable short time change in cathode bias, as large and frequent signal pulses may occur. Care has to be taken to isolate the H.T. lines to prevent feeding from one limiter into the other. The anode of the limiting valve carries a 95 ohm load in parallel with a 95 ohm cable (uniradio 31) which conveys the signal to the mixing unit and thence on to the terminating 95 ohm resistor carried in the anode system of the other limiting valve. In addition a discontinuity is produced in the cable system by the shorted stub line at the mixing unit, composed of 46 ohm cable (uniradio 4). The reflection from this produces clipping of the pulse at the mixing unit entry point and the reflected waves pass into the two terminated 95 ohm lines where they are finally absorbed. Fig. 17b illustrates the pulse at the entrance to the mixing unit in the absence of the shorted line. Fig. 17c illustrates the pulse at the same point with the shorted line present. The minimum length of 95 ohm cable between each multiplier and the mixer exceeded the shorted line path length to prevent any spurious effects from incomplete/

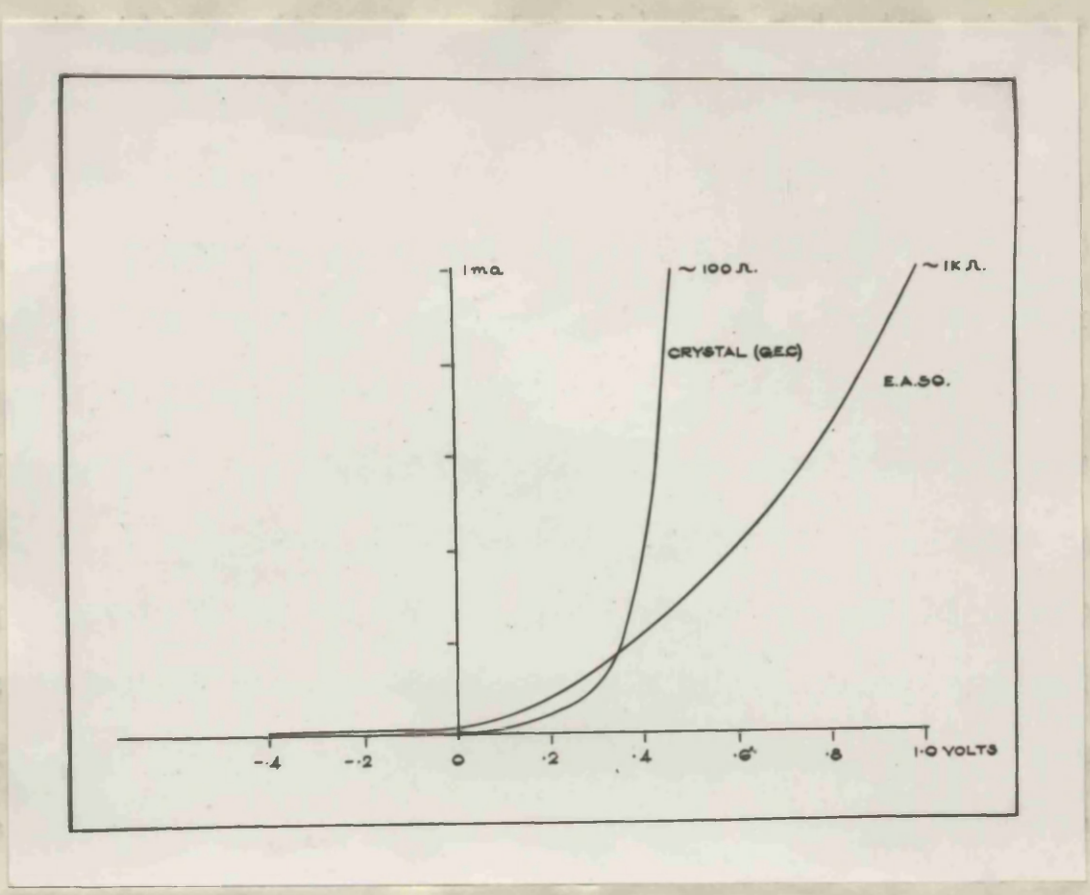

Fig. 18 .Static characteristics of valve and crystal diodes indicating the superiority of the latter for short time work.

— Double pulses

— Single pulses

Fig 19. Photograph of Output pulses (Cf. Figs 17 abc) when two scintillation counters are activated by a source. The time base is triggered here by the large double pulses associated with prompt coincidences .The small single pulses and other double pulses are displayed. The shorted stub line was here 10^{-8} sec.

incomplete terminations. In the main cable system G.E.C. plugs and sockets were employed throughout.

Mixing can be done by a valve diode following inductance compensated amplification, or it can be handled immediately on arrival by a crystal diode. The latter is preferable at fast speeds and essential at the highest speeds, and this method is shown in Fig. 16 (here the valve diode has merely a secondary role in lengthening still further the pulses delivered by the preceding crystal diode). Fig. 17d represents the voltage pulse which would be expected to appear at the far side of the mixing diode due to the single pulse. The grid earth capacity of the following pentode charges up through the forward resistance of the mixing diode and subsequently slowly drops away. (A small inherent series capacity in the mixing diode of 1 - 2 pfs slightly modifies the effects.) Fig. 17e shows the expected response of two pulses in quick succession and 17f that of two pulses arriving within the period determined by the shorted line. The effectiveness of the method of mixing depends on keeping the forward resistance of the mixing diode low, e.g., a 400 ohm impedance and an 8 pf. grid earth capacity would imply a charging time of 3×10^{-9} secs. The impedances of valve and crystal diodes can be compared from the characteristic curves of Fig. 18 obtained for specific instances. The crystal diodes appear to be adequately stable in use. Biassing of the mixing device can be employed if desired. Fig. 19 is a photograph showing the single and the double pulses in a typical arrangement, at the output of the main channel amplifier, using

a/

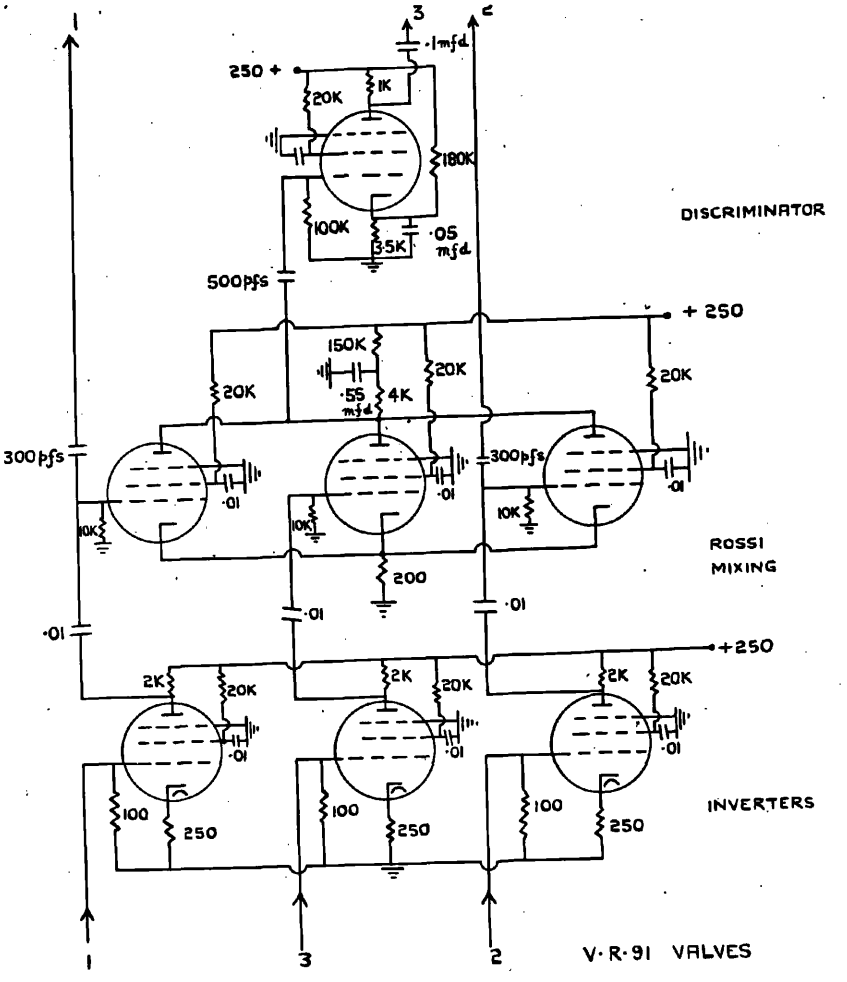

TRIPLE COINCIDENCE UNIT.

Fig. 20

a short stub length.

(iii) Side channels and the complete unit.

The side channel pulses leaving a dynode are kept fairly short (~ 1 μ. sec), to permit handling of large numbers of pulses, and activate cathode followers.

The following amplifiers (A_1, A_2) like the central channel amplifier are bolted close to the discriminators to keep the output time constants short, to permit simultaneous firing of the three disciminators (and triple unit) for simultaneous pulses. In the amplifiers A_1, A_2 are two stages with diode lengthening. The discriminators are of T.R.E. design (cf. Higginbotham, Gallagher and Sands (1947)). The discriminator output pulses were broadened to ~ 1 μ.s to produce slightly more tolerance in the firing times.

The triple unit is of conventional pattern. The circuit is shown in Fig. 20.

(iv) Operation.

For any source of radiation, of energy E, the tube volts would be raised at least so that limiting pulses were observed. The tube was then suitably set for working with radiations of higher energy.

With the tube volts set appropriately the discriminators on the corresponding side channel could then be set to exclude radiations of energy E. The other multiplier system could be similarly treated. The middle channel discriminator was set at any/

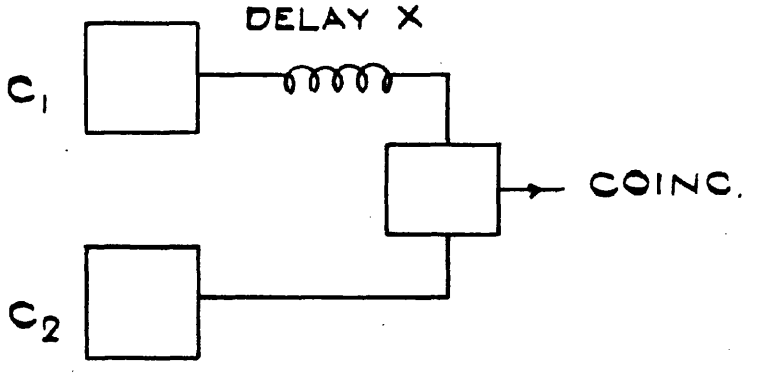

Fig. 21.

The delayed coincidence method

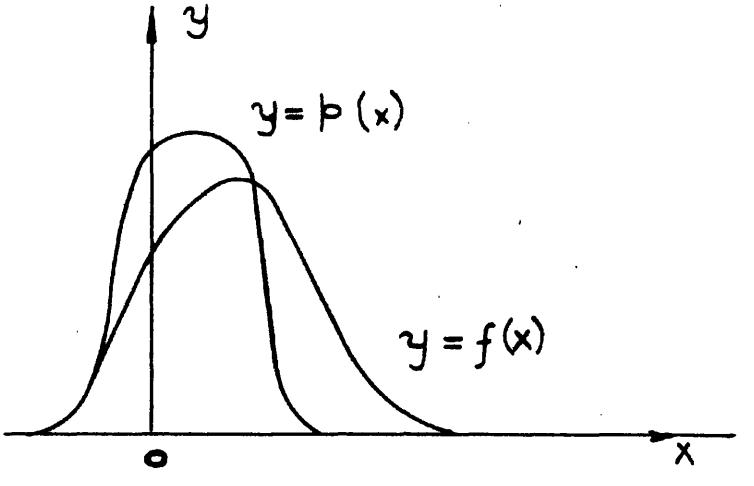

Fig . 22. Prompt and delayed coincidence curves.

any setting such that single pulses were certainly excluded from both multipliers separately.

Lastly it is necessary to stress one point of importance, a point of difference between the operation of fast and slow coincidence units. The variation of pulse shape and timing with input light energy has to be taken into account. Bigger pulses arrive faster at the output of the multiplier. Delayed coincidence curves can only be compared at the highest speeds when identical electron pulse energy distributions are involved in the two sets being compared. This matter complicates the method, and additional apparatus has to be introduced to generalise the applications of the method. This can involve spectrometers (cf. Bell, Graham, Petch, 1952) in the case of β-rays, or Kicksorter devices (cf. Ferguson and Lewis (1953), and § 4) more generally. (The counting rates should be kept as low as possible, per channel; e.g 1000 counts/sec).

Methods of handling random counts are on a comparison basis or involve cable reversals. The electron pulse energy distributions must be kept the same; here the side channels are important

(v) Resolving Time.

Fig. 21 illustrates an experimental arrangment showing variable delay x in time units inserted in the channel of counter C_1, Fig. 22 shows a possible coincidence probability curve $\left(\text{probability} = \frac{p(x)}{p_{max}}\right)$, plotted as $y = p(x)$, when prompt events from some sources are supposed present. The displacement in Fig. 22 would be due to slower response in the counter C_2. Let N_1 and N_2 be the counting rates in the two counters when the pulses are/

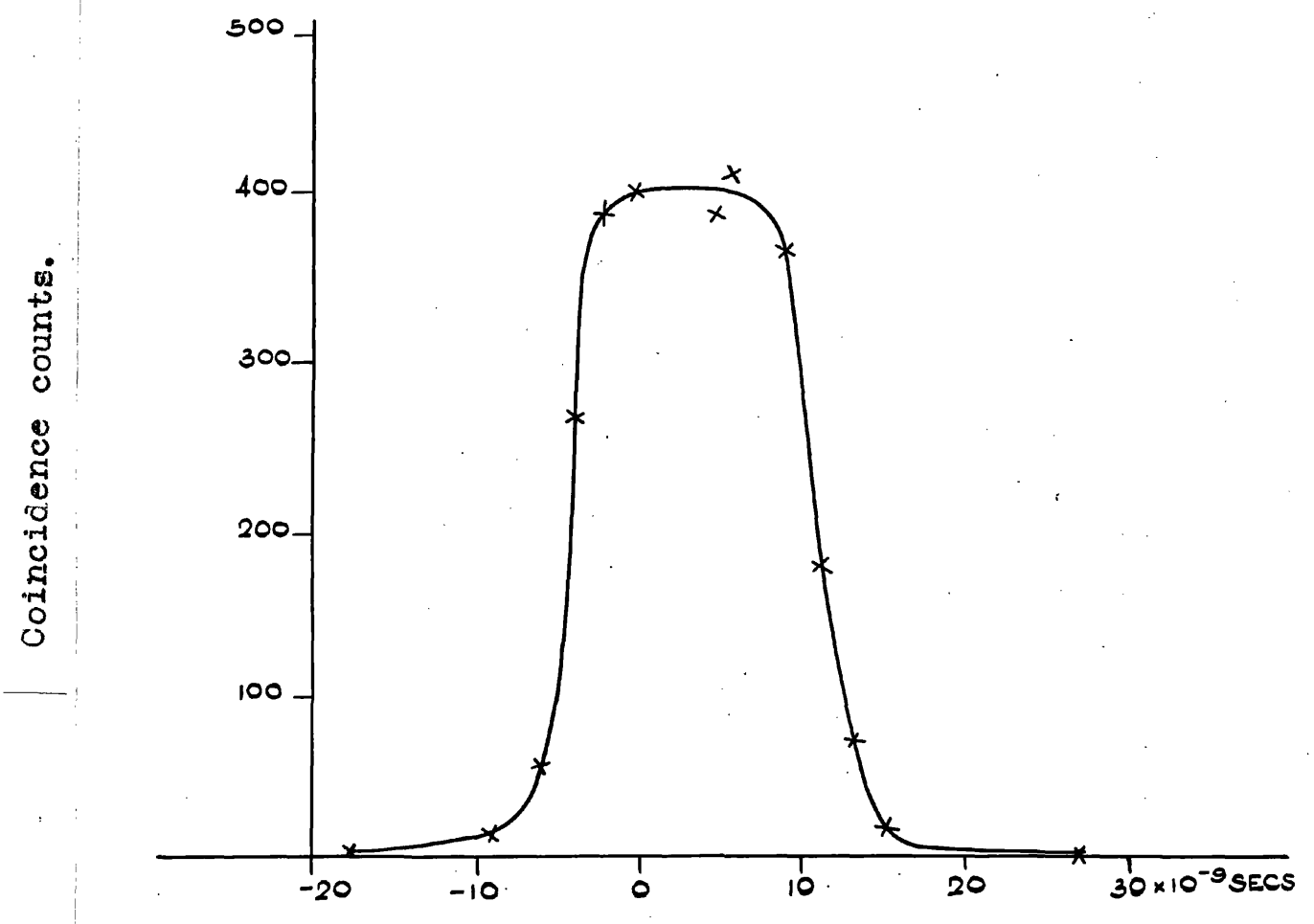

Fig 23. Resolution curve obtained between 1.28 mev. γ- ray of Na^{22} and annihilation radiation of positrons in aluminium, showing flat top . The resolving time is about 7×10^{-9} sec.

are randomly distributed (e.g., using two independent sources of type S). The random coincidence rate N_c is given by:

$$N_c = \int_{-\infty}^{+\infty} N_1 . N_2 . \frac{p(t)}{p_{max}} dt \equiv 2 N_1 . N_2 . T_o$$

where T_o is the defined resolving time of the unit, i.e.:

$$2T_o = \frac{\int_{-\infty}^{\infty} p(x)dx}{p_{max}} = \frac{\text{Area}}{\text{Max. Height}} \qquad (14)$$

Fig. 23 shows a coincidence resolution curve between the 1.28 Mev nuclear γ-ray of Na^{22} in the one counter and 0.51 Mev. radiation produced by annihilation of positrons from Na^{22} in aluminium. Evidence will be given later that these events are approximately prompt (the delay is actually $\sim 1.6 \times 10^{-10}$ secs; cf. § 4). Fig. 23 is flat topped and the efficiency is close to 100%. As the resolving time is reduced further the relatively flat top is found to disappear; these rounded tops are found to be characteristic of short resolving time work.

Limitations on the attainable resolving times arise in the phosphor as well as in the multiplier and circuitry. (cf. Post and Schiff (1950)). Considering the phosphor contribution only, if the phosphor produce at the cathode a large number N of photo-electrons and the phosphor lifetime be T, the mean time of arrival $\bar{t}$ of the first electron and the root mean square deviation $\sqrt{\overline{t^2} - \bar{t}^2}$ have been given by Post and Schiff. Approximately

$$\sqrt{\overline{t^2} - \bar{t}^2} = T/N$$

The shorted line has to be longer than T/N, in time units for reasonable coincidence efficiency. For a shorted line nT/N, with n exceeding unity the coincidence efficiency is in fact then $(1 - 1/e^n)$. In estimating N allowance has to be made for the geometry using 1P21 tubes and for the small fraction of the electrons/

[The chance of the first photoelectron appearing in time nT/N can then be shown $(1-e^{-n})$.]

electrons which travel by the direct path in the case of E.M.I. tubes (cf. Allen and Engelder (1951)). With 100 Kev electrons in terphenyl in toluene a resolving time of $\sim 10^{-9}$ secs. is possible (e.g., $N \sim 6$, $n \sim 3$) with efficiencies close on 90%. Emission times for 1P21 multipliers have been discussed by Post (1952).

(vi) The delayed coincidence method.

If every event arriving at the counter C_1 is associated with the chance $f(t)$ of an event arriving at C_2 a time t later, a different curve is obtained from $y = p(x)$ of Fig. 22. Suppose

$$f(t) = \lambda e^{-\lambda t} \qquad (15a)$$

corresponding to one lifetime, $\frac{1}{\lambda}$. The curve (cf. Fig. 22)

$$y = F(x) = \int_0^\infty p(x-t)\, f(t)\, dt \qquad (15b).$$

would then be obtained. Beyond points x where $p(x) \sim 0$ the plot of the curve $y = F(x)$, from first principles, decreases as $e^{-\lambda x}$. This tail, if readily obtainable, gives the lifetime. Otherwise the lifetime may be obtained from the centroid shifts of the curves $y = p(x)$ and $y = F(x)$ - (cf. Bay 1950). A deduction as follows can be based on a lemma by Newton (1950).

Letting $u = x-t$, (15a), (15b) give:

$$F(x) = \lambda e^{-\lambda x} \int_{-\infty}^{x} e^{\lambda u}\, p(u)\, du \quad , \quad \frac{dF}{dx} = \lambda\left[p(x) - F(x)\right] \qquad (15c)$$

Therefore

$$\int_{-\infty}^{\infty} p(x)\, dx - \int_{-\infty}^{\infty} F(x)\, dx = 0, \text{ if } \left[F(x)\right]_{-\infty}^{\infty} = 0$$

showing the areas of the prompt and delayed curves are the same for the normalised function (15a). Conversely if the prompt and delayed experimental curves are plotted to the same area, (15a) represents single period decay. Further if $\left[xF(x)\right]_{-\infty}^{\infty} = 0$,

$$\int_{-\infty}^{\infty} xF.\, dx - \int_{\infty}^{\infty} xp.\, dx = \frac{1}{\lambda} \int_{-\infty}^{\infty} F.\, dx \qquad (15d)$$

giving/

giving the lifetime in terms of centroid shift.

For two periods $\frac{1}{\lambda}$, $\frac{1}{\mu}$ present in the ratio $\alpha/(1-\alpha)$, one may write

$$f(t) = (1-\alpha)\mu e^{-\mu t} + \alpha\lambda e^{-\lambda t} \qquad (16a)$$

The periods could be observed directly far from the prompt curve. If the delayed and prompt curves are close, analysis has to be employed. For $f(t)$ given by (16a) the areas of the prompt $(y = p(x))$ and delayed $(y = F(x))$ curves are again the same, or conversely. Writing $F(x)$ as a sum of two parts, viz., $F = F_1 + F_2$

where $F_1(x) = \int_0^\infty p(x-t)\,\alpha\lambda\, e^{-\lambda t}\, dt$,

application of the above reasoning leads to

$$\int_{-\infty}^{\infty} x F\, dx - \int_{-\infty}^{\infty} x p\, dx = \left(\frac{\alpha}{\lambda} + \frac{1-\alpha}{\mu}\right) \int_{-\infty}^{\infty} p\, dx \qquad (16b)$$

$$\int_{-\infty}^{\infty} x^2 F\, dx - \int_{-\infty}^{\infty} x^2 p\, dx = 2\left(\frac{\alpha}{\lambda} + \frac{1-\alpha}{\mu}\right)\int_{-\infty}^{\infty} x p\, dx + 2\left(\frac{\alpha}{\lambda^2} + \frac{1-\alpha}{\mu^2}\right)\int_{-\infty}^{\infty} p\, dx \qquad (16c)$$

If $\mu \gg \lambda$, the terms involving μ can be omitted, giving two equations for α and λ . The equations will be referred to in § 3 and § 4 (cf. too Ferguson and Lewis (1953)).

§ 2 THEORETICAL ASPECTS CONCERNING THE SPIN RELATIONSHIP OF AN ELECTRON POSITRON PAIR IN TWO QUANTUM ANNIHILATION.

The time studies will be later much concerned with the annihilation process and the spin systems involved. Dirac (1930) derived the two quantum annihilation probability of a positron electron system. Wheeler stated that the equations require the system/

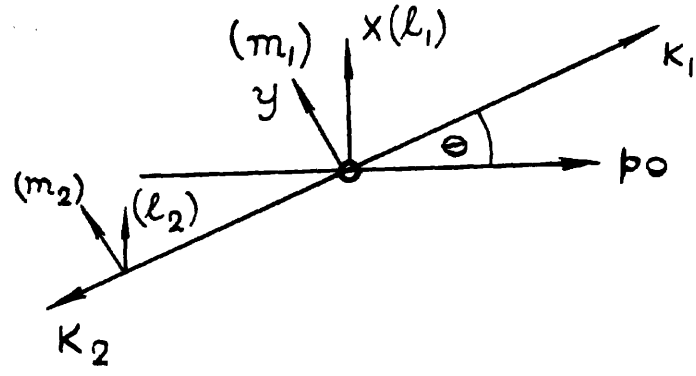

Fig. 24.

Two quantum annihilation.

system to be in a singlet state (Wheeler 1946). General selection rules on symmetry grounds have been derived by Yang (1950). As no direct proof seemed readily available it seemed desirable to check on this, from the initial relations of Dirac, as given below, (particularly because of experiments involving iron, later, where the spins of the d-shell electrons are aligned).

Consider the annihilation of an electron and positron travelling towards one another each having energy Eo and momentum Po equal in magnitude. Taking the centre of mass as origin, let the emitted quanta K_1, K_2 (each having energy Eo) have polarisations (l_1,m_1), $(l_2 m_2)$ where the resolutes l_1, l_2 are along the X axis, the $\vec{X}$ axis being perpendicular to the plane of $\vec{P}o$ and $\vec{K_1}, \vec{K_2}$ (cf. Fig. 24). The $\vec{Y}$ axis is then perpendicular to the $\vec{X}$ axis at $(90 + \theta)$ to $\vec{P_o}$ where θ is the angle between $\vec{po}$ and $\vec{K_1}$.

The annihilation occurs in two stages by the emission of $\vec{K_1}$ first and $\vec{K_2}$ after, or vice versa. The electron of energy Eo (state A) makes a transition to an intermediate state designated 1 or 2 respectively, having four possibilities of spin and energy, and thence to the final negative energy state (state F) of -Eo. Momentum is conserved in these transitions. Then (cf. Heitler "The Quantum Theory of Radiation" Oxford 1947, p206, eqn.(5)) the transition probability χ per unit solid angle can be written:

$$\chi = \frac{2\pi}{\hbar} \rho_F \left| \sum_1 \frac{H_{A1} H_{1F}}{E'} + \sum_2 \frac{H_{A2} H_{2F}}{E''} \right|^2 \qquad (17a)$$

where ρ_F is the density of final states per unit energy interval, E^1/

E^{1} and E^{11} are the energy changes involved in reaching the intermediate state; and H_{A1}, H_{1F}, H_{A2}, H_{2F} are matrix elements for the transitions, Σ_1 and Σ_2 refer to summation over the four spin and energy possibilities of the intermediate states.

Substituting for ρ_F and evaluating the matrix elements,

$$\chi = a \left| \Sigma_1 \frac{(u_0^* \alpha_1 u')(u'^* \alpha_2 u)}{E'} + \Sigma_2 \frac{(u_0^* \alpha_2 u'')(u''^* \alpha_1 u)}{E''} \right|^2 . \quad (17b)$$

where a is a constant (actually $a = e^4 c$); α_1, α_2 are the components of the Dirac operator $\vec{\alpha}$ along the polarisation vectors of the quanta $\vec{K}_1$, $\vec{K}_2$ respectively. Uo refers to the four components of the wave function of the initial state A. u^1, u^{11}, u refer similarly to the other states designated 1, 2, and F.

The main purpose is to determine what states A and F contribute to this expression χ.

E^1, for instance, is given by the electron energy:

$$(E')^2 = \mu^2 + p_0^2 + K_1^2 - 2 p_0 K_1 \cos\theta .$$

where μ is the rest mass; and the speed of light is taken as unity here for convenience.

Moreover the momenta of the intermediate states can be written $(\vec{p_0} - \vec{K_1})$ and $(\vec{p_0} - \vec{K_2})$, so that:-

$$H' u' = E' u' \quad \text{and} \quad H'' u'' = E'' u''$$

where

$$H' = (\vec{\alpha} \cdot \vec{p_0} - \vec{K_1}) + \beta\mu \quad , \quad H'' = (\vec{\alpha} \cdot \vec{p_0} - \vec{K_2}) + \beta\mu$$

in virtue of the Dirac equation.

Eq^n (17b) may be written:

$$\chi = a \left| \left(\frac{1}{E'}\right)^2 \Sigma_1 (u_0^* \alpha_1 H' u')(u'^* \alpha_2 u) + \left(\frac{1}{E''}\right)^2 \Sigma_2 (u_0^* \alpha_2 H'' u'')(u''^* \alpha_1 u) \right|^2$$

Therefore:

$$\chi = a \left| \left(\frac{1}{E'}\right)^2 \left(u_0^* \alpha_1 H' \alpha_2 u\right) + \left(\frac{1}{E''}\right)^2 \left(u_0^* \alpha_2 H'' \alpha_1 u\right) \right|^2 \qquad (17c).$$

Whence

$$\chi = a \left| \left(\frac{1}{E'}\right)^2 u_0^* \left(l_1 \alpha_x - m_1 \alpha_z \sin\theta - m_1 \alpha_y \cos\theta\right)\left(\beta_0 \alpha_z - K_1 \overline{\alpha_z \cos\theta - \alpha_y \sin\theta} + \beta\mu\right)\left(l_2 \alpha_x - m_2 \alpha_z \sin\theta - m_2 \alpha_y \cos\theta\right) u \right.$$
$$\left. + \left(\frac{1}{E''}\right)^2 u_0^* \left(l_2 \alpha_x - m_2 \alpha_z \sin\theta - m_2 \alpha_y \cos\theta\right)\left(\beta_0 \alpha_z + K_2 \overline{\alpha_z \cos\theta - \alpha_y \sin\theta} + \beta\mu\right)\left(l_1 \alpha_x - m_1 \alpha_z \sin\theta - m_1 \alpha_y \cos\theta\right) u \right|^2$$

Restricting the problem to that of slowly moving particles the terms involving β_0 may be omitted in the matrix elements, and $E^{1^2} = E^{11^2} = 2\mu^2$. Writing $m_1 l_2 - l_1 m_2 = \sin\theta$, χ reduces to:-

$$\chi = \frac{a}{\mu^2} \sin^2\theta \left| u_0^* \alpha_x \alpha_y \alpha_z u \right|^2 \qquad (17d.)$$

where θ is the angle between the polarisation vectors.

Taking $u_0 \doteq (1,0,0,0)$ corresponding to an electron of spin 1/2 along z, and E_0 positive and $u \doteq (0,0,1,0)$ corresponding to an electron of spin 1/2 along z and Eo negative, and writing the total annihilation rate $R = 2\pi\chi$, (θ varying from 0 to π only.)

$$R = \frac{2\pi a}{\mu^2} \sin^2\theta \qquad (\text{ie } R = 2\pi r_0^2 c \sin^2\theta) \qquad (18a).$$

If however $u \doteq (0,0,0,1)$ corresponding to an electron with spin -1/2 along z, and Eo negative, giving a triplet positron electron state

$$R = 0 \qquad (18b)$$

This is the result sought after; two quantum annihilation occurs only for the singlet state. Moreover, as is well known, (cf. e.g., Yang 1950) (18a) shows the quanta are always polarised at right angles.

The relation of the results to Eqn. (10) is clear. It should be mentioned however that in comparing theoretical annihilation rates/

rates with experimental values, that the theory does not take into account the attractive forces which the positron and electron have for one another. These forces would produce distortion of the wave function, increasing the annihilation probability, especially at lower speeds. [To illustrate this distortion, the positron probability density very close to a fixed negative point charge would be increased by the Coulomb factor

$$F(1,E) \sim \frac{2\pi e^2/\hbar v}{1-\exp(-2\pi e^2/\hbar v)}$$

where v is the speed of approach (cf. Temple (1928), Mott and Massey (1949)). To assess orders of magnitude Deutsch (1953) has proposed that v be associated with valency electron speeds; F(1,E) is then $\sim 2\pi$ at the centre of attraction.]

§3 ANNIHILATION OF POSITRONS IN THE GASES FREON AND OXYGEN.

(i) Preliminary studies and development work.

As mentioned in the introduction, Deutsch (1951) had shown the existence of a lifetime for positrons against annihilation, in freon, only slightly dependent on the pressure over the region 0 - 2 atmospheres, and that it had a value near 1.4×10^{-7} sec. Preliminary measurements were made here with freon using a coincidence unit of resolving time 3×10^{-8} secs., with two scintillators of terphenyl in toluene, in containers 2" x $1\frac{1}{2}$" diam., over a gas.pressure range extending to 5 atmospheres. Delayed coincidences were observed between the 1.28 Mev γ -ray of Na^{22} and the annihilation radiation. The findings of Deutsch were/

were found to be valid over the extended range. A check was made too on the annihilation time in oxygen, which was known to be inversely proportional to pressure. More accurate experiments were carried out later (cf. (iii) below).

It was decided to investigate if possible, the delayed annihilation radiation spectrum associated with this 1.4×10^{-7} sec. period in freon, and to compare it with the theoretical predictions of Ore and Powell. This method, whilst selecting the required long period radiation would also eliminate γ-radiations from the source and gas container.

The two crystal method was first tried, using an organic crystal ~ 1 cm^3 as spectrometer, back scattered radiation being picked up by a ring of sodium iodide. The nuclear 1.28 Mev γ-ray was picked up in a liquid organic scintillator as before. The small organic crystal could operate the Kicksorter if a suitable delayed coincidence occurred between the organic scintillators, and if a pulse within 1 μ sec appeared in the iodide crystal. The efficiency of the system was found, as feared, to be too low.

It was therefore necessary to measure the annihilation radiation in a large sodium iodide crystal directly, and the carrying out of the investigation therefore depended on the possibility of producing a suitable moderately fast coincidence unit using sodium iodide on the one side instead of an organic scintillator. The rise time of sodium iodide had been reported to be about $\frac{1}{4}$ μ sec (Hofstadter (1949)). It was hoped that by driving the photo-tube hard, the leading edge of the pulses could be made sufficiently steep/

Fig. 25

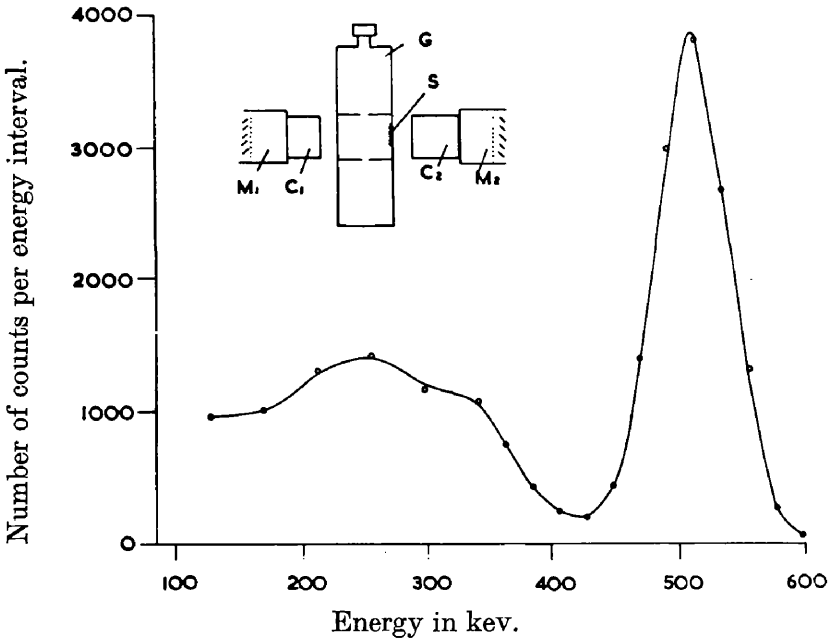

Pulse height distribution obtained for the annihilation radiation of ^{64}Cu positrons in copper.
Inset : experimental arrangement ; S, source ; G, gas container ; C_1, C_2, scintillators ; M_1, M_2, multipliers.

steep for the first 2V rise (the grid base of the CV138 valve) to provide an unit of resolving time $\sim 5 \times 10^{-8}$secs. with the γ energies in the 3-quantum annihilation continuum. Moreover the exact resolving time curve would have to be positioned in an approximately constant manner also irrespective of energy (cf. iii below). Tests of a coincidence unit using sodium iodide on the one side and a terphenyl counter on the other were carried out. The arrangement was very successful immediately. Using Hg^{203} γ -rays as a source, coincidences between the γ-ray and the scattered compton γ -ray, involving energies $\sim$ 100 Kev could be readily utilised, with resolving times of 3×10^{-8}secs. The other requirements were also met as described in (iii) below.

(ii) Experimental arrangement.

A source of Na^{22} of strength $\sim 2\mu$c. was mounted and covered by an aluminium foil 0.005" thick. It was placed inside a cylindrical gas container 2" diam., the walls of which were of 0.012" copper kept thin to reduce scattering errors (inset fig. 25). Two perforated phosphor bronze plates 0.005" thick, $1\frac{1}{2}$" apart were used to restrict the positrons to the central region of the container. The toluene scintillator, C_2 (2" x $1\frac{1}{2}$" diam.) referred to above was placed near the source. Opposite this was placed the spectrometer counter used for measuring the energy of the delayed annihilation radiation from the gas. The scintillator on this counter was a sodium iodide block, $1\frac{1}{4}$" cube (C_1), composed of two pieces cemented together along a common plane with silicon grease, as no single crystal/

Fig. 26

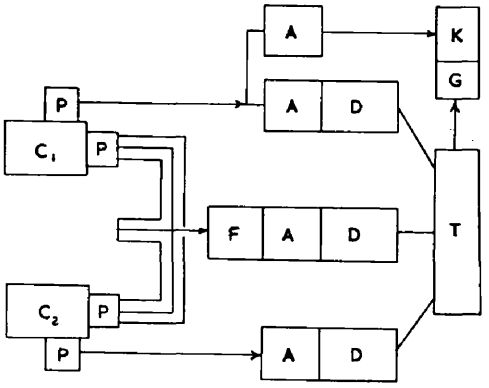

Block diagram : C_1, C_2, counters ; P, preamplifier ; F, unit receiving fast coincidences ; A, amplifier ; D, discriminator ; T, triple coincidence unit delivering selected fast coincidences ; G, gate ; K, kicksorter.

crystal of this suitable size and shape was available. The scintillator was packed in magnesium oxide, the iodide crystal being sealed inside. 14 stage E.M.I. tubes were used. The ends of the iodide and terphenyl scintillators were situated 1" and $\frac{1}{2}$" respectively from the container. To reduce scattering of delayed annihilation radiation from the surroundings, to the spectrometer crystal, the system was set up on a light plywood table, and supports, etc., reduced to a minimum.

The electronic arrangement is shown in fig. 26 and uses, with additions, the coincidence electronics essentially described in § 1. Variable amounts of uniradio 31 could be introduced in the main channel system.

The side channel delivering attenuated pulses from the terphenyl counter permitted the passing of pulses from γ-rays above $\sim$600 Kev only, i.e., from the nuclear 1.28 Mev γ-ray only here. On the sodium iodide channel pulses were taken from the tenth dynode to avoid saturation effects. Some condenser attenuation was also used. The initial grid resistance leading from the multiplier shown in fig. 16 was kept high to avoid severe differentiation at this stage. The discriminator was set so as to cut off low energy pulses (actually $\sim$140 Kev) to ensure satisfactory performance from the coincidence unit. The output from the triple coincidence unit opened the gate of the Kicksorter analysing the pulses from the iodide crystal, giving a bright spot on the cathode ray tube which could be scanned by a multiplier, or photographed, in the manner described earlier. The resolving time used here

was/

Fig. 27

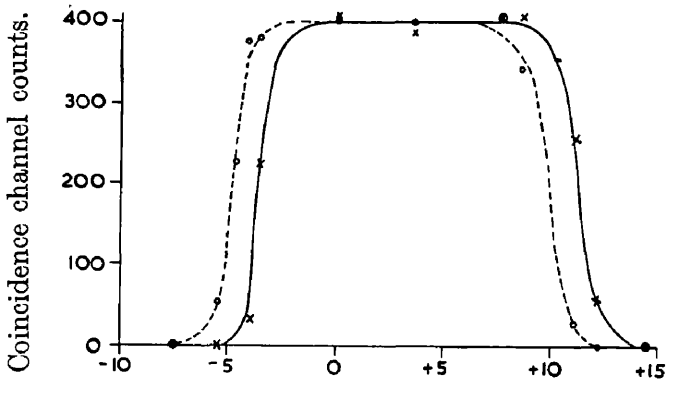

(*a*)

Delay cable length in metres.

Coincidence resolution curve between prompt pulses of a given height in the sodium iodide counter and 1·2 Mev γ-pulses in the other counter.
x——electron energy, 200 kev ; o- - -electron energy, 400 kev.

was 5×10^{-8} secs, as discussed below.

(iii) The resolution curve and the determination of annihilation times of positrons in freon and oxygen.

The coincidence resolution curve was investigated with the container evacuated. The delay between the appearance of annihilation radiation from positrons from Na^{22} in metals after the nuclear γ -emission is of order 10^{-10} secs. (cf. §4, cf. too the measurements of Bell and Graham (1953) on copper). The curve can therefore be considered an approximately prompt resolution curve. When more than 20 metres of delay cable were inserted on the 1.28 MeV γ side, the coincidences observed were only random coincidences. (Insertion of 1 metre of cable was equivalent to a delay time of 5×10^{-9} sec.). Any pulses appearing here with a gas present would indicate delayed annihilation radiation.

It was necessary to determine how the resolution curve varied with the energy of the pulse being measured in the iodide crystal. For the determination of delayed spectra the unit should have resolving times roughly independent of the pulse energies in the iodide crystal (above the figure of 140 Kev previously specified). Furthermore the position of the curve should not appreciably vary with these pulse energies; otherwise distortion of the true spectrum occurs. Fig. 27 shows the plots of coincidence counts with delay cable length for narrow energy bands of pulses from the iodide crystal. One plot is obtained using electrons in the neighbourhood of 200 KeV, the other using electrons of about 400 KeV. These/

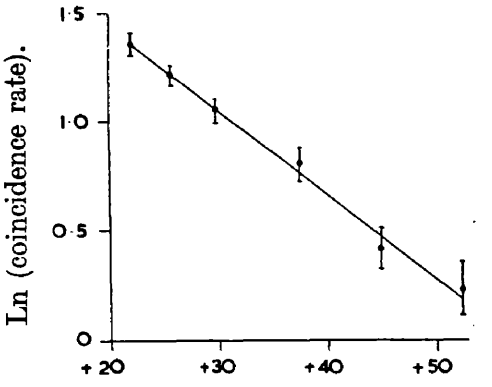

Fig. 28

(*b*)

Delay cable length in metres.

Variation of coincidence rate with delay for positrons in freon at 4·8 atmospheres.

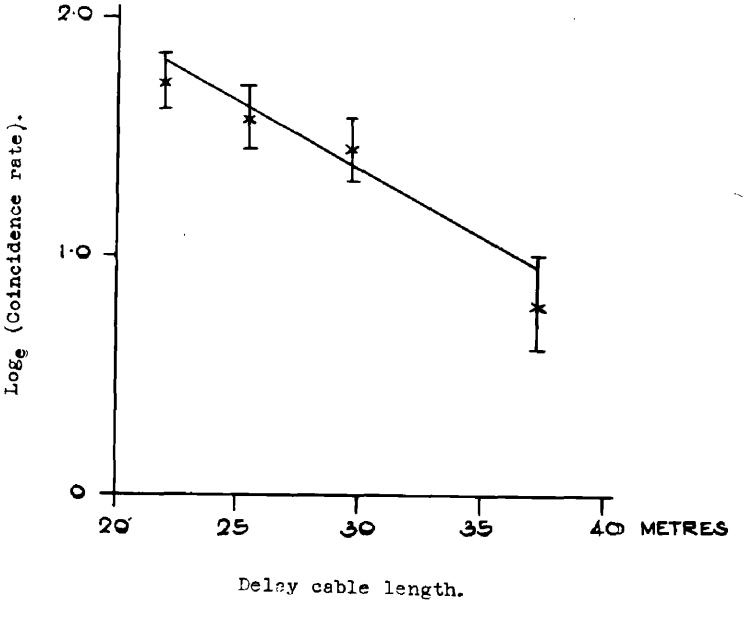

Fig 29. Determination of the positron lifetime in oxygen at 2.4 atmospheres pressure.

These particular coincidence counts are obtained as the output counts of first one and then the other of two narrow channels of the gated Kicksorter, corresponding to these particular energies. The resolving time is seen to be approximately the same in the two cases. There is a displacement of the equivalent of $1\frac{1}{2}$ metres of cable, corresponding to 7.5×10^{-9} sec only for the 200-400 KeV change involved, the bigger pulses arrive earlier. This time is small compared with the annihilation times in the gases under the conditions of this experiment, as is seen below. The effect of the displacement is to produce a small exaggeration of the low energy components in the spectrum.

Fig. 28 shows a delayed coincidence curve obtained when freon was present in the container to a saturation pressure of 4.8 atmospheres, circumstances approximating to those existing when the spectra were determined. The lifetime from this and similar curves was $(1.25 \pm 0.10) \times 10^{-7}$ sec. This annihilation time is only a little shorter than that quoted by Deutsch (1951), from his experiments at lower pressure. The variation of this annihilation time with pressure is at most slight. Fig. 29 shows a curve for oxygen at 2.4 atmospheres at room temperature. This leads to a value of 8.8×10^{-8} sec. with an error of roughly $\pm 1.5 \times 10^{-8}$ secs, in agreement with the value given by Deutsch of 8×10^{-8} secs.

(iv) The delayed annihilation spectrum of positrons in freon, and in oxygen.

The spectrometer characteristics of the sodium iodide crystal and multiplier were examined. Fig. 25 shows the annihilation spectrum/

spectrum obtained when positrons annihilated in copper, using only the iodide counter and Kicksorter. Kubitschek (1950) has shown the 1.38 MeV γ -ray of Cu^{64} to be only of $1\frac{1}{2}\%$ relative intensity. The experimental curve agrees with rough expectations for a crystal of this size. The main peak is partly photoelectric in origin involving capture of any associated iodine X-rays. It is due to the ready absorption of back scattered Compton radiation which eliminates the Compton edge. The gap at $\sim$ 420 KeV corresponds to the gap which would occur in a smaller crystal between the Compton edge and photopeak. The small low energy bulge (above 1000 counts) in the multiple Compton distribution can be explained in some measure by back scattering of γ-rays from the rear parts of the crystal mounting.

Similar curves were obtained using Na^{22} in an evacuated container with the two counters in prompt coincidence, when the counter detecting nuclear γ-radiation was placed so as to minimise the prompt coincidences from its back scattered Compton radiation. This experiment was carried out using a low (10^{-6} sec.) resolving time as a further check.

The linearity of response with γ-ray energy of the spectrometer side was checked using the 280-KeV γ -ray of H_g^{203}, the annihilation radiation of Cu^{64} positrons in copper, and the 660 KeV γ -ray of Cs^{137}. Further the effect of source positioning was examined. It was necessary to determine what effect the positioning of the positron at annihilation would have on the observed spectrum. The Cu^{64} source, enclosed in copper, was placed at various/

Fig. 30

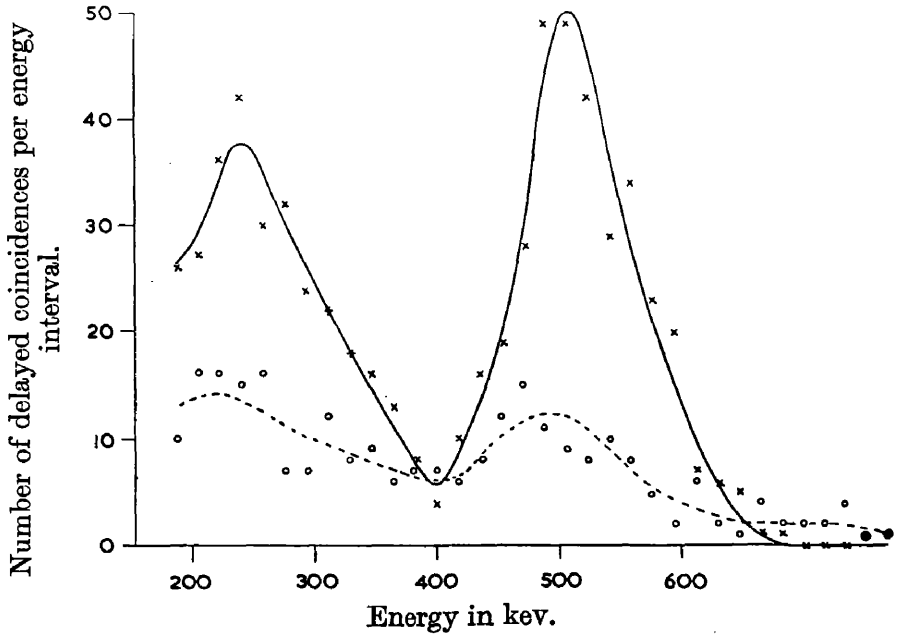

Pulse height distribution obtained for the delayed annihilation radiation of positrons in oxygen.
x——real counts, after subtracting randoms ; o- - -random counts.

Fig. 31

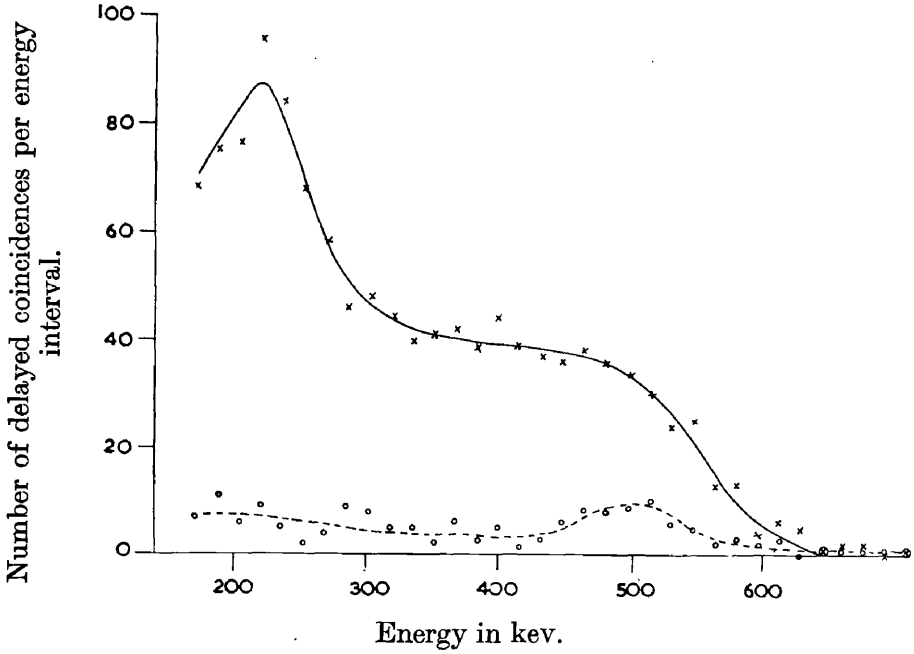

Pulse height distribution for the delayed annihilation radiation of positrons in freon.
x——real counts, after subtracting randoms ; o- - -random counts.

various points at distances of 1" - 3" from the iodide crystal, and the spectra examined. The Hg^{203} and Cs^{137} sources were likewise examined (screened where necessary from conversion X-rays). The spectral distributions did not vary appreciably, the variation in the ratio peak counts to total counts being less than about 5%.

For the determination of the delayed coincidence spectrum, the nuclear γ-ray channel was delayed by 25 metres of cable. This working point is the point + 25 in fig. 27 (produced) and in figs. 28, 29. The delayed coincidence pulses obtained under these circumstances at the Kicksorter cathode ray tube were photographed. Pulses clear of the 140 KeV threshold amployed were recorded. The spectra of the random coincidences were obtained by transferring the 25 metres of delay cable to the other side, i.e., to the iodide channel. This point is the point -25 on fig. 27 (produced back). The random pulses should show up the characteristics of the total radiation picked up from the Na^{22} source and from annihilation in the gas and surroundings.

The results obtained with oxygen in the gas container at a pressure of 2.4 atmospheres at room temperature are illustrated in fig. 30. The random counts are shown dotted. The real counts after subtracting the random counts point for point are shown by the full line. An annihilation peak at 510 KeV is seen. A low energy bulge corresponding to that in fig. 25 appears, but which is more prominent in height. The reasons for this are given below.

The results for freon in the container, at a pressure of 5.2 atmospheres, at room temperature are shown in fig. 31. The random counts are here relatively less in number. The full curve again shows/

shows the real counts after subtraction of random counts,, point for point. Here the 510 KeV radiation peak is absent, and the presence of a broad band of energies is clearly indicated. The precise shape and its relation to the theory are examined in detail below.

(v) Analysis of results and comparison with theory.

For oxygen, in fig. 30, the height of the 510 KeV peak is lower, relative to that of the low energy bulge, than it is for the spectral curve of fig. 25. The width of the 510 KeV peak at half height in fig. 30 is however greater. (20%, compared with 14% for fig. 25). This increased width is due to slight variation in gain over the several hours of running time involved in the measurements and to a lesser extent to a slight gradual deterioration in the crystal since the experiments first began. The lowering in height is in great measure due to the increased width. There are other factors which accentuate this lowering. The displacement of the resolution curve with pulse energy in the iodide crystal (cf. iii) would cause a further 10% rise in the low energy pulses. Also measurements on scattering suggest an additional rise of 5% at the lower energies, particularly from the neighbouring toluene scintillator. It therefore seems clear over the range examined that γ-rays of energy 510 KeV only are emitted from the annihilation of positrons in oxygen.

The precise shape of the freon curve will be discussed. The Ore - Powell theoretical curve for the distribution of γ-ray energy in/

Fig. 32

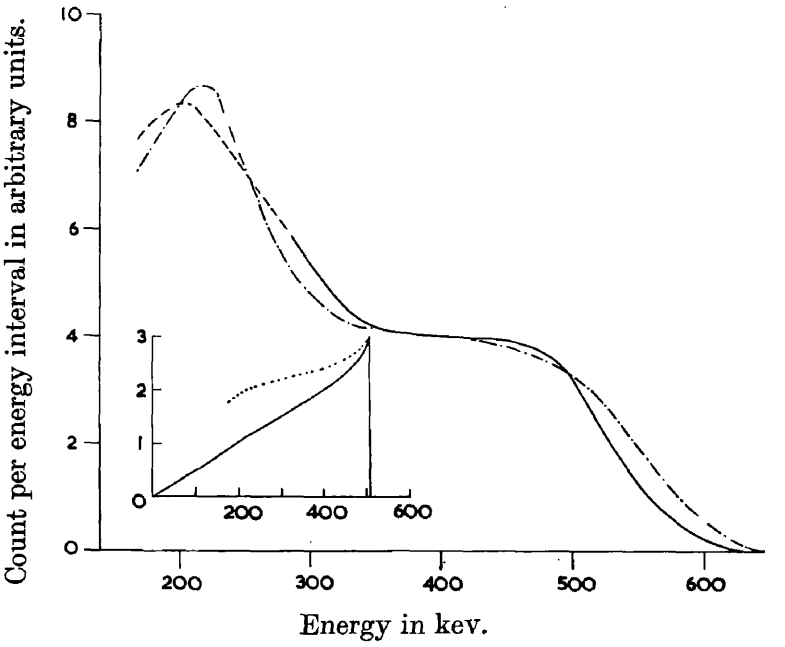

Main curves——-- Pulse height distribution expected ;
.—.—.—. Experimental curve of fig. 5.
Inset :-———Ore–Powell theoretical curve for three-quantum annihilation ;
..... expected photon response with particular NaI crystal.

in three quantum annihilation is shown in fig. 32 inset. The iodide crystal absorbs the lower energy quanta preferentially and this preference is slightly increased by the nearness of the source points to the crystal. The dotted inset curve shows the relative numbers of γ-rays which would be absorbed by the crystal in the range considered. The curve was computed using the absorption data given by Heitler (1947) (cf. too introduction).

In considering the electron energy distribution which would be produced in the crystal, allowance has to be made for the fact that more electrons are produced in the peak for the lower energy γ-radiations, primarily because of the increased importance of the photoelectric effect. The ratio of electrons in the peak to the total number energised were 0.35, 0.43, 0.65 for the 660, 510, 280 KeV radiations referred to previously. The expected electron spectrum not allowing for varying peak widths is shown in fig. 32. The lower energy portion is shown by dashes and involves slight extrapolation, but the errors are estimated at less than 5%, this part of the curve being essentially correct in shape. The experimental curve of fig. 31 is shown for comparison and is in close agreement with the theoretical predictions of Ore and Powell over the range studied.

The probability of two quanta registering simultaneously has not been introduced. For most of the radiations would come from positrons near the source, both for freon and oxygen. Again two quanta running close together are not favoured from an inspection of the phase space aspect of any theory. The phase space allocated per unit solid angle for three annihilation radiations K_1, K_2, K_3 is/

is (cf. Ore and Powell 1949) $\rho = \alpha K_1 K_2 K_3 dK_1 dK_2$, where α is a normalisation constant. The full Ore-Powell theory obtained by multiplying this expression by transition matrices shows a little more tendency for smaller angular spacing than the statistical estimate, (cf. too Siegel , Deutsch (1953)).

(vi) Discussion.

The experimental results for freon, and the Ore-Powell curves, have been shown to be in close agreement. To establish the experimental verification of the theory reasons should be advanced for believing that the long period decay in freon is associated with only triplet bound electron positron states.

Annihilation from a triplet state has to be a third order process (cf. § 2), unlike that from bound singlets. It is therefore likely to be slow. Furthermore at the high densities involved in the experiment, annihilation of free positrons was expected to be very fast (cf. too oxygen and § 4). That it is so in fact is proved experimentally in (vii). This latter would occur, of course, with two and three quantum processes in competition. Again the small pressure dependence of the annihilation time indicates that few triplets are converted to singlets by collision, so that the state must be close to pure triplet. Confirmation of the state and verification of the theory comes therefore from the proximity of the experimental value in freon of the decay time to the theoretical Ore-Powell triplet time of 1.4×10^{-7} sec, and the closeness of the experimental and theoretical spectra associated with these times. It should be mentioned that theoretical calculations

leading/

leading to lifetimes for the triplet bound state have been given by Radcliffe (1950) confirming these predictions, also by Lifshitz (1948) and by Ivanenko and Sokolov (1948) who calculated lifetimes of 8.8×10^{-8} sec. and 6.4×10^{-7} sec. respectively.

Consider the case of oxygen on the other hand, with a pressure dependent lifetime, having a value near 8×10^{-8} sec. at 2.4 atmospheres. If there were any triplet positronium, the lifetime against annihilation could be reduced by transitions to the singlet state (which latter annihilate in 10^{-10} secs). If the 8×10^{-8} sec. period were associated with such triplet states, an appreciable amount of them would have to be present. But the spectrum associated with this period showed no sign of them. It would therefore seem that the 8×10^{-8} sec. period in oxygen does not involve positronium. It could arise from positrons annihilating by collisions and this can include the possibility of forming positive ions with subsequent annihilation.

Lastly reference should be made to the annihilation time in oxygen. Using formula (10) and assuming all electrons available, the lifetime of positrons in oxygen would be 1.5×10^{-7} sec. The lifetime is shorter than given by the formula, still more so as the inner electrons are not readily reached. This is found to be true for the fast period in freon also (cf. vii) and for the solids (cf. § 4(i)).

(vii) Fast annihilation processes in freon.

The existence of a triplet state of positronium enables one to/

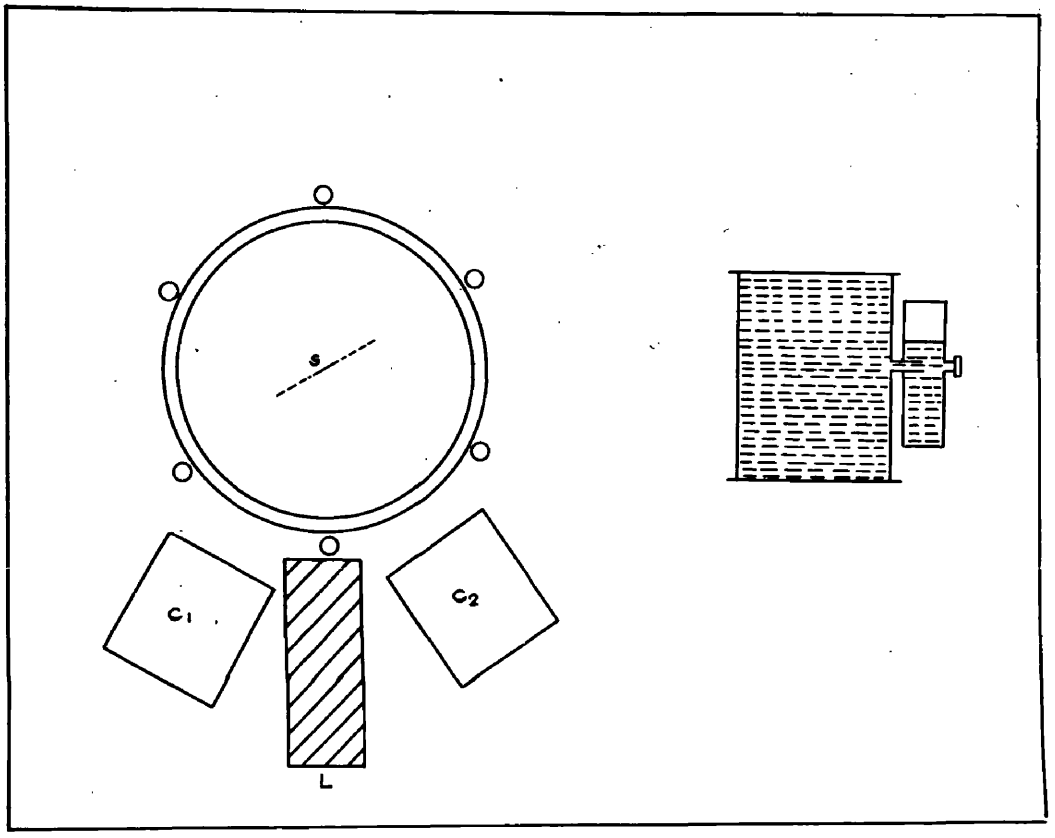

Fig. 33a. Diagram of one arrangement used for determining the fast annihilation time for positrons in freon.

Fig 33b Construction of a scintillator cell.

to infer the probability of existence of the singlet state also. It seemed desirable to look for, and examine, the fast decay in freon, even though it might involve at least two processes, viz., singlet decay and collision annihilation. Experiments by Pond, (1952), using nitric oxide to quench the triplet state indicated that in the gases examined by him, viz., hydrogen, nitrogen, argon, and helium, only about 1/4 of the annihilations involved triplet positronium. Singlet formation can be expected to be three times as rare as triplet formation. At high positron energies, however, triplet positronium might break up by collision before annihilation so that the ratio of singlet annihilation to triplet may greatly exceed 1/3.

A thin source of Na^{22}, ~5μ.c. in insulin, was mounted on aluminium foil 0.25 mgm/sq.cm. The thickness of the source and insulin was shown to be less than 0.25 mgm/sq.cm. The thickness limit was determined by partially collimated α-particle absorption measurements using a zinc sulphide scintillation counter, sensitive only to α-radiation. (Further the sodium was known to be present as sulphate, and apart from possible sodium impurity in the initial magnesium target (from which the source was produced), the source thickness was known to be considerably less than the figure above. The optical appearance of comparison layers of ordinary inactive sodium sulphate on aluminium confirmed the above limit). The source was placed at the centre of a gas chamber 4" diameter and 6" long as shown in fig. 33, one of the experimental arrangements used. The source occupied a rectangular area 1 cm. wide by 2 cms. long, its length being parallel to that of the gas cylinder. The aluminium/

Fig. 34. Delayed coincidence curves showing fast positron annihilation in freon, and specifying directly the triplet positronium abundance.
x - - Annihilation in aluminium (1.28 Mev γ-ray of Na^{22} and annihilation radiation)
o——— Annihilation in freon (1.28 Mev. γ-ray of Na 22 and annihilation radiation).

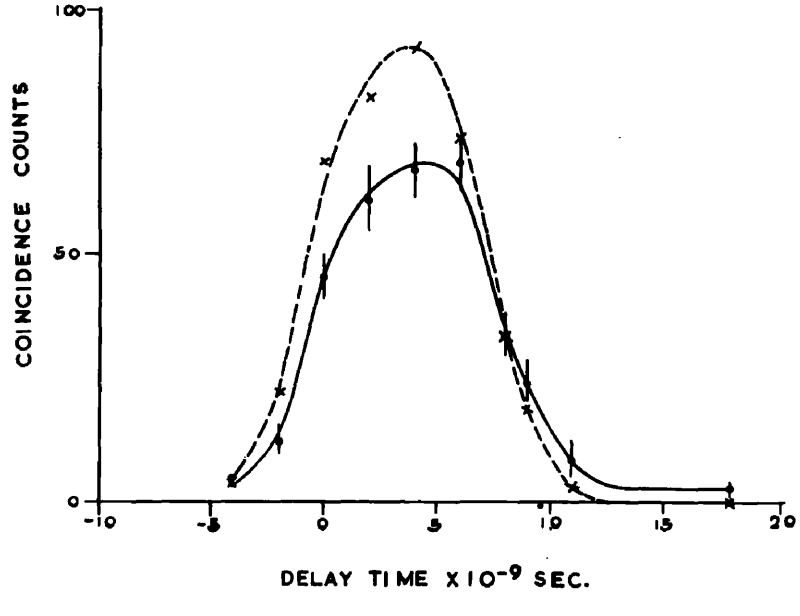

aluminium foil was 1½" wide by 2" long, its length being also parallel to the lengthof the gas cylinder. The foil was supported on a wire (30 SWG) bent to form a rectangle. The source could be covered by aluminium plates, or alternatively the gas chamber could be filled with freon at various pressures. At a saturation vapour pressure of nearly 5 atmospheres about 95% of the positrons annihilated in the gas. (This was shown by absorption measurements in a separate gas chamber with a window, in which the number of positrons reaching an anthracene scintillator crystal inside was determined, at various pressures).

In the arrangement of fig. 33, one counter picked up the 1.28 MeV nuclear γ-radiation, the other picked up the annihilation radiation. A lead block screened the two counters from Compton effects. Pair production by the nuclear 1.28 MeV γ-radiation in lead was of no account because of the heavy biassing of the discriminator in the 1.28 MeV γ-counter and because of the attenuation in the lead. The counters used terphenyl in toluene liquid scintillator cells (the cells are shown in fig. 33b, designed to eliminate the presence of a bubble in the main compartment whatever its position, the side compartment being painted black; sealing is done with polythone plugs).

One of the several pairs of delayed coincidence curves obtained by this method is shown in fig. 34, with a freon pressure of 4.5 atmospheres at 25°C. The period is immediately seen to be very short. Also the difference between the maximum ordinates (or better the areas, correcting for the tail) indicates approximately

the/

the number of positrons decaying three quantum-wise from the long lived triplet state. It is 25%. The centroid shift associated with the fast period or periods, as observed, was $4 \pm 2 \times 10^{-10}$ sec. The time for positrons to come to rest in the gas is probably $1 - 2 \times 10^{-10}$ sec. The lifetime of positrons in aluminium, as indicated in § 4 is near 1.6×10^{-10} sec. Assuming the fast period or periods to be associated with two quantum annihilation, the lifetime would seem to be less than about 6×10^{-10} sec. This period is exceptionally fast, far shorter than expected from ordinary collision. Some of it is certainly to be associated with singlet positronium, though some of it may be due to a collision process analogous to ion formation. On reducing the pressure to 2 and 1 atmospheres evidence of very small successive shifts to longer lifetimes occurred. The main results given above have been obtained too with a slightly thicker source and with one of different origin.

In a recent article Deutsch (1953) quotes the fraction of positrons forming positronium in the case of freon to be around 25% from the results of a quenching method.

It is necessary to refer to the energy restrictions on formation of positronium. The ionisation energy of positronium is 6.8 ev. (cf. Ruark 1945). The ionisation energy F of freon is 11.7 ev. (Baker and Tate (1938). Only if the positrons have an energy exceeding (F - 6.8) can formation of positronium be expected.

Deutsch (1953) has suggested the explicit ratio (F - 6.8)/F as a rough measure of the amount of triplet state in several gases.

§ 4/

§ 4 ANNIHILATION IN CONDENSED MATERIALS, NUCLEAR LIFETIMES, CONCLUDING REMARKS.

(i) Comparison measurements on annihilation times and their consequences.

As mentioned in the introduction, the theory of positron annihilation as given by eqn.(10) predicted a lifetime proportional to electron density, though it was realised that the positive charge near the core would reduce the number of electrons available to slowly moving positrons. Experiments to determine the comparative and absolute lifetimes in various condensed materials seemed important.

The lifetimes of positrons in various materials may be compared, by obtaining sets of delayed coincidence curves between the nuclear γ-ray of Na^{22} and annihilation radiation for any two of the materials in succession; (spurious Compton coincidences being minimised); using this method (cf. Ferguson and Lewis (1953) cf. preface) positron lifetime differences of less than 5×10^{-11} secs. were indicated for the metals, aluminium, magnesium, and iron compared to lead. Centroid shifts of $\sim 2 \times 10^{-10}$ secs. for mica, wax and water relative to lead indicated a longer positron lifetime in these materials. Reference too should be made to the further work of de Benedetti and Richings (1952), (cf. introduction §3, iii) published in this field in the meanwhile.

Assuming all the electrons are available in the metals, eqn.(10) would give the absolute lifetime values for lead, aluminium, magnesium/

magnesium and iron as 0.6×10^{-10}, 1.8×10^{-10}, 2.7×10^{-10}, 0.7×10^{-10} secs. respectively. If valency electrons only are available the absolute lifetimes could be 10×10^{-10}, 8×10^{-10}, 16×10^{-10}, 9×10^{-10} secs. respectively. As has been mentioned in § 3, there is evidence that the innermost electrons do not contribute to the slow annihilation of positrons. Du Mond, Lind, and Watson (1951) examined the width of the annihilation line from positrons annihilating in copper. The results based on Doppler broadening, suggested that only valency electrons played an essential part in the process. Assuming the positron to be almost at rest in the metal, they deduced the electron energy at annihilation as 16 ev corresponding to the conduction electrons. Confirmation of the dominant role of the outer electrons follows from the angular correlation experiments on the two γ-rays by De Benedetti, Cowan, Konneker and Primakoff (1950)for instance, leading to similar electron energies.

It seemed possible that the domain structure of iron would produce a slightly longer period, since the d-shell electrons would have their intrinsic spins orientated. The fact that iron lines up with the other metals indicates that the d-shell electrons do not decisively influence the annihilation process. This again tends to support the role of the valency electrons.

It could therefore be that singlet bound states are formed, of lifetime 10^{-10}secs; at any rate the simpler process neglecting positron electron attractive forces did not fit the facts. The determination of the absolute time of annihilation in the solid state/

state, as opposed to the comparison methods became therefore a matter of urgency. Experiments to determine the absolute decay time are discussed in (ii).

Meanwhile another line was investigated. The experiments on the gases substantiated the existence of a triplet bound state in gases. This indicated the possibility of a triplet bound state in condensed materials. Moreover as discussed above there was a possibility of explaining the two quantum emission of the metals by singlet positronium formation. A search was therefore made for a second period in metals, particularly in iron, using various resolving times, and also with a magnetic field applied. One counter accepted the nuclear γ-radiation, the other could accept radiation of the continuous type from triplet annihilation, if any. No delayed coincidences were obtained above the random rate.

Bell and Graham (1952) searching for a similar effect reported the existence of a second period in some non metals. The earlier measurements on non metals here had not been continued to the long delays necessary for determination of a second period.

The examination of the second period in certain materials seemed desirable, to determine its dependence on the mode of preparation and treatment., also to find out if any three quantum annihilation could be associated with it. For distrene (cf. Ferguson and Lewis (1953) by the comparison method, eqns.(16b) and (16c) of § 1 give about $\frac{1}{4}$ of the positrons associated with a second period of 2.5×10^{-9}secs. Results of similar type have been reported by Bell and Graham (1953). It is of interest to note/

note that the amount of second period decay is very close to that found for freon (viz., 25%). For investigating three quantum annihilation, two methods appeared appropriate both employing Cu^{64} as source. The first employs three counters, e.g., at 120°, operating a slow coincidence unit. The second utilises two counters at 180°, about 20 cms. apart; the change in the two quantum coincidence rates when annihilation occurs in distrene and in aluminium being noted. With these methods (cf. Ferguson and Lewis (1953)) small effects were indicated, but certainly less than 2% of the annihilation was three quantum wise. This result is not unexpected. The short second period compared with the undisturbed triplet decay rate of 1.4×10^{-7} sec. indicates that about $\frac{1}{2}$% of three quantum radiation might be emitted. (Experiments recently reported by Pond (1954) accords with such reasoning, only a few triplet states survive therefore in sheltered places of the lattice). Of course some three quantum annihilation should occur on collision theory (cf. introduction) and reference can be made in this connection to the searches for triple coincidences in copper by Rich (1951) and Stone (1952).

(ii) Absolute determination of positron lifetime; allied work.

As indicated in § 1 (iv) the positioning and form of a resolution curve depends on the energies of the pulses in the two counters. An example of this was given in fig. 27. The above comparison methods in (i) have all involved comparisons based on 1.28 MeV - 0.51 MeV coincidences. To obtain an absolute lifetime determination/

Fig. 35

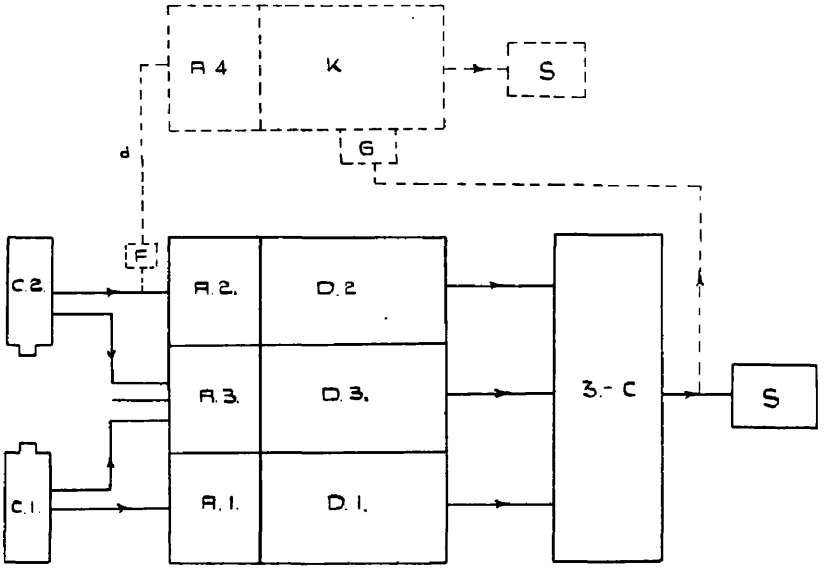

Block diagram of apparatus. Full line shows basic apparatus. Dashed line shows later additions. C.1, 2—counters; A.1, 2, 3, 4—amplifiers; D.1, 2, 3—discriminators; K—kicksorter; 3–C—triple coincidence unit; F—cathode follower; G—gate; d—1·25 μsec delay line.

determination involves comparison with a source of prompt or nearly prompt events generally having different energies from 1.28 Mev and 0.5 Mev. One possible standard involves the two annihilation quanta from Cu^{64}. The most suitable comparison source appeared to be Co^{60} having γ-ray energies of 1.17 and 1.33 MeV, (near 1.28 Mev, on either side of it). The $\gamma-\gamma$ cascades involve two electric quadrupole transitions (cf. introduction and Ch. 3). The lifetime of the intermediate state in Ni^{60} (cf. introduction eqn. (8)) could be expected to be less than 10^{-11}sec. The measurements below indicate that it is in fact less than a few times 10^{-11}secs. (Recently Bay, Henri, and McLernon (1954) have reported it less than 10^{-11}sec.). The Na^{22} γ lifetime can also be expected to be shorter than 10^{-11}sec, if it be dipole or electric quadrupole. A higher order transition would be expected to show a lifetime readily detectable. The comparison with Co^{60} should lead to the annihilation time of a positron (cf. Ferguson and Lewis (1953)). The mean pulse height distribution from the two Co^{60} radiations and from the 1.28 MeV γ-ray of Na^{22} could be expected to be similar. This was shown to be the case with the 1" diam. 1" long scintillator of terphenyl in toluene, in the pulse energy range passed by the side channel discriminator concerned. In the other channel it is then necessary to select only a narrow range of pulses.

The full apparatus is shown in fig. 35, Essentially it implies kicksorting after mixing. The arrangement bears some relation to that used in fig. 26, with the kicksorter fulfilling a different purpose/

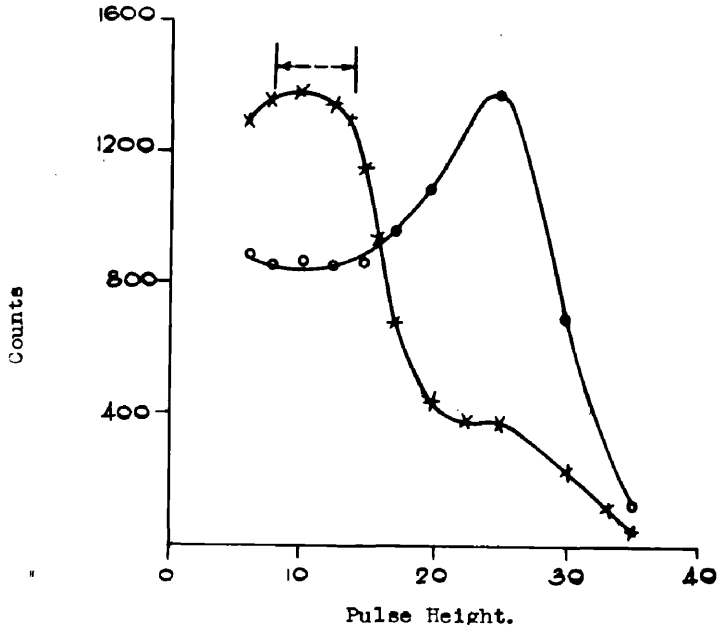

Fig. 36. Pulse height distributions due on the one hand(x-) to the γ- ray of Na^{22} and the annihilation radiation of its positrons in aluminium, and on the other hand (o-)to the γ-rays of Co^{60}. The kicksorter setting is indicated.

Fig. 37.

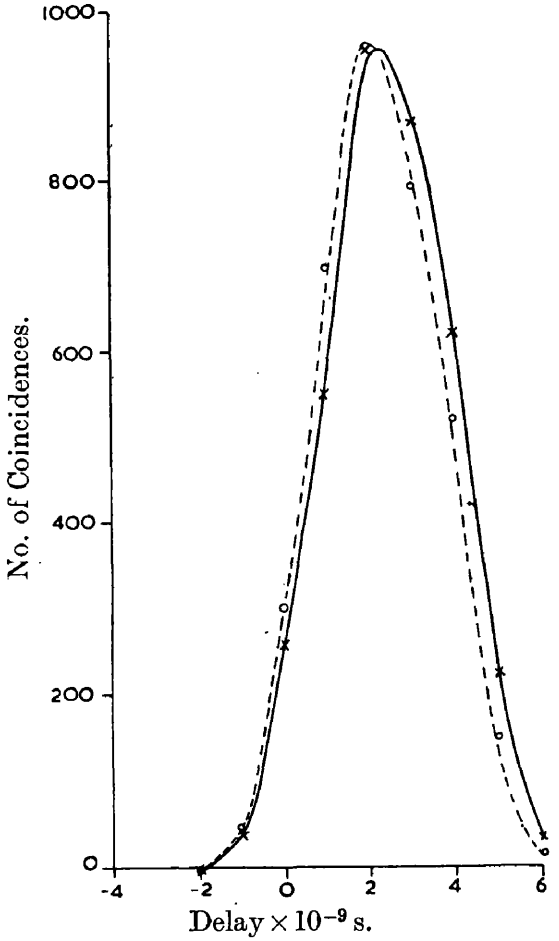

Coincidence resolution curves of coincidences between
×—— 1·28 Mev γ-ray of ^{22}Na and 511 kev annihilation radiation from aluminium.
○- - - 1·17 Mev and 1·33 Mev γ-rays of ^{60}Co.

purpose. The method of taking resolution curves is essentially related to that used in obtaining fig. 27, and in this respect stems from this earlier work. Counter C_1 can handle in turn the nuclear γ-ray of Na^{22}, or either of the γ-rays of Co^{60}. Counter C_2 received either the $\frac{1}{2}$ MeV radiation from the annihilating positrons of Na^{22}, or the other of the γ rays of Co^{60}, at a coincidence. Only those counts from the triple unit which correspond to a selected narrow range of electron pulses in C_2 are recorded in the scaler system linked with the Kicksorter channel. This band was positioned where the pulse height distributions associated with the $\frac{1}{2}$ MeV and Co^{60} γ-rays were both fairly flat. Fig. 36 shows the spectra and the approximate channel setting. The pulses fed to the Kicksorter were of order 10^{-7} secs. duration here. So a delay of order 1 μ.s. was inserted by using Z.14M cable appropriately terminated, so that the pulses might coincide with the opening of the Kicksorter gate activated by the triple unit output.

The thin Na^{22} source of weight $\sim$ 1 mgm/sq. cm.^{2} mounted on aluminium was placed between aluminium plates. The Co^{60} source was of much the same strength. Fig. 37 shows a set of delayed coincidence curves taken with the two sources in turn. Several runs, in succession, were made. Each pair of curves took about two hours with counting rates of a few hundred per minute at peak. Errors were mainly due to possible energy drifts of the side channels. The centroid shift obtained from this and analogous arrangements was $(1.6 \pm 0.6) \times 10^{-10}$ sec. It should be noted that either γ-ray from Co^{60} (unlike Na^{22}) can activate either counter first. The curve for/

for Co^{60} is in fact the sum of two resolution curves. The centroid shift of fig. 37 is not then a function, to a first order, of the Ni^{60} lifetime; however because the curves of fig. 37 lie very closely at the larger negative delays, the lifetime of Co^{60} is seen to be extremely small. Bearing in mind the earlier remarks on Na^{22}, the positron lifetime in aluminium is therefore $(1.6 \pm 0.6) \times 10^{-10}$ sec. This agrees well with the value obtained by Bell and Graham (1953), $(1.5 \pm 0.3) \times 10^{-10}$ sec. using a different method. (Minton (1954) has reported in an abstract a value of $(2.9 \pm 0.3) \times 10^{-10}$ sec.)

It follows from these measurements that the absolute time in most materials investigated particularly the metals is very short. It would appear that capture of the positron by the electron, or at least distortion of the wave function somewhat analogous to capture, can occur (cf. too § 2). The time period in the metals is certainly close to that predicted for the singlet state.

The above method could be readily extended to determine lifetimes in γ cascades or allied processes, for instance employing two annihilation $\frac{1}{2}$ MeV γ radiations as prompt standard. A band of energies would be selected from counter 1 also. With the particular cathode ray tube type of Kicksorter used here this affords no difficulty for pulses from channels 1 and 2 can be associated with X and Y deflections on the tube face. These pulses are brightened at a fast coincidence, the output scaler being associated with a required region of the XY plane of the tube.

CHAPTER 3

γ-RAY ANGULAR CORRELATIONS

CHAPTER 3: γ-RAY ANGULAR CORRELATIONS.

§ 1 THE EXPERIMENTAL METHOD, AND THE CASCADING RAYS OF Co^{60}

In the work of the previous chapter, the angular correlation between the simultaneous γ-rays emitted has been a dominant feature. The work in this chapter refers to correlations between successive γ-rays from a nucleus.

The theoretical basis underlying double cascade processes has been referred to in the introduction. As mentioned there to investigate the experimental method, work of an approximate nature on Co^{60} was carried out in the first instance.

In this experiment single crystals of naphthalene-anthracene, containing about 5% of anthracene were used as detectors, 2" diam. x $1\frac{1}{4}$" thick(In the making of these the author wishes to acknowledge some assistance from Mr. F. A. Black). Each crystal was packed in magnesium oxide and mounted on 1" cathode E.M.I. tubes using a $\frac{1}{2}$" length of perspex cylinder as junction. At the time in question (cf. introduction §4 ii)2" cathode tubes and efficient liquid scintillators had not been developed. To guard against spurious scattering particularly near the 90° position of the counters, (cf. Brady and Deutsch, 1947, 1948), some lead shielding 1/32" thick was placed around the sides, and a disc $\frac{1}{8}$" on the outer face of the crystals, and the discriminators employed set appropriately. The counters were raised above the table level using light supports. The cylindrical surfaces of the crystals faced the source of cobalt, which/

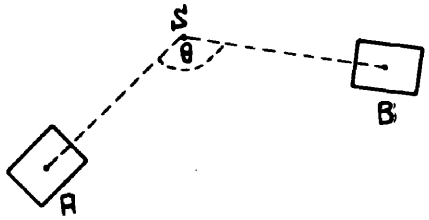

Fig. 38. γ-γ angular correlation.

which was in the form of metal of about 4 sq. mm, placed slightly below the centre of the crystals to reduce source absorption effects. The crystals were situated with their centres 6" from the source; one counter was kept fixed and the other could be rotated about the source, at a fixed distance from it, with a constant orientation. The γ-rays of 1.17 and 1.33 MeV could activate either counter. The resolving time used was 10^{-7} sec.

It is necessary to discuss the coincidence rates recorded in the two counters, when the two γ-rays are not distinguished. Let fig. 38 represent the conditions with a point source. Suppose the source have N disintegrations per second. Let the centres of crystals A and B be distant respectively r_A and r_B from the point source. Then the mean counting rate per second in A due to one of the radiations $\gamma 1$ will be:

$$N \frac{A}{4\pi r_A^2} \cdot \varepsilon_A'$$

where A is the cross sectional area of the crystal A, and ε_A^1 an efficiency factor (slowly varying with r_A). Let ε_A^{11} be a similar efficiency factor for the other radiation $\gamma 2$ in the crystal A. Let ε_B^1, ε_B^{11} be the factors for $\gamma 1$, $\gamma 2$, in the crystal B. Then the counting rate in A will be N_A per second, and in B will be N_B per second, where:-

$$N_A = N \frac{A}{4\pi r_A^2} \cdot (\varepsilon_A' + \varepsilon_A'') \; ; \quad \text{and} \quad N_B = N \frac{B}{4\pi r_B^2} (\varepsilon_B' + \varepsilon_B'') \qquad \ldots(19a)$$

If the variation of the angular correlation function $f \equiv f(\theta)$ over the solid angle of the counter be neglected, at least in the first instance, the coincidence rate Nc/sec is then given by:

$$N_C = N \cdot \frac{A}{4\pi r_A^2} \cdot \frac{B}{4\pi r_B^2} \cdot (\varepsilon_A' \varepsilon_B'' + \varepsilon_A'' \varepsilon_B') f \qquad \ldots(19b)$$

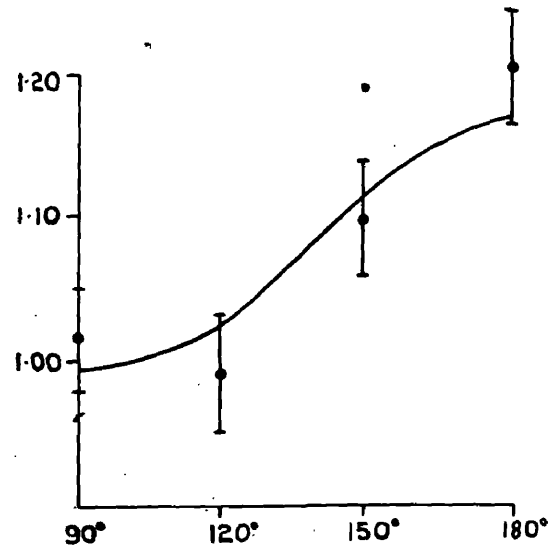

Fig. 39 . Co^{60} γ-γ angular correlation.

Thus $$f = \frac{N \cdot N_c}{N_A \cdot N_B} \cdot \frac{(\varepsilon_A' + \varepsilon_A'')(\varepsilon_B' + \varepsilon_B'')}{(\varepsilon_A' \varepsilon_B'' + \varepsilon_A'' \varepsilon_B')} \qquad (19c)$$

For exact concentricity $$f \propto \frac{N_c \cdot N}{N_A \cdot N_B} \qquad (19d)$$

Furthermore $f / \left(\frac{N_c \cdot N}{N_A \cdot N_B}\right)$ varies only slowly with r_A, r_B. These conclusions will be generalised in § 2 and will be required later.

{More accurately expressing $f(\theta)$ as a sum of Legendre polynomials $f(\theta) = \sum_{n=0}^{m} a_n \cdot P_n(\cos\theta)$, the variation of $f(\theta)$ over the solid angle can be allowed for (cf. Rose (1953)). For crystals symmetric about the lines joining their centres to the source, eqn. (19b) is replaced by:

$$N_c = N \cdot \frac{A}{4\pi r_A^2} \cdot \frac{B}{4\pi r_B^2} \cdot \varepsilon \cdot \sum_{n=0}^{m} a_n \cdot b_n \cdot P_n(\cos\theta).$$

where ε, b_n, vary only slowly with r_A, r_B; and depend on the sizes and absorption coefficients of the crystals, and $b_n \longrightarrow 1$ for small crystals. (19d) is replaced by:

$$\sum_{n=0}^{m} a_n b_n \cdot P_n(\cos\theta) \quad \propto^{l} \quad \frac{N_c \cdot N}{N_A \cdot N_B} \qquad (19e).$$

These corrections are referred to in § 2 later}.

The function f given by eqn. (19d) was determined experimentally. Making no correction for solid angle effects, preliminary measurements indicated an anisotropy ratio at 180° to 90° of 1.14 ± .04; further results are shown in fig. 39. The plotted function is

$$f(\theta) = \frac{1}{8}\cos^2\theta + \frac{1}{24}\cos^4\theta.$$

corresponding to a 4-Q-2-Q-0 transition. Taking the spin of Ni^{60} as zero, and the radiations to be pure dipole or quadrupole, no other/

other transition is compatible with the results. This agrees with the findings of Brady and Deutsch (1947, 1948) and others.

§ 2 ANGULAR CORRELATION OF γ-RAYS IN THE $B^{11} + p$ REACTION.

(i) Nature of the problem, and preliminary considerations.

The $B^{11}(p,\gamma)C^{12}$ reaction is one of the most suitable reactions for the study of γ-ray angular correlations. Furthermore at the time of the investigation only very little information existed on the spatial distribution of the γ-radiations.

γ-rays of approximately 4, 12, 16 MeV had been observed by Fowler, Gaerttner, and Lauritsen (1938) using 900 KeV protons with a thick target; (cf. too Walker (1950)). The energy measurements suggested that the 4 and 12 MeV. radiations were emitted in cascade, and that the 16 MeV. radiation was emitted in parallel. Furthermore the energy of the intermediate state involved was apparently, more exactly, 4.4 MeV above the ground state. This state could seemingly also be reached by other reactions (cf. for instance Terrell (1950)). The lowest resonance lies at 162 KeV and is narrow (cf., e.g., Morrish (1949)). There are also very broad higher resonances. They are now believed to exist at 670 KeV and 1370 KeV (cf. Huus and Day (1952)).

Jacobs, Malmberg, and Wahl (1948) reported observations on the angular distributions of the γ-rays just above the lowest resonance. A 10% assymetry was believed a better fit than isotropy. Further work was reported by Kern, Moak, Good, and Robinson (1951).

The/

The 12 MeV γ-ray distribution was given as about $(1+0.15\cos^2\theta_1)$, θ_1 being the angle made with the incident beam direction; the 16 MeV γ-ray was given as isotropic, the possible error being maybe more than 10%. The bombarding energy was not given but a figure of $\sim$ 200 KeV is mentioned by Ajzenberg and Lauritsen (1952) in a later review article.

There are many ways in which an angular correlation can be carried out in a reaction initiated by particle capture. It was decided to investigate the angular correlation when the directions of the γ-rays made the same fixed angle with the incident proton beam, this angle being as near to 90° as the experimental arrangement would conveniently allow (it was actually 100°). The correlation function was then dependent on the azimuthal angle between the two γ-ray directions. There was no necessity then from this viewpoint of distinguishing one γ-ray from the other, and no distinction was in fact made. The coincidence counting rate was then higher than it would be otherwise, this was very desirable in view of the low γ-ray yield at the lower set voltages involved, and particularly with the crystals available at the time of this experiment. (On the other hand discrimination against possible scattering was poorer without energy selection).

It is necessary to consider the coincidence counting rate due to two radiations γ_1, γ_2, in cascade when a third radiation γ_3 is also present, and to extend appropriately eqn. (19c). Suppose that $\left(k/1+k \right)$ denote the function of disintegrations resulting in the production of the radiation γ_3 (This factor K appropriate to the

16/

16 MeV radiation near the lowest resource was believed to be small {cf. Fowler, Gaerttner, and Lauritsen (1938)} and in fact is so.

Letting ε_A^+, ε_B^+ be the efficiency factors for this radiation and using the other symbols introduced in § 1, the coincidence rate can be deduced as before. If the variation in f over the solid angle be neglected (the extension can be examined as before);

$$f = \frac{N.N_C}{N_A.N_B}\left[\frac{(\Sigma_A' + \Sigma_A'' + \varepsilon_A^+ k)(\Sigma_B' + \Sigma_B'' + \varepsilon_B^+ k)}{(\varepsilon_A' \varepsilon_B'' + \varepsilon_A'' \varepsilon_B')(1+k)}\right] \qquad (20a)$$

where the expression involving the efficiency factor is only a slowly varying function of geometry.

Again: $$f \propto \frac{N.N_C}{N_A.N_B} \qquad (20b)$$

For a change in position of the source, e.g., where r_A and r_B alter, the main solid angle factors $\frac{1}{4\pi r_A^2}$ and $\frac{1}{4\pi r_B^2}$ are not involved. Only the slow variations in the efficiency factors produce error. Further K has no significance in these measurements. The geometrical arrangement of an angular correlation experiment therefore differs appreciably from that of an angular distribution measurement. In the angular correlation experiments on the boron reactions, proton beams, under the best working conditions, of $\sim$ 50 μa had to be used to generate the γ-ray flux necessary for the coincidence measurements, and apertures of order $\frac{3}{8}$" - $\frac{1}{4}$" diam. had to be employed. For an angular distribution experiment on the other hand a very fine slit, and emphasis on concentricity, are vital.

(ii) Experimental arrangement and procedure.

The/

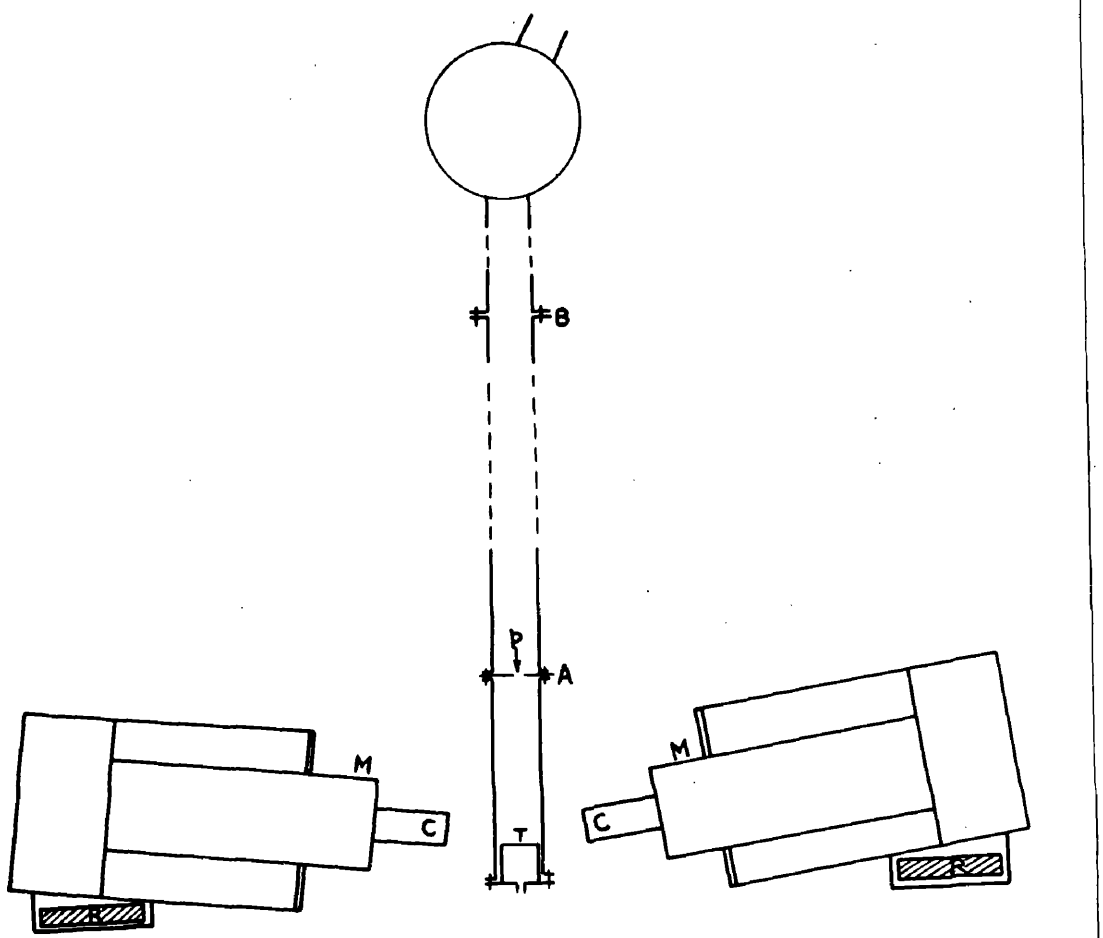

Fig .40a. Experimental arrangement: C-crystal, M-multiplier, R-track, p- proton beam, T-target, A-aperture plate.

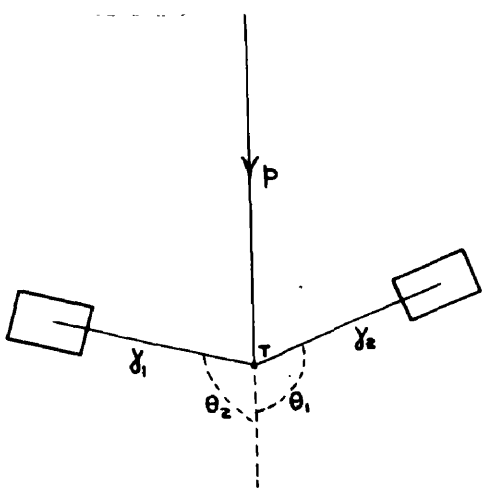

Fig. 40b Triple cascade geometry In the experimental arrangement $\theta_1=\theta_2$ .Azimuthal angle φ is $|(\varphi_1 - \varphi_2)|$ .Angle between the counters may be written θ'.

The target and counting arrangements are illustrated in fig. 40a. The beam of protons after deflection by a magnetic field travelled down a 1" diam. copper tube BA of length 24", in an approximately field free space before striking the aperture plate at A, which was water cooled. The aperture diameters used were $\frac{3}{8}$" initially and $\frac{1}{4}$" later. The beam tube below this was 5" long and 1" diam., of 1/32" copper. The target T projected into this about 1", the target backing was of 1/32" copper, cooled by water beneath. It was desirable to keep the distance between the aperture plate A and the target T short to prevent beam spread, possible scattering from the region of the aperture plate had however also to be considered. The target and its mounting were insulated from the beam tube so that later the beam could be found and positioned. The two copper tubes were aligned and the aperture centralised; it was convenient to centre the target backing position also.

The counters travelled on a raised circular aluminium track, which could be rigidly set in the cross sectional plane of the main beam tubes with its centre on the common axis of the beam tubes. The counters could then slide on this track at a constant inclination to the cross sectional plane. The scintillation crystals of the counters then remained at a fixed distance from the target centre and in a fixed orientation to it as the counter moved around the track. In each set of runs one of the counters was clamped in position, and the position of the other only varied. The azimuthal angle φ between the two counters was varied between 90° and 180° (cf. Fig. 40b).

Each/

Each scintillator consisted of a thallium activated sodium iodide block, $\frac{3}{4}$" diam. x $1\frac{1}{2}$" long mounted in paraffin in a perspex container, surrounded by aluminium foil as reflector. E.M.I. multipliers were used. The crystal blocks had their leading faces 2" from the target centre. The counters were tilted at a little over 5° to the cross sectional plane of the beam tube with the lowest points of the crystal level with the target as shown in the figure so that the γ-rays observed did not travel through the target backing. The lines joining the crystal centres to the target centre made therefore about 100° with the beam direction.

Amplified pulses activated disciminators which could operate a coincidence unit of resolving time 0.7 μ sec. The pulses were led through appropriate cables giving a relative delay of $2\frac{1}{2}$ μ secs to a similar unit measuring random coincidences. The true coincidence rate could be found. (The use of a coincidence unit of faster resolving time using large crystals of anthracene naphthalene mixtures had been contemplated but it offered no advantages at low proton energies and was not employed in these measurements). The single counting rates had to be measured at the same time, and generally required fast scaling units or their equivalent. A monitor counter had also to be employed. This used too a scintillation counter employing an iodide crystal $\frac{3}{4}$" diam. x $\frac{3}{4}$" long situated about 10" from the target. A beam swing of $\pm \frac{1}{8}$" would cause errors of order $\pm 2\frac{1}{2}\%$ at this distance. Scattered γ-rays from the main crystals to the monitor would not be important (the main crystals, and the monitor were on opposite sides of the target).

The/

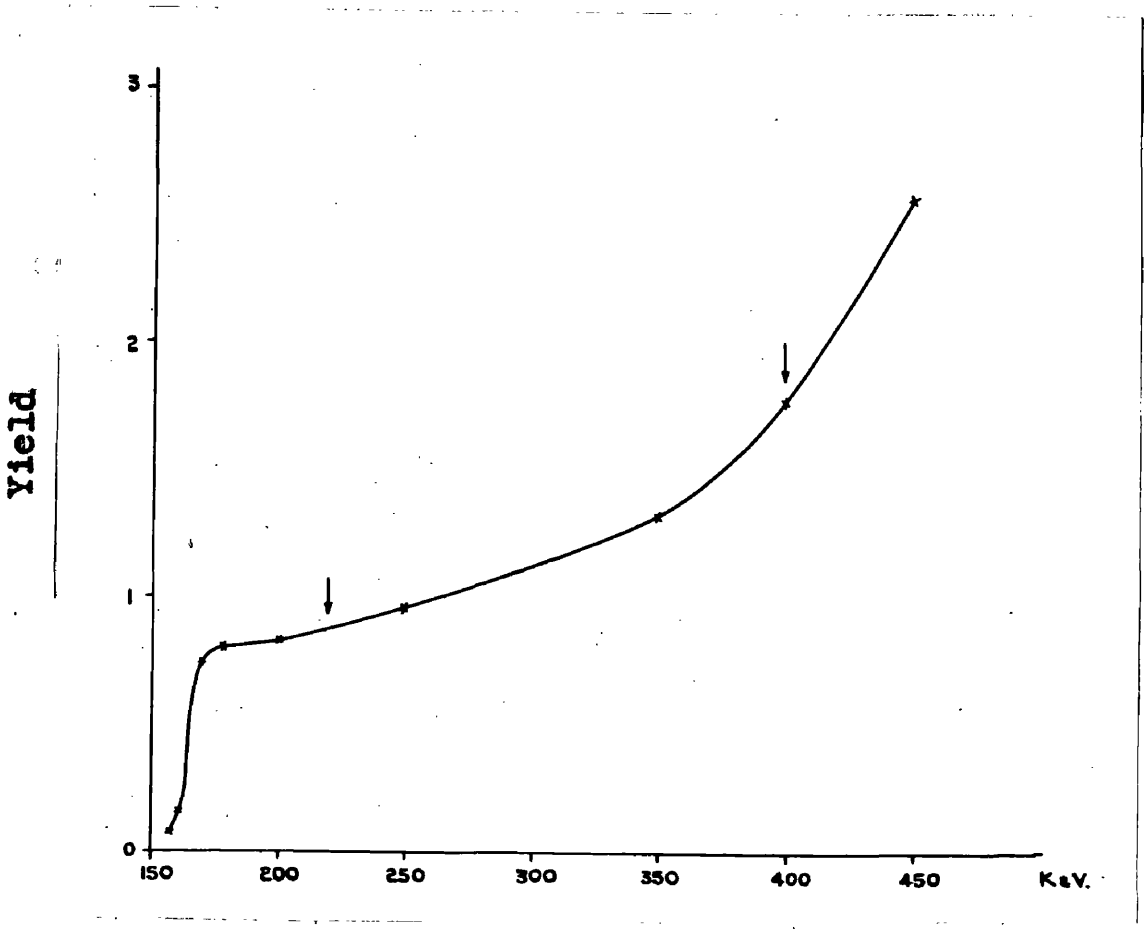

Bombarding energy.

Fig 41 Excitation curve: approximate thick target yield as a function of bombarding energy for the B^{11} proton capture reaction.

The discriminators activated by the two main counters were set to reject γ-rays of less than 1.2 MeV. Thus annihilation radiation from positrons at rest would be eliminated, and that from positrons in flight and bremsstrahlung, would be reduced. Compton scattering would be avoided for the angular separations used.

(iii) Experimental work and results.

A rough resonance curve for the thick target yield, as a function of target current measured on an integrator is shown in fig. 41. The yield is the mean of that measured by the two main counters biassed as in (ii). The 162 KeV resonance appears together with the subsequent slowly rising yield associated with the higher resonances.

γ-ray angular correlations were carried out with thick targets of boron at bombarding energies of 400 KeV and later of 220 KeV. At 400 KeV, less than 50% of the lowest resonance radiation was obtained. At 220 KeV ~ 94% of the radiation was associated with the lowest resonance. The maintaining of adequate beam current through the small apertures much below 220 KeV, (e.g., at 160 KeV), appeared difficult and experiments were not carried out at a lower voltage than this.

The coincidence counting rates immediately demonstrated that the 4 and 12 MeV radiations formed a cascade. Comparison of the rate with the single counting rates established further that the 4 and 12 MeV radiations were a dominant part of the emissions at these voltages. {γ-ray measurements by Huus and Day (1952), cf. too Ajzenberg/

Fig 42

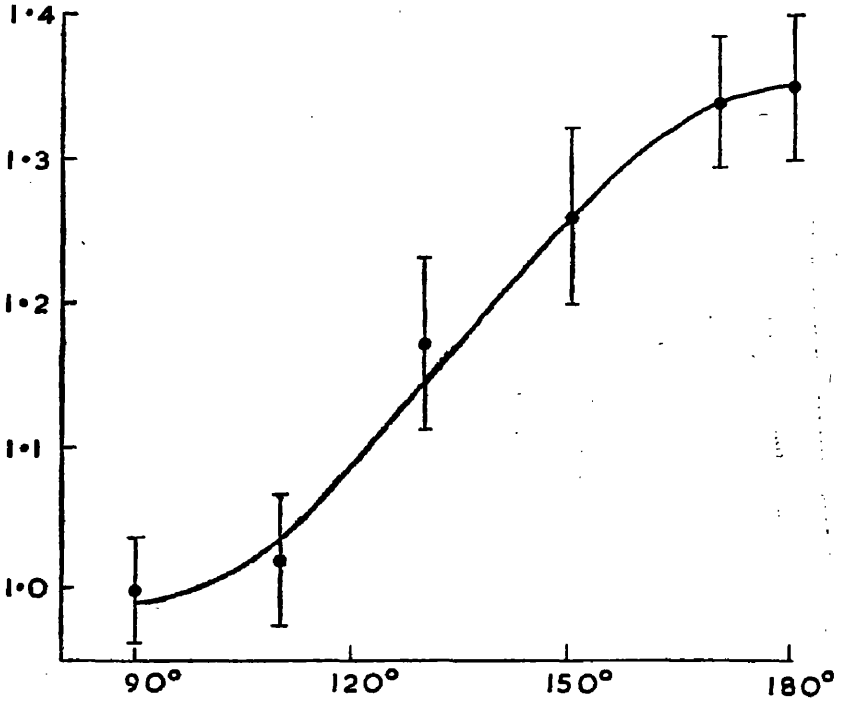

γ–γ angular correlation using 220 kev protons.

(using a thick target)

Ajzenberg and Lauritsen (1952) indicate that little 16 MeV radiation is associated with the two lower resonances.}

As discussed in (i) the angular correlation function is given by equation (20b). If N_B be associated with the counting rate in the fixed counter, in any given run, it was found experimentally that the ratio N/N_B, involving of course the monitor counter too, was a constant within the small drift errors of the amplifier and discriminator systems. The correlation function could then be taken as N_C/N_A. The counting rates N and N_B were always measured in all the runs as a check, though the correlation function used was N_C/N_A.

The yield at the 220 KeV working point was low and the random count rate / real count rate rarely exceeded 5% even with the larger aperture. At 400 KeV the ratio was some 10% - 15%, according to aperture size.

The work with 220 KeV protons is indicated first. Preliminary measurements were made using a $\frac{3}{8}$" diam. aperture. Later measurements were made using the $\frac{1}{4}$" aperture. The results were similar. Under the best conditions about 30 mins. running time gave about 250 coincidences with the $\frac{3}{8}$" aperture at a single setting of the moveable counter or about half this number with the $\frac{1}{4}$" aperture. It was necessary to take several runs with the fixed counter in various positions on the circular track. About three long runs were made with the $\frac{3}{8}$" aperture and two with the $\frac{1}{4}$" aperture. Fig. 42 illustrates the mean values obtained using the results for both kinds of aperture. The curve drawn is of the function $(1 + 0.365\cos^2\phi$

The/

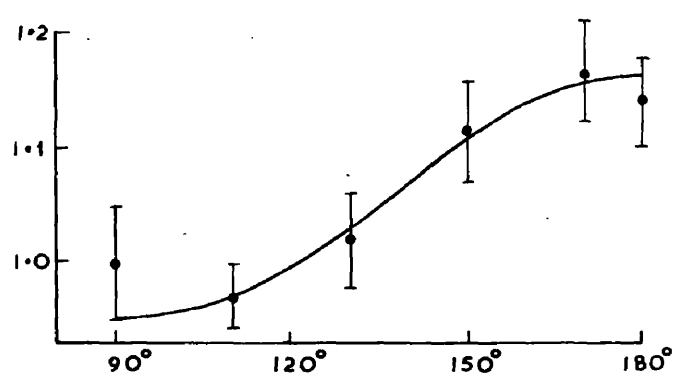

Fig 43 γ-γ correlation using 400kev .protons on boron. (using a thick target)

The estimated error was $\pm$ .06 $\cos^2\varphi$, φ being the azimuthal angle of one counter relative to the other. The best results with the smaller aperture favoured an anisotropy near the upper limit.

It was necessary to check on the spurious results which might arise from scattering, particularly from one crystal to the other, through the causes referred to in (ii), viz., by annihilation in flight and bremsstrahlung. The bombardment of Li by protons yields single γ-rays of 14 and 17 Mev only. A target of LiOH was there-bombarded by a small amount of protons near the lowest resonance energy. The coincidence rate N_C/N_A was obtained. It was low in the region 180° - 110° but showed a tendency to rise near 90°, where the counters are nearest together. Assuming that the scatter-ing in the boron case would be due to the 12 MeV γ-ray only (in view of the bias applied) and utilising the observations in the region 110° - 180°, a correction of 1½% was made giving for the mean result $\sim$ 38% anisotropy. (In retrospect, this correction could be as much as 3½%).

The measurements with 400 KeV protons were of a preliminary character, and mostly done with the larger aperture ($\frac{3}{8}$" diam.). The results are indicated in fig. 43. The curve $(1 + 0.22 \cos^2\varphi)$ is given for comparison, ignoring the 90° position. In this case there is clearly a decrease in anisotropy and evidence of interfer-ence effects which will be mentioned briefly below. This case will not be referred to quantitatively as knowledge of the higher resonance states is required.

In interpreting the results several points have to be borne in/

in mind, (a) the inclination of the γ-rays passing through the crystal centres is 100° relative to the beam direction, (b) allowance has to be made for the solid angle subtended by the crystals, (c) the voltage is off resonance. Restricting attention to the 220 KeV case, consideration of all these factors makes the anisotropy large. Considering first the correction (c), this can be shown to depend on the intensity of higher resonance radiation (cf. too vi); as the amount of the latter at 220 KeV is small ($\sim$ 1/16), this correction is a small one. The off resonance contribution is a function of energy (cf. vi); however, if the rather simple assumption is made that the fall in anisotropy to 400 KeV is typical a correction of about 3% could be expected from this cause. This makes the mean anisotropy which would have been measured at a bombarding energy of 162 KeV $\sim$41% or in the notation of Biedenharn, Arfken and Rose (1951)

$$W(100^\circ, 100^\circ, \varphi) = 1 + 0.41 \cos^2\varphi . \qquad (\sim \pm 0.06 \cos^2\varphi)$$

The correction (b), yet to be applied, depends on the assumed theoretical correlation function (cf. below). The discussion is initiated below:

(iv) Initial consideration of result.

The spin of B^{11} is 3/2 (Gordy, Ring and Burg (1948)) giving rise on proton capture to channel spins of 1 and 2. The γ-ray angular distributions at the time (§ 2 i) suggested that the C_{12} state formed was probably orientated. It was of interest however to compare the result in the first instance with the simple $\gamma - \gamma$ double cascade formula (12c), true for S wave protons, (and in special/

special cases only for higher wave protons (cf. below)). Considering only dipole and quadrupole transitions leading to a ground state of spin 0, only the transitions 2-D-2-Q-0 and 2-Q-1-D-0 give correlations approximating the experimental value, both giving $1 + 3/7 \cos^2\theta^1$ where θ^1 is the angle between the rays. (cf. Hamilton 1940). Moreover the transition 2-Q1-D-0 is less favoured than 2-D-1-D-0 and can be set aside. The predicted anisotropy for the experimental arrangement (between $\varphi = 90^\circ$ and $\varphi = 180^\circ$), allowing for the inclination effect (a), and solid angle effect (b), referred to above (cf. eqn. (19e), for the 2-Q-2-D-0 transition is only 35%. The experimental results at resonance indicate a higher anisotropy than this. Capture of higher wave protons leading to an orientated 16 MeV state has therefore to be considered, and the more general theory of triple cascade processes has to be invoked.

(v) Triple cascade processes.

The work described in the introduction §4, (i) has to be extended to include the case of two γ-rays in cascade following particle capture. The derivation of eqns. (21a), (21c) below is essentially due to Biedenharn, Arfken and Rose (1951). The essential linkage of the processes with the multipole order approach given in the introduction seemed however worth pointing out. Taking the incidence direction of the particle as Z axis of quantisation as before, $\chi_{m_1}^{11}$, (eqn. (11b)) gives the population densities of the states $(j_1 m_1)$ of the nucleus following capture. Let $(j_2 m_2)$ and $(j_3 m_3)$ denote the angular momentum and z momentum resolute of the states/

states following emission of the successive quanta $\vec{K_1}$ (θ_1,φ_1) and $\vec{K_2}$ (θ_2,φ_2) of multipole orders ℓ_1 and ℓ_2 respectively. Remembering the mode of derivation of eqns. (12a) and (12b)the chance W of a correlation for the given triple cascade can be written:

$$W = \sum_{m_1 m_3 p_1 p_2} \chi''_{m_1} \cdot \left| \sum_{m_2} \left(j_1 m_1 \middle| H(\vec{K_1} p_1) \middle| j_2 m_2\right)\left(j_2 m_2 \middle| H(\vec{K_2} p_2) \middle| j_3 m_3\right)\right|^2 \quad (21a)$$

Here $\sum$ refers to summation over the magnetic quantum numbers m_1, m_3 and the polarisations. The $\sum m_2$ summation exhibits the coherency.

The first matrix element in (21a), for instance contains the factor $(j_1,\ell_1,m_1,m_2-m_1 \,|\, j_2,m_2)$. Goertzel (1946) has shown that.

$$\left(j_1 m_1 \middle| H(\vec{K_1} p_1) \middle| j_2 m_2\right) = C\left(j_1 \ell_1 m_1\, m_2-m_1 \,|\, j_2 m_2\right) \cdot D^{\ell_1}_{m_2-m_1,\,p}(\phi_1,\theta_1,0). \quad (21b)$$

where C is a constant and $D^{\ell}_{m_2-m_1,p}$ are the $(m_2-m_1)^{th}$, p^{th}, elements of the rotational group:

The eqn. (21b) corresponds to the eqn.:

$$\sum_{p=\pm 1} \left|\left(j_1 m_1 \middle| H(\vec{K} p) \middle| j_2 m_2\right)\right|^2 = C_0^2 \left(j_1 \ell_1 m_1\, m_2-m_1 \,|\, j_2 m_2\right)^2 \cdot F_{\ell}^{\,m_2-m_1}(\theta).$$

used in deriving (12c) and shows the significance of the D elements in relation to the intensity functions F of the multipole fields.

Here $$\sum_{p=\pm 1} \left| D^{\ell_1}_{m_2-m_1\,p}(\varphi_1,\theta_1,0)\right|^2 = F_{\ell_1}^{\,m_2-m_1}(\theta_1).$$

The final formal eqn., derived by Biedenharn, Arfken and Rose (1951), taking $\varphi_1 = 0$, and $\varphi_2 = \varphi$, may therefore be written:

$$W(\theta_1\,\theta_2\,\varphi) = \sum_{m_1 m_3 p_1 p_2} \chi''_{m_1} \cdot \left| \sum_{m_2} \left(j_1 \ell_1 m_1\, m_2-m_1 \middle| j_2 m_2\right) D^{\ell_1}_{m_2-m_1,p_1}(0,\theta_1,0) \cdot \left(j_2 \ell_2 m_2\, m_3-m_2 \middle| j_3 m_3\right) D^{\ell_2}_{m_3-m_2,p_2}(\varphi,\theta_2,0)\right|^2 \quad (21c).$$

(vi) Discussion.

As/

As shown in (iv), the possibility of p wave capture has to be considered. Combination with the channel spins 1 and 2 can yield orientated states $J_1 = 1,2,3$. This C_{12} state is believed to be the same as that, associated with the same resonance, which gives an α and Be^8 nucleus, this latter giving two α particles. The Be^8 nucleus must therefore have even parity, (cf., e.g., Fermi (1950)), and therefore even spin. The C_{12} state involved would then have even J and even parity or odd J and odd parity. From the parity of B^{11}, the only state which can be expected from p wave protons is a 2^+ state.

The choice of the channel spin ratio and intermediate state remains. Taking into account the forbiddenness of the 16 MeV radiation, the intermediate state could involve only $J_2 = 1,2,3$. Eqn. (21c) has been explicitly determined for a 2-D-2-Q-0 transition by Biedenharn, Arfken and Rose, and the computation confirmed here. Not correcting for solid angle, the theoretical value appropriate is:

$$W(100^\circ, 100^\circ, \varphi) = (42.6-29.1x) + (0.4+0.6x)\cos\varphi + (0.7+21.2x)\cos^2\varphi \quad (22a)$$

where X is the channel spin factor $\left\{\alpha(1)/(\alpha(1) + \alpha(2))\right\}$ in the notation of eqn. (11b). The term in cos φ is a small one. The anisotropy ratio R between the values at 180° and 90° is then given by $R = 1 + (20.6x + .3)/(42.6 - 29.1x)$ (22b).

Making an approximate correction for the solid angle effect referred to as (b), on lines discussed in § 1, the observed ratio would be less, viz., R^1. R and R^1 increase with X. Some values of R and R^1 are given by:

X/

X	=	.50	.55	.60	.65	.70
R	=	1.38	1.43	1.50	1.58	1.66
R^1	=	1.35	1.40	1.46	1.53	1.61

The case x = .50 is that considered already in (iv), the magnetic substates of the initial state, $J_1 = 2$, being then equally populated.

If the figure of 41% be taken (cf. too later) for the anisotropy and if the error limit for this resonance estimate be kept as narrow as 6%, the 2-D-2-Q-0 transition could be predicted, with a channel spin factor x of $\sim 0.56 \pm .05$, the best results indicating the greater likelihood of the factor being near the upper value 0.61, (and considering the scattering correction).

Independently angular correlation measurements were published by Hubbard, Nelson and Jacobs (1952) for two different planes, different from the above, agreeing with a 2-D-2-Q-0 transition as above and permitting $.1 \leq x \leq 1$ and $.4 \leq x \leq .85$ respectively, viz.,

$$W(\theta_1, 0) = 1 + (0.39 \pm 0.15)\cos^2\theta_1$$

$$W(\theta_1, \tfrac{\pi}{2}) = 1 - (0.2 \pm 0.1)\cos^2\theta_1$$

in the notation of Biedenharn, Arfken and Rose (1951).

They also gave angular distribution results for the 12 MeV γ-ray agreeing with a 2-D-2-Q-0 transition but requiring x to be between 0.66 and 0.74, viz., the distribution

$$1 + (0.23 \pm 0.04)\cos^2\theta_1 \qquad \begin{pmatrix} \\ \text{cf. (i)} \end{pmatrix}$$

The α-particle distribution in the $(B^{11}p, Be^8\alpha)$ reaction studied by/

by Thomson, Cohen, French and Hutchison, indicates a 2-D-2-Q-0 transition with x near 0.7.

The angular distribution of the 16 MeV radiation has been anomalous, being near to isotropy near resonance (cf. (i)), instead of being anisotropic. It has been examined by Rutherglen, Grant, Flack and Deukars (1954), the abnormally low angular distribution has been associated with the interference between the radiations from the higher resonances developed at 162 KeV.

It is desirable in conclusion to indicate how an angular correlation of the above type, associated with a reaction product contrasts with that from a radioactive source, and to indicate qualitatively, for the sake of brevity, its relation to bombarding energy. It should be mentioned first that in these experiments little proton scattering occurs and the protons travel approximately in the initial direction, until well below the lowest resonance energy. For a thin target, or for a thin target element of a thick target, in this boron case, more than one compound nucleus contributes generally to the emission of γ-rays. Thus for a thin target at 200 KeV, say, competition arises between the two higher resonances with every single proton at capture; interference occurs and the angular correlation associated depends on the amplitude and the phase of the two states contributing.

For a thick target, each thin target element gives its quota independently, since the γ-ray energies differ; these quotas from the individual elements add in an intensity fashion (as opposed to emplitude). Since the radiations from 220 KeV protons on/

on a thick target are predominantly from the resonance energy, the contributions from the higher bombarding energies are of only small effect as has been stated earlier. With 400 KeV protons on a thick target the radiation from the 162 KeV resonance will produce its characteristic anisotropy, but superposed will be the contributions by intensity from the individual target elements. One last point; the radiation emitted at the lowest resonance energy region itself will contain a very small contribution ($\sim$ 1/250) from the higher resonances there, producing a small amplitude ($\sim$ 1/16 total) interference; no regard has been paid to this in comparing the lower resonance experimental values with equations (21c) and (22).

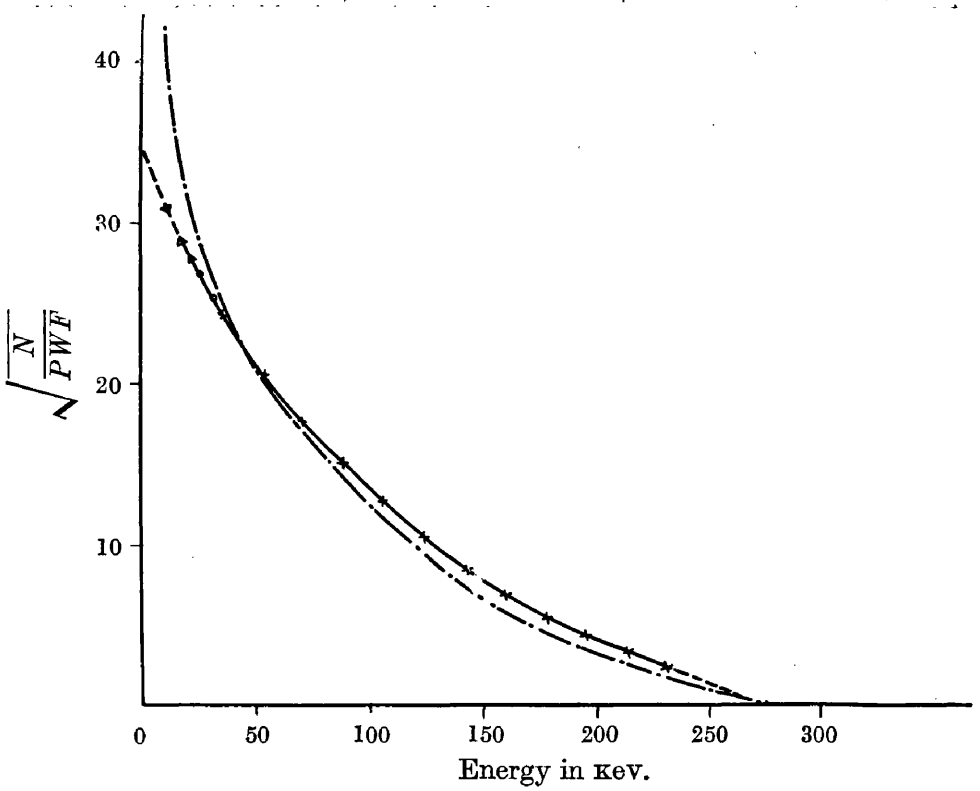

Solid curve —Fermi plot of ^{87}Rb β-spectrum obtained with activated rubidium iodide crystal. .—.—. Fermi Plot obtained by Curran, Dixon and Wilson (1951) with the proportional counter.

Fig. 44.

APPENDIX - THE RADIOACTIVITY OF Rb^{87} (continued)

The energy distribution N(W).dW of the electrons emitted in β-decay may be written:-

$$N(W).dW = C.F_o(W,Z).(W_o-W)^2.(W^2-1)^{\frac{1}{2}}.W.dW \qquad (23)$$

Here Wo is the maximum β-ray energy, and Fo(W,z) is the Fermi Coulomb correction factor for an allowed transition. C is a constant for an allowed transition, but is in general a function of energy, the form of the function being determined by the type of interaction and degree of forbiddenness (cf. Fermi (1934), Konopinski and Uhlenbeck (1941), Greuling (1942)).

Fig. 44 shows the Fermi plot, [the function $\sqrt{C}.(Wo - W)$], of the results of fig. 15. Points near the end of the range are not shown here. The results of proportional counter work by Curran, Dixon, and Wilson (1951) are shown for comparison. There are more counts at the higher energy end and less at the lower energy end than obtained in the proportional counter work. This is only to be expected as the higher energy particles would be efficiently absorbed, and there would be no back scattering at the lower energies in the crystal. The end point is indicated at 275 KeV, as determined from fig. 15. (Recent results by McGregor and Wiedenbeck (1954) using a lens spectrometer accord above about 70 KeV). The total counting rate above 17.4 KeV was found using appropriate paralysis, as indicated previously. Allowing for loss of proper counts through the possibility of coincident arrival within the paralysis time (0 - 3 milliseconds), 1975 counts per minute were obtained from the crystal of weight 0.1487 gms.

Extrapolation/

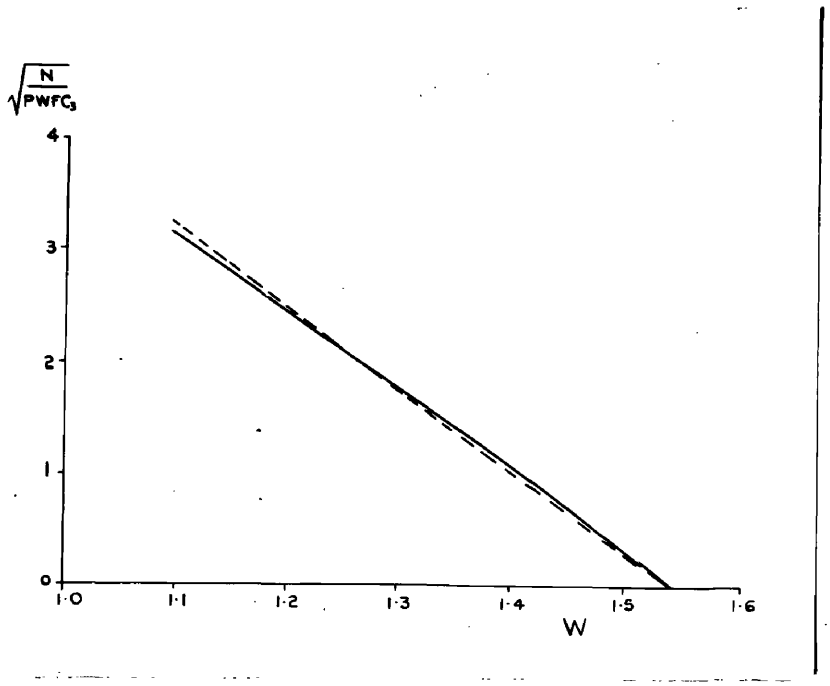

Fig. 45. Linearisation of the Fermi plot for Rb^{87} on introducing the correction factor C_3.

Extrapolation to zero energy along the dotted Fermi plot (which actually includes the point near 13 KeV) involves an extra 600 counts/min. The Rb^{87} abundance figure is 27.2%, giving a half-life figure of $(5.90 \pm 0.3)10^{10}$ years. (Recent results of Flinta and Eklund (1954) accord too with this figure).

The transition has a log ft value therefore of 17.5 indicating a third forbidden transition. The nuclear spin change in the decay $Rb^{87} \rightarrow Sr^{87}$, viz., 3/2 → 9/2 agrees with this. On the shell model a parity change ($p^3/2 \rightarrow g^9/2$) is expected. Pseudo scalar interaction (3P) is then not possible. Calculations using the formulae of Greuling (1942) eliminates the possibility of scalar interaction (3S) also. The determination of C in general involves some knowledge of the nucleus. Tokozowa, Umezawa and Nakamura (1952) proposed that polar vector (^3V) or tensor interaction (3T) alone gave good fits with the experimental data. They deduced (using one parameter) a correction factor C_3 such that $\sqrt{(N/PWFC_3)}$ plotted against (Wo - W) differed little from a straight line (cf. Physica, (1952), 1166). Apparently there is an error of calculation in their work (cf. McGregor and Wiedenbeck (1954)). Using revised values, and a parameter value deduced on theoretical grounds by Yamada (1953) linearization of the plot is possible, as shown in fig. 45.

In concluding this appendix, it should be mentioned that measurement of strontium content enables age determinations to be made on the basis of the Rb^{87} lifetime figure; e.g., the age of lepidolite beds, amongst the oldest, can be assessed at 2×10^9 years (cf. Strassman and Walling (1938)).

REFERENCES

Abraham (1914), Phys. Zeits., 15, 914.

Aeppli, H., Bishop, A.S., Frauenfelder, H., Walter, M. and Zuntli, W., (1951), Phys. Rev., 82, 550.

Agnew, H.M., (1950), Phys. Rev., 77, 655.

Ajzenberg, F. and Lauritsen, T., Rev. Mod. Phys., (1952), 24, 321.

Allen, J.S. and Engelder, T.C., (1951), Rev. Sc. Inst., 22, 401.

Anderson, C.D., (1932), Science, 76, 238.

Austin, L. and Starke, H., (1902), Ann. Phys., 9, 271

Baker, R.F. and Tate, J.T., (1938), Phys. Rev., 53, 683.

Bannerman, R.C., Lewis, G.M. and Curran, S.C., (1951), Phil,Mag., 42, 1097.

Bay, Z., (1950), Phys. Rev., 77, 419.

Bay, Z., Henri, V.P. and McLernon, F.I., (1954), Bull. Am. Phys. Soc., 1, 43.

Beach, L.A., Peacock, C.L. and Wilkinson, R.G. (1949), Phys. Rev. 76, 1624.

Becquerel, H., (1896), Comptes Rendus, 122; 501.

Bell, P.R., (1948), Phys. Rev., 73, 1405.

Bell, P.R., Cassidy, J.M. and Davis, R.C., (1950), Nucl. Data Supp. N.B.S. circular, 499, 20.

Bell, R.E. and Graham, R.L., (1952), Phys. Rev., 87, 236.

Bell, R.E. and Graham, R.L., (1953), Phys. Rev., 90, 644.

Bell, R.E. and Petch, H.L., (1949), Phys. Rev., 76, 1409.

Bell, R.E., Graham, R.L. and Petch, H.E., (1952), Con.Jour.Phys., 30, 35.

Beringer, R., (1943), Phys. Rev., 63, 23.

Beringer, R. and Montgomery, C.G., (1942), Phys. Rev., 61, 222.

Biedenharn, L.C. Arfken, G.B. and Rose, M.E., (1951), Phys. Rev. 83, 586.

Biedenharn, L.C. and Rose, M.E., (1953), Rev. Mod. Phys., 25, 729.

Birks/

irks, J.B., and Szendrei, M.E., (1953), Phys. Rev. 91, 197.

ishop, G.R., Wilson, R. and Halban, H., (1950), Phys. Rev., 77, 416.

itter, F., (1950), "Nuclear Physics", Addison Wesley Press Inc.,Camb., Mass.

lackett, P.M.S. and Occhialini,,G.P.S., (1933), P.R.S., A, 139, 699.

latt, J.M. and Weisskopf, V.F. (1952) "Theoretical Nuclear Physics", Wiley, N.Y.

leaney, B., (1951), Phil. Mag., 42, 441.

rady, E.L. and Deutsch, M., (1947) Phys. Rev., 72, 870.

rady, E.L. and Deutsch, M., (1948)a Phys., Rev., 74, 1541.

rady, E.L. and Deutsch, M., (1948)b Phys., Rev., 78, 558.

roser, I. and Kallman, H., (1947)a Zs f. Naturf., 2a, 439.

roser, I. and Kallman, H., (1947)b Zs f. Naturf., 2a, 642.

utement, F.D.S., (1951), Nature, Lond., 167, 400.

erenkov, P.A., Compt. Rand. U.S.S.R. (1934), 8, 451.

hariton, J. and Lea, C.A., (1929), P.R.S., A, 122, 304.

harpak, G. and Suzor, F., (1951), Comp. Rendus, 233, 1356.

olgate, S.A. and Gilbert, F.C., (1953), Phys. Rev., 89, 790.

ompton, A.H., (1923), Phys. Rev., 21, 483.

ondon, E.U. and Shortley, G.H., (1951) "The Theory of Atomic Spectra", Camb. Univ. Pr.

rookes, W., (1903), P.R.S., 71, 405.

urran, S.C. and Baker, W., (1944) (cf. Rev. Sc. Inst. (1947), 19, 116)

urran, S.C., (1952), Physica, 1166.

urran, S.C., Dixon, D. and Wilson, H.W., (1951), Phys., Rev., 84, 151.

aniels, J.M., Grace, M.A. and Robinson, F.N.H., (1951), Nat., 168, 780.

avey, W.G. and Moon, P.B., (1953), Proc. Phys. Soc., 66, 956.

e Benedetti, S., Cowan, C.E., Konneker, W.R. and Primakoff, H., (1950), Phys. Rev., 77, 205.

e Benedetti, S. and Richings, H.J., (1951), Phys. Rev., 81, 310.

e/

De Benedetti, S. and Richings, H.J., (1952), Phys. Rev., 85, 377.

De Benedetti, S. and Siegel, R., (1952), Phys. Rev., 85, 371

Delbrück, M. and Gamow, G. (1931), cf. Gamov, G. and Critchfield, C.L., (1949), "Theory of Atomic Nucleus and Nuclear Energy Sources", Oxf. Press, 192.

Dennison, D.M., (1940), Phys. Rev., 57, 454.

Deutsch, M., (1951), Phys. Rev. 83, 866.

Deutsch, M., (1953), "Progress in Nuclear Physics III", Pergamon Press, London.

Deutsch, M. and Dulit, E., (1951), Phys. Rev., 84, 601.

Devons, S., (1949), "Excited States of Nuclei" Camb. Univ. Press.

Devons, S., and Hine, M.G.N. (1949), P.R.S., A, 199, 73.

Dirac, P.A.M., (1928), P.R.S., A, 117, 610.

Dirac, P.A.M., (1930), Proc. Camb. Phil. Soc., 26, 361.

Du Mond, J.W., Lind, D.A. and Watson, B.B., (1949), Phys. Rev., 75, 1226.

Dunworth, J.V., (1940), Rev. Sci. Inst., 11, 167.

Elliott, L.G. and Bell, R.E., (1949), Phys. Rev., 76, 168.

Elliott, L.G. and Wolfson, J.L., (1951), Phys. Rev., 82, 333.

Engstrom, R.W., (1947), J. Opt. Sc. Amer., 37, 420.

Falkoff, D.L. and Uhlenbeck, G.E., (1950), Phys. Rev., 79, 323.

Ferguson, A.T.G. and Lewis, G.M., (1953), Phil. Mag., 44, 1339.

Fermi, E., (1934), Zeits. f. Physik., 88, 161.

Fermi, E., (1950), "Nuclear Physics", Univ. of Chicago Press.

Flinta, J. and Eklund, S., Arkiv. f Fysik., (1954), 32, 401.

Fowler, W.A., Gaerttner, E.R., and Lauritsen, C.C., (1938), Phys. Rev., 53, 628.

Fowler, W.A., and Lauritsen, C.C., (1949), Phys. Rev., 76, 314.

Franz, W., (1950) Z. Physik, 127, 363.

Furst/

Furst, M., Kallman, H. and Kramer, B., (1953), Phys. Rev., 89, 416.

Garlick, G.F.T., and Wright, G.T., (1952), Proc. Phys. Soc. Lond.B65,415.

Goertzel, G., (1946), Phys. Rev., 70, 897.

Goldhaber, M. and Sunyar, A.W., (1951), Phys. Rev., 83, 906.

Good, W.M., (1948), Phys. Rev., 70, 978.

Gordy, W., Ring, H. and Burg, A.B., (1948), Phys. Rev., 74, 119.

Graham, R.L., and Bell, R.E., (1951), Phys. Rev., 84, 380.

Greuling, E., (1942), Phys. Rev., 61, 568.

Guggenheimer, K.M., (1943), P.R.S., A, 181, 169.

Hafstad, L.R. and Teller, E., (1938), Phys. Rev., 54, 681.

Hallwachs, W., (1888), Wied. Ann., 33, 301.

Hamilton, D.R., (1940), Phys. Rev., 58, 122.

Hanson, A.O., (1949)., Phys. Rev., 75, 1794.

Haxel, D., Houtermans, F.G. and Kemmerich, M. (1948), Phys. Rev., 74,1886

Hayden, R.J., Reynold, J.H. and Inghram, M.G. (1949), Phys.Rev., 75,1500.

Heitler, W., (1936) Proc. Camb. Phil. Soc., 32, 112.

Heitler, W., (1947) "Quantum Theory of Radiation", Oxf. U.P., 2nd Ed.

Heitler, W. and Sauter, F., (1933) Nature, 132, 892.

Higginbotham, W.A., Gallagher, J., and Sands, M., (1947) Rev. Sc. Inst., 18, 706.

Hofstadter, R. (1948), Phys. Rev., 74, 100.

Hofstadter, R. (1949), Phys. Rev., 75, 796.

Hofstadter, R. and McIntyre, J.A., (1950)a Phys. Rev., 78, 619.

Hofstadter, R. and McIntyre, J.A., (1950)b Phys. Rev., 80, 631.

Hollander, J.M., Perlman, I. and Seaborg, G.T., (1953) Rev. Mod. Phys. 25, 469.

Hopkins, J.I., (1951), Rev. Sc. Inst., 22, 29.

Hubbard/

Hubbard, T.P., Nelson, E.B. and Jacobs, J.A., (1952), Phys.Rev., 87, 378.

Huus, T. and Day, R.B., (1952), Phys. Rev., 85, 761.

Inghram, M.G., Hayden, R.J. and Hess, D.C., (1947), Phys. Rev., 71, 643. (cf. too (1950), Suppl., Nuclear Data, Nat. Bur. Stand. Circular 499.

Jackson, J.A. and Harrison, F.B., (1953), Phys. Rev., 89, 322.

Jacobs, J.A., Malmberg, P. and Wahl, J.S., (1948), Phys. Rev., 73, 1130.

Jaeger, J.C. and Hulme, H.R., (1935), P.R.S., 148, 708.

Jaeger, J.C. and Hulme, H.R., (1936), Proc. Camb. Phil. Soc., 32, 158.

Johannson, S.A.E., (1950), Nature, 166, 794.

Kendall, H.W. and Deutsch, M. (1953), Bull. Am. Phys. Soc., 6, 28.

Kern, B.D., Moak, C.D., Good, W.M. and Robinson, G.P., Phys. Rev.,(1951), 83, 211.

Klein, O. and Nishina, Y., (1929), Zs.f. Physik., 52; 853.

Konopinski, E.J. and Uhlenbeck, G.E., (1941) Phys. Rev., 60, 308.

Kikuchi, S., Watase, Y., and Itoh, J., (1942) Zeits f. Phys., 119, 185.

Kubitschek, H.E., (1950)., Phys. Rev., 79, 23.

Latyshev, G.D., (1947), Rev. Mod. Phys., 19, 132.

Lee, M.R. and Katz, R., (1954), Phys. Rev., 93, 155.

Lenard, P., (1903), Ann. Phys., 12, 449.

Lewis, G.M., Phil. Mag., (1952)a, 43, 690.

Lewis, G.M., Phil. Mag. (1952)b, 43, 1070.

Lewis, G.M. and Ferguson, A.T.G., (1953), Phil. Mag., 44, 1011.

McGregor, M.H. and Wiedenbeck, M.L., (1952), Phys. Rev., 86, 420.

McGregor, M.H. and Wiedenbeck, M.L., (1954), Phys. Rev., 94, 138.

Malmfors, K.G., (1952), Ark. Fys., 6, 49.

Mandeville, C.E. and Scherb, M.V., (1948), Phys. Rev., 73, 1434.

Mann, L.G. and Axel, P., Phys. Rev., 84, 221 (1951).

Marinsky/

Marinsky, J.A., (1949), Thesis M.I.T. and Progress Rep. Lab. Nuclear Sci. Eng. (July).

Mayer, M.G., (1949), Phys. Rev., 75, 1969.

Mayer, M.G., Moszkowski, S.A. and Nordheim, L.W., (1951), Rev. Mod. Phys. 23, 315.

Meric, S., (1949), Ph.D. Thesis, Univ. of Glasgow.

Metzger, F. and Deutsch, M., (1950), Phys. Rev., 78, 551.

Miller, L.C. and Curtiss, L.F. (1946), Phys. Rev. 70, 983.

Minton, G.H., (1954), Bull. Am., Phys. Soc., 1,21.

Mitchell, A.C.G., Langer, L.M. and Brown, L.J.,(1947), Phys.Rev., 71,140.

Moak, C.D., Good, W.M. and Robinson, G.P. (1951), Phys. Rev., 83,211A, 241A.

Morrish, A.H., (1949), Phys. Rev., 76, 1651.

Mott, N.F. and Massey, H.S.W., (1949), "The Theory of Atomic Collisions", Oxf. Press; 49.

Newton, T.D., (1950), Phys. Rev., 78, 490.

Nyquist, H., (1928), Phys. Rev., 32, 110.

Ollano, Z., (1941) Il Nuovo Cimento, 18, 11.

Ore, A., and Powell, J.L., (1949), Phys. Rev., 75, 1696.

Osborne, R.K. and Peacock, W.C., (1946), Phys. Rev., 69, 679.

Pond, T.A., (1952), Phys. Rev., 85, 489.

Pond, T.A., (1954), Phys. Rev., 93, 478.

Post, R.F., (1950), Phys. Rev., 79, 735.

Post, R.F. (1952), Nucleonics, 10/3, 34.

Post, R.F. and Schiff, L.I., (1950), Phys. Rev., 80, 1113.

Radcliffe, J.M., (1951), Phil, Mag., 42, 1334.

Raffle, J.F. and Robbins, E.J., (1952), Proc. Phys. Soc., 65 B, 320.

Rall, W. and Wilkinson, R.G., (1947), Phys. Rev., 71, 321.

Reynolds/

Reynolds, G.T., Harrison, F.B. and Salvini, G., (1950), Phys. Rev., 78, 488.

Rich, J.A., (1951), Phys. Rev. 81, 140.

Robinson, B.L. and Madansky, L. (1951), Phys. Rev., 84, 1067.

Roggankamp, P.L., Pruett, C.H. and Wilkinson, R.G. (1953) (cf. Rev. Mod. Phys., (1953), 557).

Röntgen, W.C., (1895), (cf. Ann. d. Phys., 64 1 , (1898)).

Rose, M.E., (1953), Phys. Rev., 91, 610.

Ruark, E., (1945), Phys. Rev., 68, 278.

Rutledge, W.C., Cork, J.M. and Burson, S.B., (1952) Phys. Rev., 86, 775.

Rutherglen, J.G., Grant, P.J., Flack, F.C. and Deukars, W.M. (1954), Proc. Phys. Soc., (to be published).

Scharff-Goldhaber, G., der Mateosian, E., McKeown, M. and Sunyar, A.W., (1950), Phys. Rev. 78, 325.

Segrè, E. and Helmholz, A.C. (1949), Rev. Mod. Phys., 21, 271.

Sherr, R., Muether, H.R. and White, M.G., (1949), Phys. Rev., 75, 282.

Shearer, J.W. and Deutsch, M., (1951), Phys. Rev., 82, 336.

Siegel,R 1952 (cf. Deutsch, M., (1953), "Progress in Nuclear Physics" III Pergamon Press)

Sommer, A. and Turk, W.E., (1950), J. Sc. Inst., 27, 113.

Spring, K.H., (1950) "Photons and Electrons", Methuen.

Stokes, G., (1852), Phil. Trans., 142, 463.

Stobbe, M., (1930), Ann. d. Phys. , 7, 661.

Stone, R.S., (1952), Phys. Rev., 87, 235.

Strassman, F. and Walling, E., (1938), Ber. d.d. Chem. Ges., 71, 1.

Stratton, J.A., (1941) "Electromagnetic Theory" McGraw Hill, Inc.

Temple, G., (1928), P.R.S.,A 121, 673.

Terrel, (1950), Phys. Rev., 80, 1076.

Thomson, D.M., Cohen, A.V., French, A.P. and Hutchison, G.W., (1952) Proc. Phys. Soc., A, 65, 745.

Thirion/

Thirion, J. and Telegedi, V.L., (1953) Bull. Am. Phys. Soc., 7, 16.

Tomozowa, Y., Umezawa, M. and Nakamura, S., (1952), Phys. Rev., 86, 791.

Walker, R.L., (1950), Phys. Rev., 79, 172.

Wattenberg, A., (1947), Phys. Rev., 71, 497.

West, H.I., Meyerhof, W.E. and Hofstadter, R., (1951) Phys. Rev.,81, 141.

Weizsäcker, C.F., von (1935) Zeits. Physik., 96, 431.

Wheeler, J., (1946), Ann. New York Acad. Sci., 48, 219.

Williams, F.C., (1936), J.I.E.E., 79, 352.

Wilson, H.W. and Lewis, G.M., (1952), Proc. Phys. Soc., A, 65, 656.

Yamada, M., (1953) Prog. Theor. Phys. Japan, 9, 268.

Yang, C.N., (1950), Phys. Rev., 77, 242.

Zworykin, V.K., Morton, G.A. and Malter, L. (1936), Proc. Inst. Rdd. Eng. N.Y., 24, 351.